



Faculty of Science and Technology

MASTER'S THESIS

| | |
|--|--|
| Study program/ Specialization: | Spring Semester 2014 |
| Offshore Technology/ Marine and Subsea Technology | Open |
| Writer: Mohammed Ali Mohammed | Writer's Signature |
| Faculty Supervisor Prof. Arnfinn Nergaard | |
| Second Supervisor - | |
| Title of Thesis Evaluation of Module Handling System on Current Riserless Light Well Intervention Units to Improve Up-time | |
| Credits (ECTS): 30 | |
| Key Words Module Handling Hydrodynamics Moonpool deployment RLWI | Pages 83 Enclosure Stavanger June 16, 2014 |

Abstract

Riserless light well intervention technology (RLWI) is the latest addition to the subsea light well intervention market. Beginning operation in mid 2005, the technology has the advantage of utilizing a special subsea lubricator to perform intervention activities in water depths of up to 1200 m without the need for marine risers. Utilizing the technology, oil companies have been able to save up to 50% on intervention costs. Nonetheless, RLWI has its own draw backs. In the last 4 years, it has seen up to 25% downtime due to waiting on weather (wow). A look at the weather criteria of one of the RLWI vessels, Island Wellserver, indicates module deployment and retrieval to be the weather limiting operation. In this thesis work, it is attempted to identify the critical elements of the module deployment system and analyze their significance in the objective of raising the operational weather limit. Hence the module handling system was carefully studied. Critical failure modes were found to be failure of crane wire due to excess loading, failure of lower cursor system due to impact loading and clashing of module to moonpool walls. Analysis of the module deployment system against these failure modes was ensued. Orcaflex simulation software was selected. System guide wires, crane wire, vessel and moonpool were modelled. DNV recommended practice with appropriate calibration was utilized to calculate hydrodynamic coefficients for the module. Asgard field data was selected, 1-year unrestricted current condition was employed, regular wave analysis for module in moonpool and irregular wave analysis for module beneath moonpool was performed. Finally, sensitivity of the failure parameters to the system particulars was studied.

The results showed the moonpool sea-state to be a defining parameter, as would be expected. However, surprisingly enough, the study found that the vessel length is not directly related to the moonpool sea-state and a longer vessel does not necessarily mean a better platform for the module deployment operation. For the rest of the particulars studied, higher guide wires tensions, wider moonpool and active heave compensation all have a positive effect in handling the environmental loads. Although, changing moonpool dimensions affect hydrodynamics positively, their significance is small due to dependency on vessel's breadth. Based on these results and available data for analysis, a recommended system particulars was tested. Significance improvement, up to 45%, in lowering the risk of failure was observed. A design weather limit for the recommended system was found to be less than $H_S = 2.5$ m. This attributes to a 28% waiting on weather per operation with an operation reference period of $T_R = 13$ h. However, estimation of complex hydrodynamic coefficients proved to be challenging and was taken conservatively. Model tests of module is recommended for this purpose. Further, a better software package like SIMO would be preferred to Orcaflex for such types of analysis.

This page is intentionally left blank

Preface

I came across this thesis project when I was employed as a summer intern at Statoil ASA in June 2013. I had the opportunity to go offshore on one of the riser-less light well intervention vessels and had a bit of experience how the operation was carried out. During my time at the office, I had learned that waiting on weather was one of the main challenges faced by the technology. I decided that I would like to understand the reason behind this challenge, and try to point out the critical parts of the system to improve the weather up time. It was my motivation to write this thesis on the topic.

I have attempted to go thorough the necessary phases to fully tackle the main challenges of waiting on weather. Chapter 1 brings the reader into the world of riser-less light well intervention, and its current importance in the oil industry. The main research problem for the thesis, and its relevance to the industry are also highlighted in this chapter.

In Chapter 2, I have summarized necessary literature and theory one needs to know and understand before attempting to analyze a marine operation, specifically, riser-less light well intervention. The reader is encouraged to read this chapter if they need to understand certain aspects of marine operation, moonpool deployment, history of riserless light well interventions and etc.... The reader can skip this chapter if he/she is knowledgeable on the subject.

In Chapter 3, the analysis basis is discussed in appropriate detail. This chapter illustrates what and why a specific method or code is used.

Chapter 4 is a presentation of the results. Chapter 5 analyzes in good detail the observed results, identifies the critical factors and further explains their implications.

Finally, in Chapter 6, I have summarized the findings and stressed the limitations and recommendations for further work.

This page is intentionally left blank

Acknowledgments

First and foremost, I would like to give my sincere appreciation and gratitude to my supervisor Professor Arnfinn Nergaard for giving me the opportunity to work with him in this project.

Secondly, I am grateful for Ole-Erik Endrerud and Arunjyoti Sarkar for their unreserved support in the initial parts of the thesis.

Next, my deepest appreciation goes to my true friend Elsa T.M for her unlimited support and companionship from the time I started working on this thesis to its end.

I would also like to extend my gratitude further to fellow engineers and classmates Adedayo, Adekunle and Arvind for their help and advice towards learning the main simulation software Orcaflex used for this thesis.

Finally, to anyone who had given me their time to listen and give me advice on how to tackle the challenges faced, my warmest thanks goes out to you.

Contents

| | Page |
|---|----------|
| 1 Introduction | 1 |
| 1.1 Background | 1 |
| 1.2 Problem Statement | 2 |
| 1.3 Key Milestones | 2 |
| 1.4 Scope | 3 |
| 1.5 Feasibility and Relevance of the Project | 3 |
| 2 Literature Review | 4 |
| 2.1 Riser-less Light Well Intervention (RLWI) | 4 |
| 2.1.1 Subsea Well Interventions | 4 |
| 2.1.2 Riser-less Technology for Subsea Wells | 5 |
| 2.1.3 RLWI Operational History | 8 |
| 2.1.4 RLWI Challenges | 9 |
| 2.2 Weather and Marine Environment | 11 |
| 2.2.1 Density | 11 |
| 2.2.2 Ocean Current | 12 |
| 2.2.3 Ocean Waves | 12 |
| 2.3 Environmental Forces | 17 |
| 2.3.1 Buoyancy Force | 18 |
| 2.3.2 Current Forces | 18 |
| 2.3.3 Wave Forces | 20 |
| 2.3.4 Hydrodynamic Coefficients | 23 |
| 2.4 Module Deployment: System and Procedure | 25 |
| 2.4.1 Vessel Station Keeping | 25 |
| 2.4.2 Moonpool | 28 |
| 2.4.3 Module handling Tower | 30 |
| 2.4.4 Coupling Wire | 31 |
| 2.4.5 Winches | 33 |
| 2.4.6 Constant Tensioned Lower Cursor System | 34 |

| | | |
|----------|---|-----------|
| 2.4.7 | Deployment Procedure | 36 |
| 3 | Analysis Basis | 38 |
| 3.1 | Define Operation Class and Select Field | 38 |
| 3.2 | Analysis Software | 39 |
| 3.3 | Marine Environment Modelling | 39 |
| 3.3.1 | Design Density | 39 |
| 3.3.2 | Design Current | 40 |
| 3.3.3 | Design Wave Parameters | 40 |
| 3.4 | Subsea Equipment Modelling | 42 |
| 3.5 | Module Handling System Modelling | 46 |
| 3.5.1 | Vessel | 46 |
| 3.5.2 | Moonpool | 47 |
| 3.5.3 | Constant Tension Guide Wires | 48 |
| 3.5.4 | Heave Compensated Crane Wire | 48 |
| 3.5.5 | Tower and Cursor System | 48 |
| 3.6 | Load Case and Load Combination | 49 |
| 3.6.1 | Load Cases | 49 |
| 3.6.2 | Load Combinations | 49 |
| 3.6.3 | Sensitivity Case | 50 |
| 3.7 | Design Principle | 50 |
| 3.7.1 | Load and Resistant Factor Design (LRFD) | 50 |
| 3.7.2 | Working Stress Design (WSD) | 51 |
| 3.8 | Acceptance Criteria | 51 |
| 3.8.1 | Failure Modes | 51 |
| 3.8.2 | Safety Factors (Failure Limit) | 52 |
| 4 | Results | 54 |
| 4.1 | General | 54 |
| 4.2 | Base Case | 56 |
| 4.3 | Sensitivity Study | 60 |
| 4.3.1 | Vessel Particulars | 60 |
| 4.3.2 | Active Heave Compensation | 61 |
| 4.3.3 | Moonpool Width | 61 |
| 4.3.4 | Guide Wire Tension | 61 |
| 4.4 | Recommended Particulars | 61 |
| 5 | Discussion | 66 |
| 5.1 | Base Case Study | 66 |
| 5.2 | Sensitivity Parameters | 69 |
| 5.3 | Base Case Vs Recommended Case | 73 |

| | |
|---|------------|
| 5.4 Effect on Up-time | 74 |
| 6 Conclusion & Recommendation | 77 |
| References | 81 |
| A Sensitivity Plots | 84 |
| B Global Hydrodynamic Coefficient Tables | 96 |
| C Added Mass Calculations | 100 |
| D Failure Mode Effects Analysis | 110 |
| E Certex Wire Properties | 112 |
| F Information on Åsgard Field | 115 |

List of Figures

| | | |
|------|---|----|
| 2.1 | Classification of subsea rigs based on capability [5] | 5 |
| 2.2 | RLWI Mark II assembly | 6 |
| 2.3 | Variation of density with temperature | 11 |
| 2.4 | Wave Parameters | 12 |
| 2.5 | Superposition of regular waves to make irregular sea [15] | 13 |
| 2.6 | Weather effect on waves (Beaufort scale) | 18 |
| 2.7 | Current Force profile with depth | 19 |
| 2.8 | motion of water particles in ocean waves | 20 |
| 2.9 | Wave theories and their range of applicability [20] | 21 |
| 2.10 | Submerged 3D body within slamming region | 23 |
| 2.11 | Module handling system on-board Island Constructor (<i>Source: Island Offshore</i>) | 26 |
| 2.12 | six degree of freedom vessel motions | 27 |
| 2.13 | Example RAO | 27 |
| 2.14 | Cofferdam moonpool walls with an estimated relative damping ration of up to 45% (<i>Picture: DeepOcean</i>) | 30 |
| 2.15 | Module handling tower on RLWI vessel | 31 |
| 2.16 | Active Heave compensation system [28] | 34 |
| 2.17 | Passive heave compensation system [28] | 35 |
| 2.18 | Lower Cursor System [27] | 35 |
| 3.1 | Complex subsea module, Well Control Package | 42 |
| 3.2 | Simplified model of module for added mass calculation | 44 |
| 3.3 | Modelling mesh on Orcaflex to account for hydrodynamic coupling coefficients | 45 |
| 3.4 | Modification for added mass proximity to water surface | 46 |
| 3.5 | Load case definition based on module elevation | 49 |
| 3.6 | Critical structural failure modes considered for analysis | 52 |
| 4.1 | Orcaflex model results | 55 |
| 4.2 | Base Case A: Results relative to moonpool at $H_S = 2.5m$ and 180° wave direction | 57 |

| | | |
|-----|---|----|
| 4.3 | Base Case B: Results relative to moonpool at $H_S = 2.5m$ and 180° wave direction | 58 |
| 4.4 | Base Case C: Results relative to moonpool at $H_S = 2.5m$ and 180° wave direction | 59 |
| 4.5 | Vessel heave RAOs at 180° wave direction | 60 |
| 4.6 | Recommended Case A: Results relative to moonpool at $H_S = 2.5m$ and 180° wave direction | 63 |
| 4.7 | Recommended Case B: Results relative to moonpool at $H_S = 2.5m$ and 180° wave direction | 64 |
| 4.8 | Recommended Case C: Results relative to moonpool at $H_S = 2.5m$ and 180° wave direction | 65 |
| 5.1 | Crane tip heave motion transfer functions | 67 |
| 5.2 | Vessel moonpool sea state RAO different wave heading | 68 |
| 5.3 | Spider diagram for sensitivity of failure parameters to system particulars (Maximum Values at $H_s = 2.5$ m for all load cases and peak periods 6 – 10 s) | 70 |
| 5.4 | Vessel RAO Vs Moonpool Heave Seastate | 71 |
| 5.5 | Vessel Surge RAO at 180° wave direction | 72 |
| 5.6 | Variance of moonpool seastate RAO for different moonpool side width at 180° wave direction | 73 |
| 5.7 | Percentage waiting on weather calculated based on expected reference period of module deployment operation | 76 |
| A.1 | Vessel Sensitivity Case A: Results relative to moonpool at $H_S = 2.5m$ and 180° wave direction | 85 |
| A.2 | Vessel Sensitivity Case B: Results relative to moonpool at $H_S = 2.5m$ and 180° wave direction | 86 |
| A.3 | Vessel Sensitivity Case C: Results relative to moonpool at $H_S = 2.5m$ and 180° wave direction | 87 |
| A.4 | Heave compensator Sensitivity Case A: Results relative to moonpool at $H_S = 2.5m$ and 180° wave direction | 88 |
| A.5 | Heave Compensator Sensitivity Case B: Results relative to moonpool at $H_S = 2.5m$ and 180° wave direction | 89 |
| A.6 | Heave Compensator Sensitivity Case C: Results relative to moonpool at $H_S = 2.5m$ and 180° wave direction | 90 |
| A.7 | Moonpool Particulars Case A: Results relative to moonpool at $H_S = 2.5m$ and 180° wave direction | 91 |
| A.8 | Moonpool Particulars Case B: Results relative to moonpool at $H_S = 2.5m$ and 180° wave direction | 92 |
| A.9 | Guidewire Tension Case A: Results relative to moonpool at $H_S = 2.5m$ and 180° wave direction | 93 |

| | | |
|------|---|-----|
| A.10 | Guidewire Tension Case B: Results relative to moonpool at $H_S = 2.5m$ and 180° wave direction | 94 |
| A.11 | Guidewire Tension Sensitivity Case C: Results relative to moonpool at $H_S = 2.5m$ and 180° wave direction | 95 |
| E.1 | Guide wire properties(Diameter-19 mm) | 113 |
| E.2 | Crane wire properties (Diameter-69.9mm) | 114 |

List of Tables

| | | |
|-----|--|-----|
| 2.1 | Different rigs which performed RLWI operations at least once | 8 |
| 2.2 | Average time spent on operation [14] | 10 |
| 2.3 | A 4 year statistics on current RLWI vessels on Norwegian Continental Shelf [2] | 10 |
| 2.4 | Operability wave (OP_{WF}) criteria present on Island Wellserver [11] | 10 |
| 2.5 | Dynamic positioning classes [24] | 29 |
| 3.1 | Acceptable return periods for H_s | 40 |
| 3.2 | 1 year current for Åsgard [35] | 41 |
| 3.3 | General MKII module data [2] | 43 |
| 3.4 | Wire Properties [37] | 48 |
| 3.5 | Basic Usage factors η_o for WSD method [33] | 51 |
| 4.1 | Global added mass coefficients for module parts | 55 |
| 4.2 | Drag coefficients used for analysis | 56 |
| 4.3 | Vessel sensitivity particulars | 60 |
| 5.1 | Comparison between base case and recommended case on handling system particulars | 74 |
| 5.2 | Comparison between base case and recommended case on maximum para- metric values for $H_s = 2.5$ m and 180° wave direction, $T_p = 6 - 10$ s | 74 |
| C.1 | CASE A: 7.6 m moonpool size | 101 |
| C.2 | CASE A: 7.8 m moonpool size | 102 |
| C.3 | CASE A: 8.0 m moonpool size | 103 |
| C.4 | CASE A: 8.2 m moonpool size | 104 |
| C.5 | CASE B: 7.6 m moonpool size | 105 |
| C.6 | CASE B: 7.8 m moonpool size | 106 |
| C.7 | CASE B: 8.0 m moonpool size | 107 |
| C.8 | CASE B: 8.2 m moonpool size | 108 |
| C.9 | CASE C | 109 |
| D.1 | FMEA of RLWI deployment operation | 111 |

Abbreviations

| | |
|------------|--|
| H | Wave height |
| H_s | Significant Wave height |
| d | Water depth |
| T | Wave period |
| S_T | Wave spectral density as a function of period |
| ω | Angular wave frequency |
| ω_o | Natural frequency |
| S_ω | Wave spectral density as a function of frequency |
| T_p | Peak Period |
| T_z | Zero up-crossing period |
| T_R | Reference period |
| f | Wave frequency = $\frac{\omega}{2\pi}$ |
| f_p | Peak frequency = $\frac{1}{T_p}$ |
| g | Gravitational Acceleration |
| U_x | Wind Velocity at x height from mean sea level |
| v_c | Current velocity |
| v_w | Wave velocity |
| C_{D_s} | Steady drag coefficient |
| C_D | Drag Coefficient |
| C_{dd} | Oscillatory drag coefficient |
| B_1 | Linear damping coefficient |
| B_2 | Quadratic damping coefficient |
| D | Diameter |
| C_A | Added mass Coefficient |
| A_{33} | Added mass in heave |
| C_m | Inertia coefficient |
| r | Position of mass |
| \dot{r} | Velocity of mass relative to earth |
| A | Cross-sectional area |
| S | Projected Area |

| | |
|------------|--|
| V | Volume |
| p | Perforation level |
| Re | Reynold's number |
| KC | Keulegan-Carpenter number |
| U_{R_j} | Relative velocity of wave to module |
| f_I | Inertia force |
| f_s | Slamming force |
| f_d | Drag force |
| F_B | Buoyancy force |
| ∇V | Submerged volume |
| ρ | Density |
| η | Surface elevation |
| γ | Peak Enhancement Factor |
| ζ | Water surface elevation inside moonpool |
| ζ_w | Water surface elevation outside moonpool |
| S_f | Safety factor |
| A_b | Base area of module |
| RAO | Response amplitude operator |
| MHT | Module handling system |
| PCH | Pressure control head |
| ULP | Upper lubricator package |
| LT | Lubricator tubular |
| LS | Lubricator section |
| LLP | Lower lubricator section |
| IWRC | Independent wire rope core |
| RLWI | Riserless light well intervention |
| LCS | Lower cursor system |
| WCP | Well control package |
| RT | Running tool |
| SWL | Safe working load |
| AHC | Active heave compensator |
| MBS | Mean Breaking Strength |
| WOW | Waiting on weather |
| E | Elastic modulus |
| G | Modulus of Rigidity |

Chapter 1

Introduction

1.1 Background

It has been well over a century since the first offshore well was drilled in Ohio (1896), and since then most of the conventional shallow water oil resources, also known as “easy oil”, have been discovered and developed. In recent years, the offshore industry found it necessary and practical to shift its focus to producing from deep-water and small-sized fields. However, traditional platform technology developed mainly for shallow water drilling proved technically and economically unviable solution for such challenges. This led to the rise of subsea technology, distinguished mainly by its use of subsea wells. Subsea wells have a characteristic feature of being located farther away from a host platform. It meant that subsea technology allowed production of deep-water and small sized fields economically. To that effect, there are now over 5000 subsea wells across the world, with their number rising rapidly. Offshore drilling seems to be heading towards subsea production systems in the future.

However, subsea production systems are still development ages and one of the biggest drawbacks is their high cost of administering well interventions. This is mainly because, unlike platform wells which can be accessed directly from host platforms, subsea wells can only be accessed by connecting floating intervention rigs to subsea trees through expensive intervention equipment. Due to this, well interventions on subsea wells are performed less frequently resulting in an estimated 20% reduction in their hydrocarbon recovery rates [1]. Hence, reducing the cost of well interventions has been a key area of concern for the subsea industry.

The introduction of riser-less light well intervention technology in the market has been partly successful at lowering some of the cost of subsea well interventions.

1.2 Problem Statement

Riser-less Light Well Intervention (RLWI) technology is latest development in the attempt to reduce the cost of subsea well interventions. The technology involves using a new riser-less subsea intervention equipment as compared to the traditional riser-based one. The absence of heavy risers on-board makes it possible to perform RLWI subsea well interventions on smaller, faster, and cheaper mono-hull vessels and hence significantly reduces cost per operation.

RLWI technology is quick and cost effective, however, it is currently highly inefficient. Based on the current RLWI vessels statistics, the vessels are at an average of 25% down time over the last 4 years [2]. This is unsatisfactory because it has resulted in fewer interventions per year, delay of potential oil recovery and subsequently affecting the project developers' yearly revenue.

The grounds for downtime is mainly associated with weather criteria on-board the RLWI units. Transiting to key side and waiting on weather (WOW) accounts to more than three quarters of the total downtime. The main reason for low operability weather limit of the vessels is found to be low design weather criteria for *module deployment operation* on the Norwegian Continental Shelf. Therefore, raising the operability criteria of module deployment system for future RLWI units plays a key role in improving efficiency.

1.3 Key Milestones

It has been established from section 1.2 that *improving the module deployment operational weather criteria* would be beneficiary. In this thesis, we have taken the challenge of identifying and evaluating the critical factors that play a part in the module deployment operation. Key milestones of the project are;

1. Describe the critical elements of RLWI module deployment operations

Riser-less light well intervention operation and sequence, vessel motions, environmental forces, module handling system, and other elements will be carefully studied and described.

2. Time domain analysis of module deployment operation

This operation is aimed at determining the current sea state limit of module deployment operation based on standard design codes. We learn and execute marine operation software and model RLWI module deployment operation as accurately as possible.

3. Perform sub-system sensitivity analysis for module deployment system

We will identify and perform sensitivity analysis on some critical elements of the module deployment system. These will include vessel length, guide wire tension, moonpool dimensions and heave compensation systems.

4. Analysis of Results

The results of the time domain analysis and optimization will be evaluated. The significance of the results with respect to increased up time, cost per operation and safety perspectives.

5. Recommendation on module deployment system configuration

Determine maximum up-time gained by evaluating combinations of various module deployment system configuration and recommend best suitable system configuration.

1.4 Scope

1. Study conducted for typical Norwegian Continental Shelf weather condition
2. Study conducted on the current RLWI subsea module (Stack) and module deployment system

1.5 Feasibility and Relevance of the Project

The Norwegian operator, Statoil ASA, started a global project known as CAT-A in 2013 [3]. The main project goal was to build a better intervention rig that could work all year round. This thesis goes hand in hand to that objective. The results of this study can be used to identify critical elements of current module deployment system. This will help decision makers of the possibilities of modification on module handling operations. In addition, the interpretation of the results would point out a way of optimizing the current RLWI units. Hence, The project is in line with solving present-day challenges of the oil industry and will contribute into reduction of cost per well work and improving safety.

Chapter 2

Literature Review

2.1 Riser-less Light Well Intervention (RLWI)

2.1.1 Subsea Well Interventions

Several definitions of the term "*Well Intervention or Well Workover*" exist in literature [4], [6]. In simple terms, well interventions is a collective term used for activities that are performed on a live production or injection well, to alter its state, for a required period of time. Such activities could range from improving efficiency of the well with respect to production to completely shutting it down. Well interventions should be performed with a recommended frequency to optimize the performance of the well.

When performing well interventions, one of the main focus is making sure safety and integrity of the well remains intact at all times. The complexity of the well work varies considerably with the type of the well. In platform wells, this is relatively easier to do since the access point to the well is located topside. However, for subsea wells, this is not the case. The subsea wells have their access points (x-mass tree) located at the seabed, hence, making it increasingly difficult to access the well safely. Therefore, subsea well interventions require sophisticated machinery and trained personnel to perform the job. The high cost of hiring such machinery and personnel makes it uneconomical to perform *subsea well interventions* with the recommended frequency. Consequently, project developers have seen a 10-30% less recovery rate potential from subsea wells compared to platform wells [2].

Recently, the offshore industry has taken an initiative to reduce the cost of subsea well interventions by developing fit-for-purpose intervention units. Consequently, different categories subsea well intervention units are now being developed depending on the type and intensity of the well work. Each category has its own scope of capabilities and improved technology as described in the following list and demonstrated in Figure 2.1 [6];

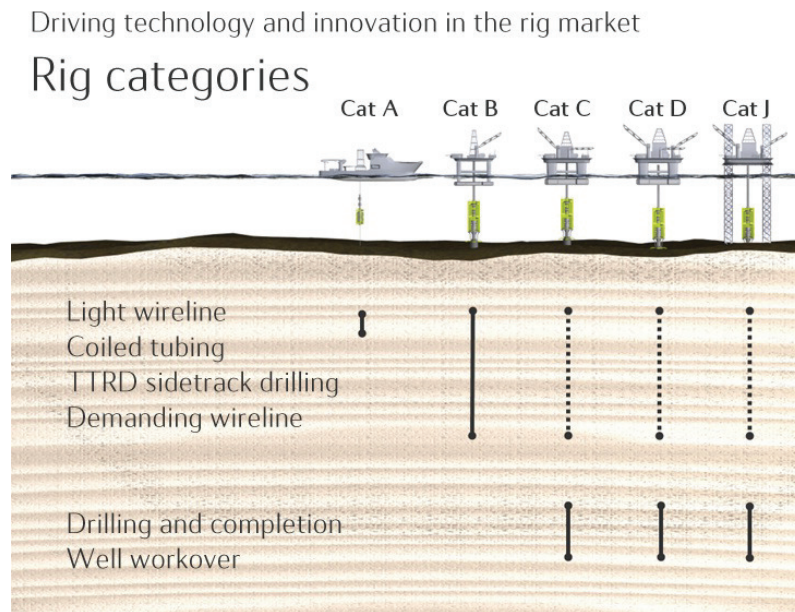


Figure 2.1: Classification of subsea rigs based on capability [5]

Category A — A small or medium sized vessel intended to perform wire-line interventions and other light well interventions. Plugging of a well is also within its capacity. DNV classifies such vessels as Well Intervention Unit 1.

Category A+ — Similar to Cat A vessel for wire-line operations, but also purpose built to perform coiled tubing operations with a 7" riser. DNV classifies such vessels as Well Intervention Unit 2.

Category B — A rig, typically a semi-submersible, in addition to performing every operation that Cat A+ does, has the capacity to perform sidetrack drilling through production tubing. However, this unit has been abandoned as of June 2013.

Category C, D, & J — These rigs are, ordinary drilling rig, optimized rig for medium water depths, Jack-up drilling rig customized for deep waters respectively. These are drilling rigs purpose built for high performance in the Norwegian Continental Shelf. DNV classifies these types of intervention vessels similar to Drilling Rigs.

2.1.2 Riser-less Technology for Subsea Wells

Traditionally, wire-line operations are performed by using riser based technology where risers are extended from topside to the sea bed. The risers act as a pressure barrier between the sea column and the hydrocarbons. Hydrocarbons are sealed off at topside facilities and intervention can commence similar to a dry tree operations. Although successful, such

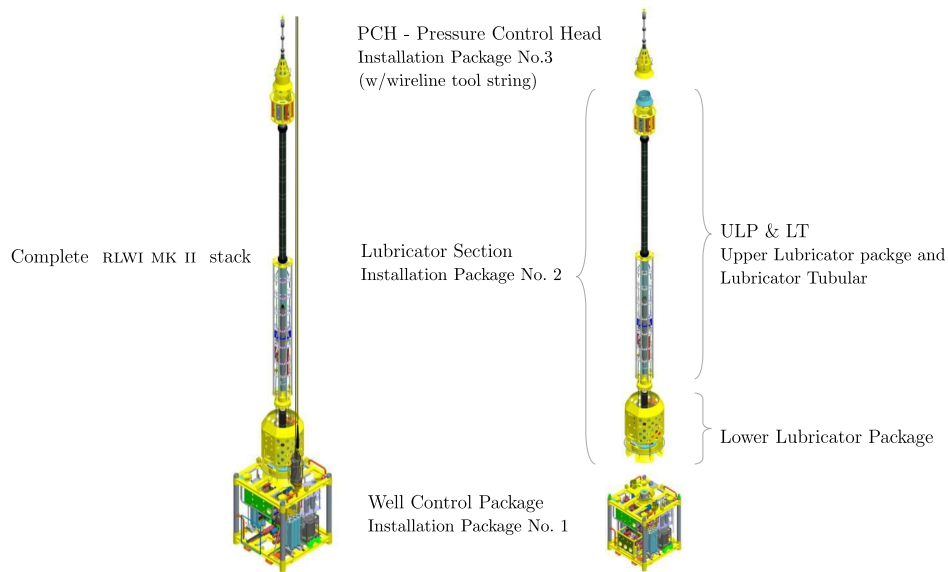


Figure 2.2: RLWI Mark II assembly

heavy risers require large rigs such as semi-submersibles, rendering the operation to be slow and costly.

Category A vessel, also known as riser-less light well intervention vessel, (see section 2.1.1) is developed to minimize the cost of wire-line interventions. It achieves this by using the a riser-less intervention technology with a patented subsea lubricator, called the RLWI *stack*. The RLWI stack utilizes *pressurized grease seal* technology that allows it to seal off hydrocarbons near the sea bottom, removing the need for risers. Therefore, wire-line interventions could possibly be carried out on smaller vessels which have lower day rates and faster transit speeds. From experience, 40-50% reduction in cost per intervention compared with conventional rigs has been attained [7].

Several FMC brochures [8] describe in detail how the technology works. Basically the RLWI stack gets its name from its comprising parts being stacked on top of one another. It has five main components as shown in Figure 2.2.

1. Pressure Control Head

The top most section of the RLWI stack is the pressure control head. It consists of a locking tool with the *upper lubricator package* as well as the flow tubes responsible for providing the grease seal function. The viscous grease located between the wires and the flow tube is viscous enough for required frictional force, and is pumped by a pump located in the *lower lubricator section*. It is important that the pressure from the water column and grease pump be higher than the wellhead pressure. The PCH

is a primary well barrier.

2. Upper Lubricator Package

The ULP, located beneath the the PCH, contains the ball valve for cutting the wireline string in case of emergency. However, the cutting ball valve is not able to cut through tools [9]. In addition, it has the grease circulation outlet and a connection hub for the PCH.

3. Lubricator Tubular

The LT is located between the lower and upper lubricator packages. It is a host for grease reservoirs but also to the injection pumps. A pair of reservoirs contains 370 liters of grease. The LT, together with upper and lower lubricator packages also act as a storage or parking facility for the intervention tools. This is necessary to pressurize the tool higher than the well head pressure before entering the live well. Up to 22 m tool string can be stored.

4. Lower Lubricator Package

The LLP houses several components that allow the control of the RLWI stack. These include, the subsea control module, the hydraulic power unit, hydraulic reservoirs, accumulators, and process control domain etc. But more importantly, the LLP is connected to the Well control package through a safety joint. The safety joint is a critical element allowing the lubricator section to bend and not transfer the bending moment to the well control package.

5. Well Control Package

The WCP is the main mechanical safety barrier of the RLWI stack. It is connected, hydraulically to the X-mass tree through an adapter suiting the type of X-mass tree. It contains a series of upper valves and lower valves, as well as the shear/seal ram. In emergencies, it is able to cut through wireline, wireline tool string, coiled tubing, as well as drill pipe and pressure shut in. During interventions, it provides communication panels from work-over control system to the X-mass tree. It is able to supply pressure and hydraulics capable of flushing hydrocarbons back into the well.

The technology has been qualified for its reliability and safety. The equipment is verified by relevant standards, such as Norsok D-002 and DNV-OS-E101 among others, to perform operations in the North Sea and Norwegian Sea for up to a depth of 500 m. Its size allows it to be deployed from a small supply vessel certified as class *Well Intervention Unit 1* by DNV offshore standard DNV-OSS-101. Therefore, riser-less light well intervention has become a reality and an attractive alternative allowing operations to be performed safely with well integrity intact.

Table 2.1: *Different rigs which performed RLWI operations at least once*

| Vessel Name | Available for RLWI | Location | Length | Breadth | DP Class | Owner |
|---------------------|--------------------|----------------|--------|---------|----------|------------------|
| Island Constructor | 2008– | North Sea | 120 | 25 | DPIII | Island Offshore |
| Island Intervention | 2011– | Gulf of Mexico | 120 | 25 | DPIII | Island Offshore |
| Island Wellserver | 2008– | North Sea | 116 | 25 | DPIII | Island Offshore |
| Island Frontier | 2004– | North Sea | 106 | 21 | DPIII | Island Offshore |
| Reggalia | 2003 | North Sea | N/A | N/A | N/A | Prosafe |
| Havila Phonix | 2009–2013 | North Sea | 110 | 23 | DPII | Havilla Shipping |
| Seawell | 2000– | North Sea | 114 | 22 | DPII | Helix Energy |
| Well Enhancer | 2009– | North Sea | 132 | 22 | DPIII | Helix Energy |
| Skandi Constructor | 2013– | Atlantic North | 120 | 25 | DPIII | Helix Energy |

2.1.3 RLWI Operational History

The first recorded RLWI operation in the North Sea was performed for the Norwegian oil company Statoil with a vessel known as Seawell back late 1990's. Statoil remained interested in the application of this new technology and initiated a contract with FMC Technologies and Prosafe to perform pilot test operation with a multi-service-vessel named Regalia. By using a first generation subsea lubricator, the partners would perform the earliest operations in Statfjord North, Visund and Åsgard fields. This was the first time RLWI was recognized as a possible alternative. Despite being deemed successful, the oil industry still welcomed the technology with a bit of skepticism. This was mainly attributed to contractual difficulties between operators and wire-line/ well control equipment/vessel service providers [10]. The next generation RLWI operations wouldn't start until 2005.

An alliance between Island Offshore, Aker well services, and FMC technologies solved the problem and formed an attractive single contract between contractors and client. Hence the earliest RLWI operation conducted by an Island Offshore vessel was in April 2005 by a vessel known as Island Frontier [11]. Since then there have been hundreds of operations performed by 9 mono-hull vessels, one of which-Havila Pheonix-is no longer in the business beginning 2014. With an average age of subsea wells reaching 15 years, North Sea's over-2000 subsea wells will continue to require more frequent interventions. On average, an estimated 1250 days of RLWI operations will be conducted annually in the coming years [12].

Currently operating RLWI vessels, shown in Table 2.1, are associated with two service contracts; Well OPS and North Sea Alliance. The latter of which has been by far the most experienced in RLWI. From the customers, operators such as Statoil and BP have been the beneficiaries of the technology, but new operators such as Eni Norge, ConoccoPhillips, Chevron, Nexen, and Shell are keen to join the market once the technology is deemed to be mature [10].

These vessels are equipped to perform light well interventions. Such well intervention jobs

include, bore hole surveys/logging, fluid displacement, gas lift valve repair, perforating, re-perforating, sand washing, setting/pulling tubing plugs, stimulation, zonal isolation etc.... [13] Some of the vessels, such as the Island Constructor are also able to perform coiled tubing operations. For a complete RLWI operation, the vessel will perform operations including sea-fastening, transiting, station-keeping, module deployment, and wire-line operations. The purpose and duration of each operation is outlined;

Sea-fastening/Mobilizing : This activity is done twice before start of the operation and at the end of it. It includes making sure all components are safe and ready for operation. Doing this twice for one well intervention job takes approximately 84 hours [14].

Transiting : This is a process of travelling from shore to the well site and back to shore. For the Norwegian Sea, port is at Kristiansund and an average of 150 km is traveled to wells. With current RLWI vessels it takes about 10 hours to reach a well.

Station keeping : Once the mono-hull vessel reaches a well site, it turns on the dynamic positioning (DP) (see section 2.4) for station keeping. The vessel will remain in DP state until the completion of wire-line operation.

Skidding Process of preparing modules for deployment. The operation is performed topside using the module handling rails and pushed into the moonpool by hydraulically powered equipment.

Module deployment : The process of deploying the well control equipment through the moonpool until it is safely positioned on the well. The deployment speed and the water depth determines the time taken to complete the operation. Normally can be performed within 30 minutes for a specific component.

Wire-line operations : Well intervention operations using a slick line or a braided wire. The operation duration depends on the total number of wire line runs and the complexity of the job. If we assume a drift run, a run for setting of isolation plug and two runs for perforation, the average time taken will be approximately 124 hours as shown in Table 2.2.

Topside operations Such operations are always carried out to follow procedures and safe preparation of equipments. Such activities, including the skidding, deployment and retrieval of equipment will take an average of 80 hours per a given intervention.

2.1.4 RLWI Challenges

Although the technology is quick and cost effective, RLWI is currently highly inefficient. Based on the current RLWI vessels statistics, the vessels are at an average of 25% down time over the last 4 years. This is unsatisfactory because it results in fewer interventions

Table 2.2: Average time spent on operation [14]

| Operation (2 off) | Average time (hrs) |
|------------------------------|-----------------------|
| Mobilizing/Sea Fastening | 84 |
| Transiting / Station keeping | 20 |
| Deployment/retrival/skidding | 93,5 |
| Well Intervention runs | 124 |
| Total | 321 |

| Vessel Name | Island Wellserver | Island Frontier |
|-----------------------------------|-------------------|-----------------|
| Average operational days | 349d | 349d |
| Waiting on weather (wow) | 22,4% | 28,6% |
| No. of expected operations (2015) | 16 | 14 |

Table 2.3: A 4 year statistics on current RLWI vessels on Norwegian Continental Shelf [2]

per year, delay of potential oil recovery and subsequently damaging the company's yearly revenue.

The grounds for downtime are mainly associated with operational weather criteria on board. Transiting to key side and waiting on weather (wow) for these operations takes more than three quarters of the total downtime. The main reasons for waiting on weather are;

1. Operational weather limits on vessels are too low compared to apparent sea states on site.
2. Low confidence on operational weather limit
3. Low confidence on on-site weather measurement method

Table 2.4 shows the operability criteria (OP_{WF}) present on Island Wellserver. It can be seen that module deployment is a critical operation based on operability criteria.

Table 2.4: Operability wave (OP_{WF}) criteria present on Island Wellserver [11]

| Design modes | Maximum Displacement (Single Amplitudes) | | | | |
|---|--|----------|-----------|-----------|----------|
| | Heave (m) | Roll (m) | Pitch (m) | Surge (m) | Sway (m) |
| Well Intervention Operations $H_s = 6.0m / T_p = 12.4sec$ | 4.2 | 4.6 | 7.9 | 3.4 | 1.8 |
| Module deployment $H_s = 4.0m / T_p = 10.1sec$ | 2.1 | 2.9 | 5.7 | 1.6 | 0.9 |
| Horizontal Skidding of module $H_s = 4.0m / T_p = 10.1sec$ | 2.1 | 2.9 | 5.7 | 1.6 | 0.9 |

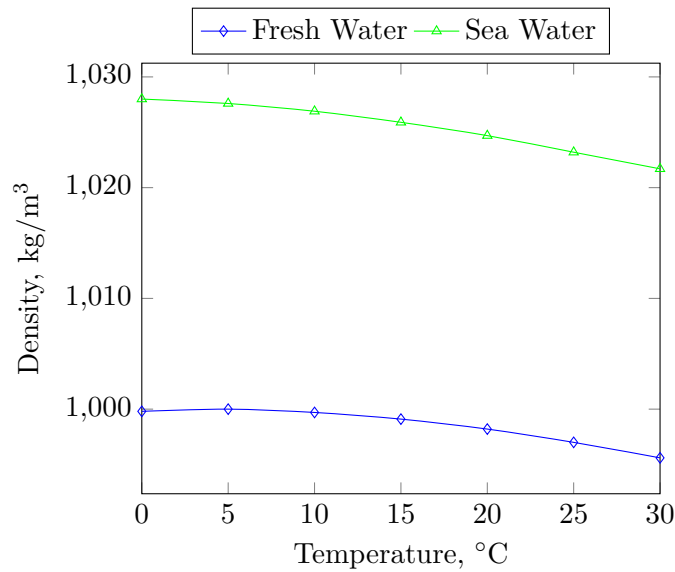


Figure 2.3: Variation of density with temperature

2.2 Weather and Marine Environment

In section 2.1, the type of operations in RLWI is discussed and it is pointed out that the main challenges of the operations came from waiting on weather. In this context, *weather* is mainly specified to wind, storm, temperature, and tidal conditions. Changes in magnitude, direction and duration of these parameters is simply a weather change. The effect weather change at a given location on a marine environment can be felt locally as well as remotely. This section describes the environment at which marine operations are performed and how this environment can be affected by weather. The effect of such environment on a marine operation is discussed in section 2.3.

2.2.1 Density

When an operation is to be carried in sea, the environment obviously changes significantly compared from on-land operations. One of the changes is the variation of density from air to water. The density (ρ) of water at 4 °C is 1025 kg/m³, about a thousand times the density of air. The density of sea water is only slightly affected by changes in weather as shown in figure 2.3. However, significant temperature decrease could result in ice formation, and hence, may have bigger implications on marine operations.

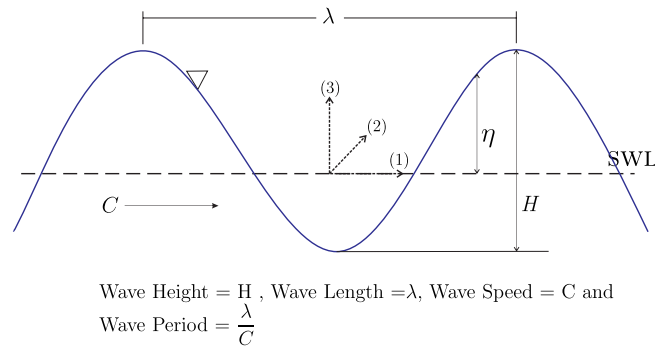


Figure 2.4: Wave Parameters

2.2.2 Ocean Current

A second distinction that is present in marine environment is an *ocean current*. This phenomenon results mainly from temperature variation in the sea, tides, and wind (surface current). The effect of such changes is a movement of the sea from one part of the ocean to another. Current magnitude vary from one time to another and highly notable changes to current magnitude happen during seasonal changes due to temperature effects. Wind and tidal rages bring daily variation of current magnitude. Ocean current is usually described by 1-year, 10-year and 100-year statistical values.

2.2.3 Ocean Waves

A third and most notable change of environment from land to sea is the presence of *ocean waves* in the marine environment. A *wave* is energy carried by and propagates through a medium (sea water in this case) and causes the medium to move in sinusoidal motion until the energy dissipates and it dies out. The medium also continues the sinusoidal motion until it gets damped and dies out. A wave is characterized by its wave period (T) and wave height (H)(see figure 2.4).

Ocean waves are a number of waves continuously formed due to energy dissipated from a windstorm to the sea. As waves travel through the sea, they cause the seawater to move in a sinusoidal motion. The higher the magnitude and duration of the windstorm, the more energy is transferred to the sea, and the stronger the waves, i.e. higher wave heights. In addition, the location and fetch area of the storm decides how frequently waves are being generated. Therefore, waves are highly affected by the weather conditions (*Storm*) of the surrounding environment.

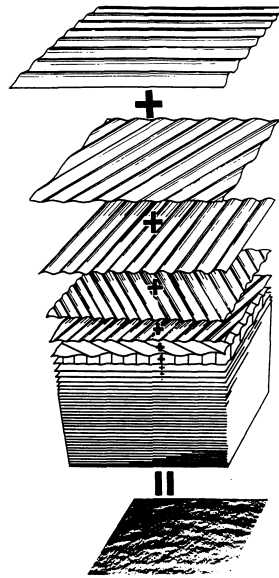


Figure 2.5: Superposition of regular waves to make irregular sea [15]

Regular and Irregular Waves

It is important to understand the behavior of ocean waves as they contain energy which could be utilized, but also, could affect marine operations. When a group of waves traveling one after another are carrying same amount of energy resulting in constant wave heights (H) and wave periods (T) in the medium, they are called *regular waves*. Regular waves are the simplest description of wave groups. However, in reality, waves are rarely formed in this fashion. The natural ocean waves are disturbed and irregular. Such types of waves are termed *irregular waves*, and are assumed to be a superposition of various regular waves having different wave heights and periods and directions (see figure 2.5).

Short term wave spectrum

Natural ocean waves have a never ending sea-state of 'irregular waves'. For a specified period of time, one may need a careful representation of such sea-states. For practical purposes, a sea-state is assumed to be stable for a short term of 3-hours. During these hours, there will be a number of waves with different wave heights and periods. The distribution such irregular waves is also an important parameter. A wave spectrum is then used to define the sea-state energy distribution with respect to wave frequency or wave period, $S(\omega)$ or $S(T)$, for the short-term of 3-hours. Example wave spectra's are shown in

equations (2.1) and (2.2), with two and four defining parameters respectively.

$$S(T) = \alpha T^3 e^{\beta T^4} \quad (2.1)$$

$$S(\omega) = \alpha \omega^{-l} e^{\beta \omega^n} \quad (2.2)$$

A sea state defined by a specific wave spectra is represented by parameters such as *significant wave height* (H_s), *peak wave period* (T_p), and other parameters depending on the type of spectrum (see descriptions below). The significant wave height is an estimate of the average of the highest third wave heights. The peak period (T_p) is the period at which the spectral energy expressed in terms of time (S_T), is at its maximum. Alternatively, *zero up-crossing period* (T_z) is sometimes used, which is the ratio of total time to the number of zero up crossings in a wave record [16]. The relationship between T_p and T_z depends on the type of spectrum.

Pierson Moskowitz

In 1964, the Pierson Moskowitz spectrum, named after its founders W.J.Pierson and L.Moskowitz, was suggested as a representative spectrum for a fully developed sea in deep water conditions. A fully developed sea in this context is a sea-state in which the energy dissipated into the sea from the local wind is in equilibrium with the energy lost. Thereby the spectrum describes the sea state in terms of the wind energy variable, the wind velocity. It is important to note that a fully arisen sea is expected when the fetch length is long enough, usually covering several kilometers.

Usually refereed as the PM Spectrum, the following expression has been seen to have good agreement with test data [17].

$$S(f) = \frac{\alpha g^2}{(2\pi)^4} \cdot f^{-5} \exp \left(-0.74 \left(\frac{f_0}{f} \right)^4 \right) \quad (2.3)$$

$$\begin{aligned} \alpha &= 0.0081 \\ \text{Where, } f_0 &= g(2\pi U_{19.5})^{-1} \\ U_{19.5} &= \text{Velocity at 19.5 m above still water level} \\ g &= \text{Gravitational acceleration} \end{aligned}$$

This formulation has been transferred to the usual H_s , T_p parameters and is given as equation (2.4). $f_p = \frac{1}{T_p}$.

$$S(f) = \frac{5}{16} \cdot H_s^2 f_p^4 f^{-5} \exp \left(-\frac{5}{4} \left(\frac{f_p}{f} \right)^4 \right) \quad (2.4)$$

JONSWAP

Generally called the JONSWAP spectrum, the Joint North Sea Wave Project was initiated by a partnership between USA, UK, Germany and Holland. The main goal of the project was to formulate a representative spectrum for small fetched sea and also to understand the transformation of waves from deep sea to shallow waters. The project started in 1967 and collected data for an area covering 160 km from island of Sylt to Bright. After analysis of a large number of data, the following JONSWAP formulation was put forward [17].

$$S(f) = \frac{\alpha g^2}{(2\pi)^4} f^{-5} \exp\left(\frac{-5}{4} \left(\frac{f}{f_m}\right)^{-4}\right) \cdot \gamma \exp\left(\frac{1}{-2\sigma^2} \left(\frac{f}{f_m} - 1\right)^2\right)$$

$$\alpha = 0.076 x^{-0.22}$$

$$x = gFU_{10}^{-2}$$

$$f_m = 3.5gx^{-0.33}/U_{10}$$

Where, $\sigma = 0.07 \quad f \leq f_p$

$$\sigma = 0.09 \quad f > f_p$$

$$\gamma : \text{Peak enhancement factor}$$

$$U_{10} : \text{Wind speed at 10 m above the still water level}$$

Transferring to usual parameters, H_s and T_p and using γ gives equation (2.5)

$$S(f) = \alpha H_s^2 f_p^4 f^{-5} \gamma^\beta \exp\left(\frac{-5}{4} \left(\frac{f_p}{f}\right)^4\right) \quad (2.5)$$

$$\alpha \approx \frac{0.064}{0.230 + 0.0336\gamma^{-\left(\frac{0.185}{1.9+\gamma}\right)}}$$

$$\beta = \exp\left(-\frac{(f - f_p)^2}{2\sigma^2 f_p^2}\right)$$

Torsethaugen Two-Peak Spectrum

Sometimes the sea could be a mixture of wind developed sea and a swell wave generated remotely. It may be necessary to find a spectrum that accounts for both waves types. In 1994, Torsethaugen and in 2004, Torsethaugen and Haver developed a two peak spectrum from data collected in the Haltenbanken and Statfjord Area, in the Norwegian Sea. They put forward a spectra defined by five parameters, H_s , T_p , γ , N , and M . In order to distinguish a sea state to be either swell dominated or wind sea dominated, equation (2.6) is used [18].

$$T_f = a_f H_s^{\frac{1}{3}} \quad (2.6)$$

| | |
|-------------|-------------------------|
| $T_p > T_f$ | swell dominated |
| $T_p < T_f$ | Wind Dominated |
| $a_f = 6.6$ | for 370 km fetch length |
| $a_f = 5.3$ | for 100 km fetch length |

The general form of the Torsethaugen spectrum is given by equation (2.7).

$$S(f) = G_0 \cdot A_{\gamma_j} \cdot \Gamma_{s_j} \cdot \gamma_{F_j} \quad (2.7)$$

This general form can be simplified by employing the parameters $N = 4$ and $M = 4$. These assumptions will lead to the following equations.

$$\begin{aligned} G_0 &= 3.26 \\ a_f &= 6.6 \\ A_{\gamma_1} &= \left(1 + 1.1 [\ln(\gamma)]^{1.19}\right) / \gamma \\ A_{\gamma_2} &= 1 \\ \Gamma_{s_j} &= f_{nj}^{-4} \exp[-f_{nj}]^{-4} \text{ for } j = 1, 2 \\ \gamma_{F_1} &= \gamma \left[\frac{1}{2\sigma^2} (f_{n1} - 1)^2 \right] \\ \gamma_{F_2} &= 1 \end{aligned}$$

The given simplified form is taken directly from the document DNV-RP-C205, Appendix A. The reader can consult the document for full detail on primary and secondary peak parameters.

Long term wave statistics

We often refer to the long term statistics of a sea-state at a given location when we decide to understand the long term situation at the location. Referring to data collected at the location for several years, say 20 years one will be able to construct probability distributions to determine the required values such as the 1-yr and 10-yr significant wave height. These values are essential in design of structures with long design life. Several representative distributions for the data exist in literature, but Gumbel's and Weibull's distributions are found to fit better than others [19].

Gumbel Distribution

The Gumbel distribution has the form

$$F = P(X < x) = e^{-\frac{x-B}{A}} \quad (2.8)$$

The two parameters of the Gumbel distribution are determined by rearranging equation (2.8) into a linear form and fitting it into a linear trend line.

$$x = A(-\ln(-\ln(F))) + B$$

Weibull Distribution

Weibull's distribution is an alternative proposed probability distribution that has well fitted to actual gathered data. The two-parameter Weibull distribution is as shown in equation (2.9).

$$F = P(X < x) = 1 - e^{-\frac{(x-B)^k}{A}} \quad (2.9)$$

Similarly, it is rearranged into a linear form,

$$x = A(-\ln(1 - F))^{\frac{1}{k}} + B$$

The value of k , also known as the shape parameter, is pre-defined. The value is an estimate and many trials can be performed before determining the most suitable value. Experienced engineers should be able to determine this parameter with less challenge.

Effect of weather on ocean waves

weather affects the marine environment in terms of waves, currents and density variations. Figure 2.6 shows a representation local wind speed effects on the significant wave heights (Beaufort scale). The effect of local storm is short, steep crested waves known as *wind sea*. They are characterized by high energy, concentrated, sharp spectrum, and higher ratio of H_s to T_p .

When the storm is generated at a location far from the location of the sea, it is called *swell*, characterized by lower peak energy and low ratio of significant wave height to peak period having a more flat wave spectrum.

In the long term, there are seasonal variances in the waves. On average, summer season has lower significant wave heights than in the winter. In addition to tidal waves change the mean sea level at different times of the day.

2.3 Environmental Forces

When operations are performed on a marine environment, presence of waves, current, and sea water density apply forces on a body within the vicinity of the environment. We call

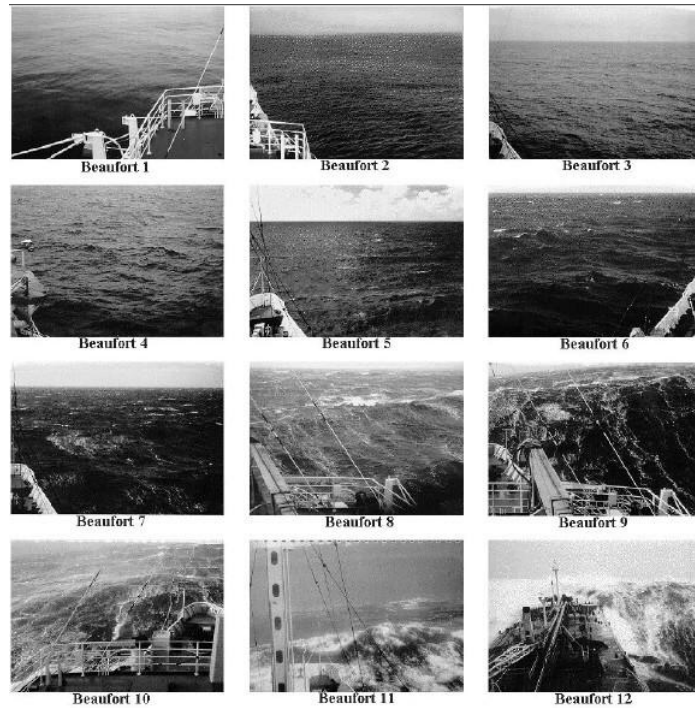


Figure 2.6: Weather effect on waves (Beaufort scale)

these, environmental forces. It is important to understand the nature and quantify the magnitude of these forces in order to perform an operation on a safe manner. In this section we look at how the marine environment can have an impact on a marine operation.

2.3.1 Buoyancy Force

Hydrostatic pressure is a result of density. This pressure acts in all directions and is dependent of the depth at which the body is within the fluid (sea water) environment. For a solid body, the hydrostatic pressure at the top of the body is less than at the bottom of the body, hence a net upward force is applied to a solid body of a specific volume. This net upward force is known as *buoyancy force* and is calculated by;

$$\mathbf{F}_{B_i} = \rho g \nabla V \quad F_B = 0 \text{ N for } j = 1, 2 \quad (2.10)$$

where ∇V is the submerged volume at any given time.

2.3.2 Current Forces

The mechanics of currents is that they can be safely considered to travel with a steady velocity for long time. They depend on depth due to the boundary layer effect. This

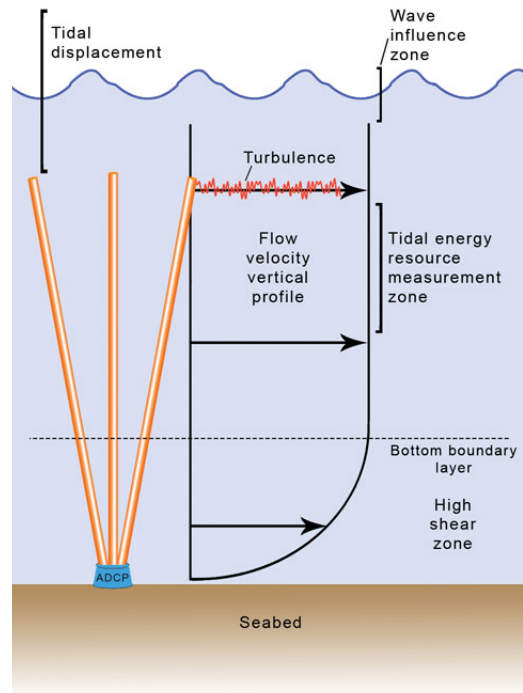


Figure 2.7: Current Force profile with depth

velocity is a result of tide, temperature circulation, and surface wind.

$$V_c(z) = V_{circ}(z) + V_{wind}(z) + V_{tides}(z) \quad (2.11)$$

The current velocity profile as a function of depth, typically and the effect on structures. Current is affected by the tidal ranges.

The presence of this steady velocity applies a *static* drag force in the direction of flow, normal to the axis of the body. Equation (2.12) is the normal drag force applied to a fixed or steadily moving slender structure. This equation is modified for a small 3D object by replacing the *diameter* D with the *projected surface area* S of the object normal to the flow as shown in equation (2.13).

$$f_{c_i} = \frac{1}{2} \rho C_{D_{S_i}} D |v_{c_i}| v_{c_i} \quad (2.12)$$

$$f_{c_i} = \frac{1}{2} \rho C_{D_{S_i}} S |v_{c_i}| v_{c_i} \quad (2.13)$$

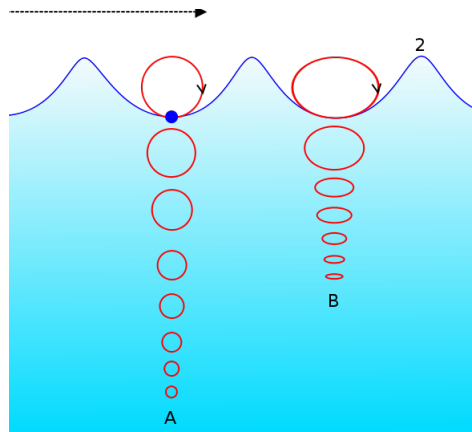


Figure 2.8: motion of water particles in ocean waves

2.3.3 Wave Forces

Determining total force on a body due to waves and the dynamic response is a complex scenario. Several theories are proposed to understand the interaction between waves and solid bodies in a marine environment. To compute the forces, first we need to understand the mechanics behind ocean waves.

Wave Mechanics

A wave behaves in sinusoidal motion as shown in figure 2.8. It makes an oscillatory motion and therefore has time and location dependent velocity and acceleration. Several theories exist that determine these vectors in terms of depth, time and location in question. Some theories are more accurate than others, while some are simple to use for hand calculations and others are made for machine computing. All of them have made assumptions of some sort. The regular wave theories are listed here based on their simplicity. Figure 2.9 shows a summary of the wave theories and their applicability ranges.

1. Linear airy wave theory
2. Cnoidal theory
3. Solitary wave theory
4. Stream Function Wave Theory
5. Stoke's Higher order wave theory

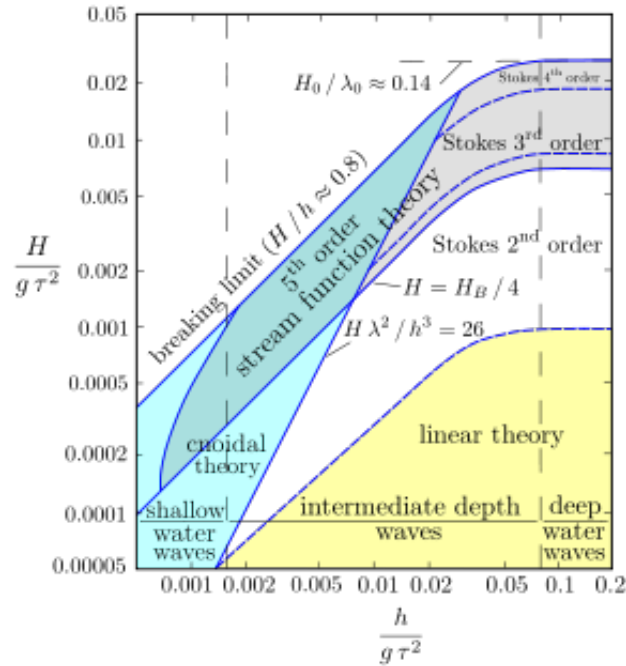


Figure 2.9: Wave theories and their range of applicability [20]

Inertia and Drag Force

A fixed body in oscillated flow will experience forces in the form of inertia force that results from the acceleration of the flow and drag force due to the relative velocity of the oscillating wave. These forces can be estimated by using the Morison's equation (2.14). Equation (2.15) is a modification of the Morison's equation for small 3D bodies as it was done for current forces in section 2.3.2.

$$f_{w_i} = \rho (\delta_{ij} + C_{A_{ij}}) A \dot{v}_{w_j} + \frac{1}{2} \rho C_{D_i} D |v_{w_j}| v_{w_j} \quad (2.14)$$

$$f_{w_i} = \rho (\delta_{ij} + C_{A_{ij}}) V \dot{v}_{w_j} + \frac{1}{2} \rho C_{D_i} D |v_{w_j}| v_{w_j} \quad (2.15)$$

These forces are determined by estimating the hydrodynamic coefficients, 1) $C_{A_{ij}}$ added mass coefficients and 2) C_D Drag force coefficient for oscillatory motion, estimated to be 2-3 times steady drag coefficient C_{D_S} [21].

Inertia and Damping

Damping is mainly a result of the viscosity opposing the motion of an object. For a submerged moving body in still fluid, the force acted by the fluid on the body is given by equation (2.16). Similar adjustment is made for a moving 3D body. \dot{r} and \ddot{r} are relative velocity and acceleration of the body respectively relative to the water.

$$f_{d_i} = -\rho C_{A_{ij}} A \ddot{r}_j + \frac{1}{2} \rho C_{d_i} A_p |\dot{r}_j| \dot{r}_i \quad (2.16)$$

Where C_{dd} the damping coefficient similarly used in equation (2.14). Equation (2.16) can equally be replaced by equation (2.17) if we take account of linear and quadratic damping coefficients B_1 and B_2 .

$$f_{d_i} = -\rho C_{A_{ij}} A \ddot{r}_j + B_{1_i} \dot{r}_i + B_{2_i} |\dot{r}_i| \dot{r}_i \quad (2.17)$$

For a moving small 3D object in still water;

$$f_{d_i} = -\rho C_{A_{ij}} V \ddot{r}_i + \frac{1}{2} \rho C_{d_i} S |\dot{r}_i| \dot{r}_i \quad (2.18)$$

or;

$$f_{d_i} = -\rho C_{A_{ij}} V \ddot{r}_i + B_{1_i} \dot{r}_i + B_{2_i} |\dot{r}_i| \dot{r}_i \quad (2.19)$$

For small values of KC, the total force of a moving body in oscillator motion can be approximated by using the relative velocity formulation ($U_{R_j} = \dot{v} - \dot{r}_j$).

Then

$$f_{I+dd_i} = \rho (\delta_{ij} + C_{A_{ij}}) A \dot{U}_{R_j} + B_{1_j} \dot{U}_{R_j} + B_{2_j} |\dot{v}_j| \dot{U}_{R_j} \quad (2.20)$$

or

$$f_{I+dd_i} = \rho (\delta_{ij} + C_{A_{ij}}) A \dot{U}_{R_j} + \frac{1}{2} \rho C_{dd_j} A_p |\dot{v}_j| \dot{U}_{R_j} \quad (2.21)$$

Slamming

For a body in the process of being submerged, there happens to be an additional slamming force in addition to the drag and inertia. In still waters this slamming is determined by [22];

$$\begin{aligned} \frac{d}{dt} (a \dot{r}_i) &= a \ddot{r}_i + \frac{da}{dt} \dot{r}_i^2 \\ &= f_{I_i} + f_{S_i} \end{aligned}$$

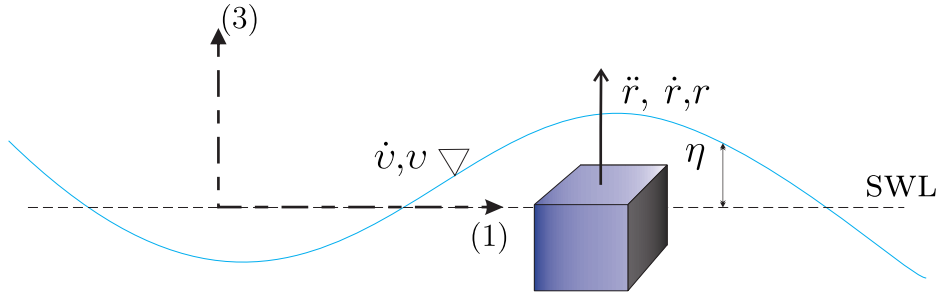


Figure 2.10: Submerged 3D body within slamming region

Using the slam coefficient C_s , we can write the slamming force on a still water environment as;

$$\begin{aligned} f_{s_i} &= \frac{da}{dt} \dot{r}_i^2 \\ &= \frac{1}{2} \rho A C_{s_{ij}} \dot{r}_i^2 \\ C_{s_{ij}} &= \frac{2}{\rho A} \frac{da}{dt} \end{aligned}$$

When a body is being submerged in a wave environment where η is the amplitude of the wave as a function of time, we have the slamming force as

$$f_{s_i} = \frac{1}{2} \rho A C_{s_{ij}} (\dot{\eta} - \dot{r}_3) (v_j - \dot{r}_j) \quad (2.22)$$

where $i = 1$ is x-direction, $i = 2$ is y-direction and $i = 3$ is the z-direction.

the total force on a moving object then is given by adding all these forces together.

$$\begin{aligned} f_i &= F_{B_{i=3}} + f_{I_i} + f_{D_i} + f_{S_i} \\ f_i &= (\rho g \nabla V)_{i=3} \\ &\quad + \rho (\delta_{ij} + C_{A_{ij}}) A \dot{U}_{R_j} \\ &\quad + \frac{1}{2} \rho C_{dd_j} D |v_i| U_{R_j} \\ &\quad + \frac{1}{2} \rho A C_{s_j} (\dot{\eta} - \dot{r}_3) (U_{R_j}) \end{aligned} \quad (2.23)$$

2.3.4 Hydrodynamic Coefficients

The hydrodynamic coefficients are an essential part of environmental force estimations. They are represented by a 6x6 matrix as shown in equation(2.24). The coefficients are

symmetric and hence $C_{ij} = C_{ji}$. This implies the total number of coefficients for any body type is 21 as shown in equation (2.24). When a body has symmetric configuration, the cross-coupling coefficients ($C_{i \neq j}$), are zero. When there is no symmetry, they are not.

$$\mathbf{C}_{ij} = \begin{pmatrix} C_{11} & C_{12} & C_{13} & C_{14} & C_{15} & C_{16} \\ C_{12} & C_{22} & C_{23} & C_{24} & C_{25} & C_{26} \\ C_{13} & C_{23} & C_{33} & C_{34} & C_{35} & C_{36} \\ C_{14} & C_{24} & C_{34} & C_{44} & C_{45} & C_{46} \\ C_{15} & C_{25} & C_{35} & C_{45} & C_{55} & C_{56} \\ C_{16} & C_{26} & C_{36} & C_{46} & C_{56} & C_{66} \end{pmatrix} \quad (2.24)$$

There has not been a specific theoretical method of determining hydrodynamic coefficient matrix and most of it has been relied on empirical calculations. O.Øritsland [22] and his team performed a variety of model tests using different shapes and determined the variation of hydrodynamic coefficients with the following parameters. His team performed a large number of the model tests by varying these parameters and determined hydrodynamic coefficients as a function of these parameters and plotted them. For a body in oscillatory flow, all parameters have an effect on the the coefficients, for a body in steady flow, only Reynold's number and body shape are taken into account.

1. **Body shape and geometry:** Body shape and geometry are self explanatory. The dimensions and configurations of the shape. Circular, 3D, sphere, ..etc.
2. **Reynold's number, (Re):** Dimensionless quantity describing type of flow. Approximate regions of flow are;

$$\begin{array}{ll} Re < 2 \times 10^5 & \text{Subcritical} \\ 2 \times 10^5 < Re < 5 \times 10^5 & \text{Critical} \\ 5 \times 10^5 < Re < 3 \times 10^6 & \text{Supercritical} \\ 3 \times 10^6 < Re & \text{Post-Supercritical} \end{array}$$

3. **Keulegan–Carpenter number, (KC):** This is a measure of the ellipse of wave oscillations. $KC = U_o \frac{T}{D}$. If $KC > 30$, then the wave has more of a flat elliptic shape, and if it near the value of 1, then it implies circular wave motion.
4. **Frequency parameter, $\left(\beta = \frac{Re}{KC}\right)$:** The ratio of Reynold's number to Keulegan-Carpenter number has also shown to be a defining parameter.
5. **Surface roughness, $\left(\frac{k}{D}\right)$:** Self explanatory.

It is possible to refer to those plots to determine some hydrodynamic coefficients if other alternatives such as model tests are not available (cf. section 3.4).

Alternatively DNV [21] has formulated some constant values of hydrodynamic coefficients for objects with various shapes by maintaining the rest of the parameters to be at a constant realistic number. Further, DNV recommended these constant values should be calibrated accordingly when the object is in close proximity to walls and water-surface and perforated by a certain amount. These modifications are necessary because of high variation in KC and Re values to the ones initially assumed by DNV. However, if higher accuracy of estimation is desired, model tests are recommended.

In conclusion, the environment applies forces on any structure with in it. Different geometry of structures in different environment will experience different magnitude of forces. It is therefore important to carefully and accurately estimate these forces and design a module handling system capable of supporting against them.

2.4 Module Deployment: System and Procedure

For an operation to be carried out safely and successfully, a verified system and procedure should be established that could cope with the dynamic environmental forces discussed earlier. In this section, we describe the system and procedure that is presently in place on riser-less light well intervention units. Specific focus is made to module deployment operation. Figure 2.11 shows the structure on board one of the latest RLWI units.

A number of suppliers of module handling systems exist in the market, such as Deep Ocean, IHC Offshore Systems, ROXAR, MACGREGOR and AXTech. A typical module deployment operation comprises of the following systems.

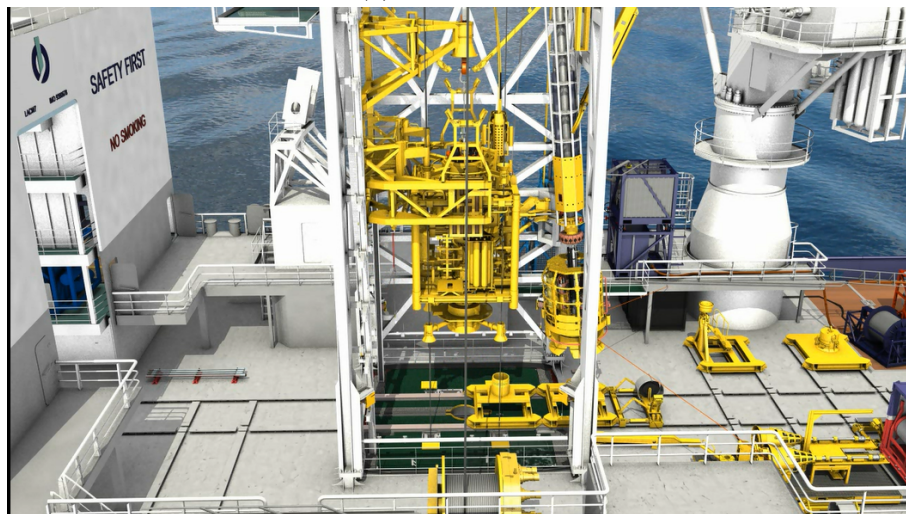
1. Vessel
2. Tower and Cursor system
3. Moonpool system
4. Guide wire system
5. Lifting Wire
6. Cursor system

2.4.1 Vessel Station Keeping

A vessel is used as a mobile platform for the deployment operation. Several factors such as transit speed, stability, safety, etc.... of vessel particulars are important. For a module deployment operation in particular, station keeping ability is highly relevant. The vessel has



(a) General layout



(b) Module in moonpool area

Figure 2.11: Module handling system on-board Island Constructor (Source: Island Offshore)

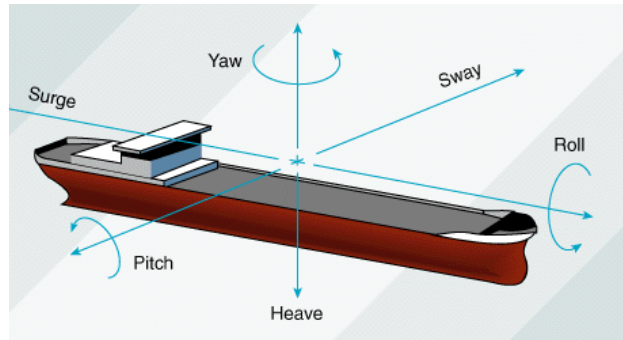


Figure 2.12: six degree of freedom vessel motions

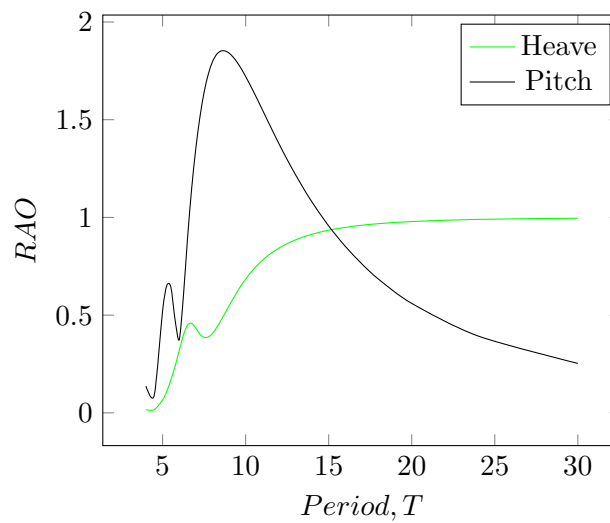


Figure 2.13: Example RAO

a six degree of freedom motion, i.e it can have translational and rotational displacements. The denotation for the vessel motions are as shown in the figure 2.12.

Station keeping ability is measured in motion transfer functions, also known as response amplitude operator (RAO). The RAO is a transfer function for every degree of freedom in terms of a ratio of the wave amplitude.

$$X_i(t) = RAO \cdot \eta_i(t) \quad (2.25)$$

where $\eta_i(t)$ is wave amplitude in the i – direction and $X_i(t)$ is vessel response in i – direction.

Available technology developed for station keeping such as mooring and dynamic positioning. For a supply vessel, the most common system is the dynamic positioning (DP). Dynamic positioning is a form of station keeping by use of thrusters automatically controlled in the

DP control room. The DP control room will get position reference information from various types of systems such as GPS satellite Systems or Augmentation Systems or Taut-Wire arrangement. In this thesis, we will not go into detail on how each system functions. The reader is advised to refer to several literature for detail information [23]. The DP system on-board is however classified by several classifying organizations such as DNV and IMO. DNV classifications have been more up-to-date and as of 2014, new DPS and DNYPOS-ER series have been added making the total number of DP class types to 9 [24].

2.4.2 Moonpool

A moonpool is an opening in the central area of the hull. The main purpose of having a moonpool is to block the effects of the wave forces by using the hull during drilling, installation, diving and other operations. Since the water motion is protected on all sides, lateral environmental forces could be completely avoided. Hence current and surge and sway forces are assumed to be no existent.

However, there is one down side to all the positive effects of the moonpool. The main flaw of a moonpool is the presence *heave resonance effect*. This is a phenomenon that occurs when the ship is in transit or during wave conditions. The resulting heave oscillations in the moonpool could be as high as three to four times the wave height. They result in unworkable conditions in DP state and resistance to transit speed.

Several designs of moonpool configurations have been attempted to dampen the moonpool resonance. Because of the complexity of the moonpool hydrodynamics, there is not a single fits-all type of solution. There are two main types of solutions which are being practiced in the market: bottom covers that prevent water flow into the moonpool at all, and moonpool side wall designs that allow water into moonpool but dampen oscillations.

The first category is seen to be well effective when it is designed to suit well with the hull design. Results show a completely dampened moonpool sea state. However, they are ineffective during high speed transits and also have their own drag. Therefore, they can only be used in certain vessels with low transit speeds [25].

The second design configuration uses devices such as perforated walls and overflow chambers to break the resonance with the sea state. Since they take space in the moonpool walls and reduce the moonpool opening size, they sometimes pose a practical challenge to the owner. They have been shown to be effective upon adequate construction. According to DNV a cofferdam moonpool design has a shown the best damping effect so far. in the well intervention vessels, a cofferdam type of moonpool was used, ref figure 2.14. Typical moonpool dimensions range from $7.2 \times 7.2 \text{ m}^2$ to $8.2 \times 8.2 \text{ m}^2$.

Table 2.5: Dynamic positioning classes [24]

| Notation Heirarcy | IMO Notation | DNV Notation | Description |
|--|-------------------|--------------------------|---|
| Notations not requiring redundancy | Not applicable | DPS 0 | Dynamic positioning system without redundancy. |
| | | DYNPOS- AUTS | Dynamic positioning system without redundancy. Additional requirements to achieve higher availability and robustness as compared to DPS 0 will apply. |
| | DP1 | DPS 1 | Dynamic positioning system with an independent joystick system back-up and a position reference back-up. |
| | | DYNPOS- AUT | Dynamic positioning system with an independent joystick system back-up and a position reference back-up. Additional requirements to achieve higher availability and robustness as compared to DPS 1 will apply. |
| Notations requiring redundancy | DP2 | DPS 2 | Dynamic positioning system with redundancy in technical design and with an independent joystick system back-up. |
| | | DYNPOS- AUTR | Dynamic positioning system with redundancy in technical design and with an independent joystick system back-up. Additional requirements to achieve higher availability and robustness as compared to DPS 2 will apply. |
| Notations requiring redundancy and separationof systems | DP3 | DPS 3 | Dynamic positioning system with redundancy in technical design and with an independent joystick system back-up. Plus a back-up dynamic positioning control system in an back-up dynamic positioning control centre, designed with physical separation for components that provide redundancy. |
| | | DYNPOS- AUTRO | Dynamic positioning system with redundancy in technical design and with an independent joystick system back-up. Plus a back-up dynamic positioning controlsystem in an back-up dynamic positioning control centre, designed with physical separation for components that provide redundancy. Additional requirements to achieve higher availability and robustness as compared to DPS 3 will apply. |

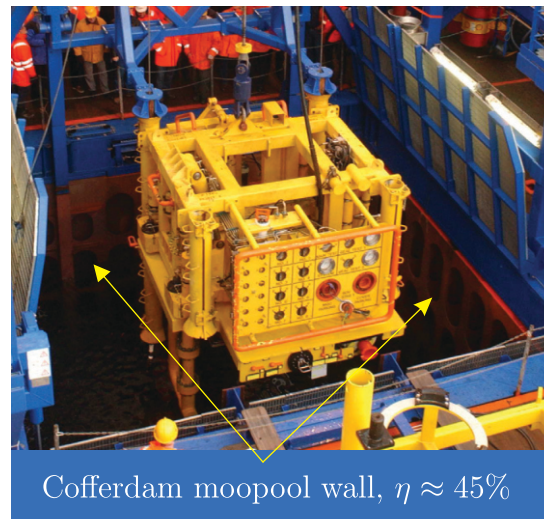


Figure 2.14: Cofferdam moonpool walls with an estimated relative damping ration of up to 45% (Picture: DeepOcean)

2.4.3 Module handling Tower

The module handling tower (MHT) is the hang-off point where the winch sheaves are located. In other terms, it is the point where the crane tip motions are calculated. The handling tower should be able to handle forces transferred to it by the module through the crane wire. The tower rigidity is an important quantity in lifting operations, although it is usually disregarded. The tower height depends on the type of lifting operation and the dimensions of the equipment to be lifted. In RLWI, the lubricator section (ULP,LT and LLP) is deployed in a single operation. The total length of the tower, should therefore be greater than the length of the Lubricator Section (23 m).

The tower is installed on top of the moonpool and therefore, its footprint should always be larger than the moonpool opening. Another important aspect of MHT is its weight. Large weight and corresponding center of gravity are always working against stability of the ship. Total weight could range from ≈ 100 to 300 t. The sheaves mounted on the MHT are hydraulically controlled and move a certain diameter to be located directly above a desired location.

The module handling tower also houses the operator cabin that is accessed from the main deck through the stairs. The operator cabin has representatives from all three companies.



Figure 2.15: Module handling tower on RLWI vessel

2.4.4 Coupling Wire

Coupling wires are an integral part of any lifting operation, on land and at sea. They are used to support loads in a given direction by using their tensile strength. However, strength is not the only criteria when selecting wire ropes. Durability, fatigue resistance, abrasion resistance, weight, diameter and other operation specific properties should be checked. The significance of one property over another depends on the type of operations they are to be used.

A coupling wire is made up of strands of wires arranged in a specific manner to obtain a desired performance. They have a 'core' wire which is surrounded by all 'outer' called stands. In this way they form a wire rope. The three main types of core used are: 1) Fiber Core ; 2) Independent Wire Rope Core and 3) Strand Core [26]. There are many configurations of strands in the market. We will not go into detail on each of them. The strands are largely responsible for the tensile strength of the wire rope. Generally, wire rope with many small diameter strands have a better fatigue resistance and strength than a wire of the same size but with larger diameter strands. However, the larger diameter strands are more abrasion resistant. It is apparent that there is no coupling wire that can do it all. Selection of the type of wire rope to be used in an application should be carefully selected. Below we describe some of the major area one should look at when choosing a wire rope.

Strength: The wire strength is usually described by the minimum breaking strength. A wire is expected to break if a load of such magnitude is applied to it in test conditions. The values found on most manuals are for newly fabricated wires. A used wire would have a lesser MBF due to wear and tear. Therefore, a wire should always have a high margin of safety from operating near the minimum breaking force. Usual design safety factors range from 3-5 according to standard regulations.

Fatigue : Fatigue resistance is the ability of the wire to resist loss of strength due to repeated bending stress. This usually happens when the wire has to pass through sheaves and drums, as is the case on RLWI operations. Larger number and smaller diameter strands perform better than large diameter, smaller number strands. Alternatively, avoiding cyclic loading by having large enough sheaves can be practiced.

Crushing Resistance : The ability of wires to resist lateral crushing loads is termed crushing resistance. When external pressure is applied during reeling of wire into the drum or when passing through sheaves, the strands on the core might crush and lose their original configuration. The resulting wire would react abnormally to loads and affects operation. IWRC ropes are more crush resistant than fiber core ropes, and large diameter strands are more crush resistant than smaller diameter stranded wire ropes [26].

Abrasion Resistance : when a wire rope has been used for sometime, the outer most strands experience metal loss from actual wearing. The resulting wire is now smaller in diameter and changed the shape of the cross-section. This will result in lower breaking strength. Abrasion resistance is a term used to describe the ability of a wire to resist metal loss. Large diameter strands perform better with respect to this criteria.

Weight : When we decide to perform deep water installations, the weight of the wire comes into question. Lighter ropes are often preferred than regular steel wire ropes. Most commonly, fiber core wire ropes are much lighter than IWRC or strand core wire ropes.

Rotation Resistance : when a wire is loaded, the strands stretch and unwind resulting in a torque. The torque will then transfer into the load causing it to rotate. In single strand wire ropes, the rotation resistance is not possible. But double strand ropes can be laid in opposite directions and could subtract the torque generated by one another.

Therefore, our choice of coupling wire should be justified. The guide wire are mainly used as a lateral guides and will be in constant exposure to abrasion. Therefore, one should find abrasion resistant wires. Moreover, they are also exposed to cyclic loading, meaning, a fatigue resistant rope is required. Weight and strength are are not primary features of

concern due to the wires being in pre-determined constant tension. The crane wire should give priority to rotation resistance and strength, while also considering fatigue. The water depth of 500 m is a concern for weight, however, most RLWI operations are carried out in depths of up to 450 m [3].

2.4.5 Winches

Winches are used for a number of purposes. They are fasted to the main deck of the vessel and the wire rope is spooled around their drum. The wire is paid out from the winches when required.

Vessels today have automated winches which can encode the movement of the ship and hence perform a desired functions. Among these winches, active heave compensated winches, passive heave compensated winches and constant tension winches are widely used in lifting operations. Recent developments on winches have allowed to perform two or more functions at the same time.

Active Heave Compensated Main Winch

The main wire rope found in current RLWI vessels is active heave compensated. The capacity of the compensator could be up to 300 t. The main principle of an active heave compensator is shown in figure 2.16. The main principle lies is that an accelerometer will sense the motion of the ship and sends a message to a computer which will interpret it. The computer then sends a signal which will control the motion of the winch wire. The specific active heave compensation system shown uses a hydraulic cylinder and an accumulator. The connection between these two balances the force from the load. The main advantage of the system is it utilizes less power. However, it has limited movement and requires additional space for installation of the equipment. Alternatively, a hydraulic motor could be used. This system has very high capacity and very little residual heave. It will require full power consumption.

Passive Heave Compensation

The umbilical winch found on a the current RLWI units is passive heave compensated [27]. The main difference between the two modes of motion control is utilization of external power. A passive heave compensator adapts to any change in load by giving or pulling away accumulated energy. Figure 2.17 illustrates the mechanism. Although it does have advantage of using no external power, it will require loads with high resistance against movement. Additionally it will result in high residual heave and in worst case scenario

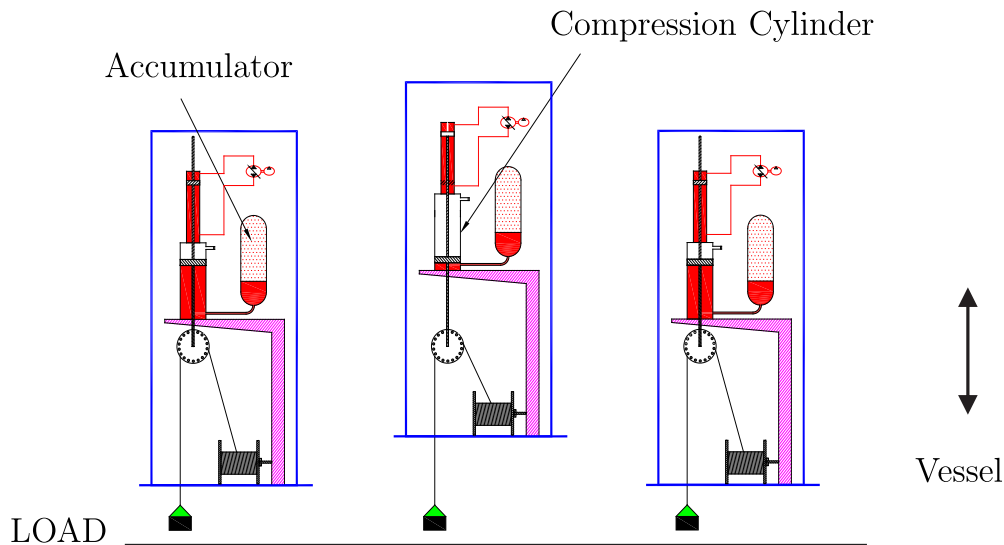


Figure 2.16: Active Heave compensation system [28]

might even exasperate the motion. Hence, Passive heave motion control should be used with caution and depending on the type of operation.

2.4.6 Constant Tensioned Lower Cursor System

When the module is in between the moonpool, it requires support from horizontal motions to prevent any form of clashing. RLWI vessels have taken a note of this types of failure and hence a dual cursor system is in place [27]. The upper cursor system is stationed above the lower cursor and it functions as a lateral support at the termination point between the main hook and the module. The lower cursor, shown in figure 2.18, is supported by a constant tensioned winch connected to the tower. Constant tensioned winches are also in place for guide wire winches. The main purpose of the LCS is to provide lateral support to the module by holding it in place. It utilizes rubber prongs that are in place in each of the four sides of the rectangular frame. It will be allowed to travel at the same speed as the module once it grips the module from the bottom of the keel to the main deck. Aside from any help from remotely operated vehicles, the LCS is equipped with lights and camera to enable visual confirmation of the module as it arrives the keel of the vessel. However, the LCS is not meant to provide vertical load support. Maximum loads on the LCS are expected to happen near the keel due to higher lateral motion of the module. In practice, the LCS is deployed a few decimeters above the keel level to avoid failure of such fashion. Guide wires are, therefore, expected to provide the necessary lateral support.

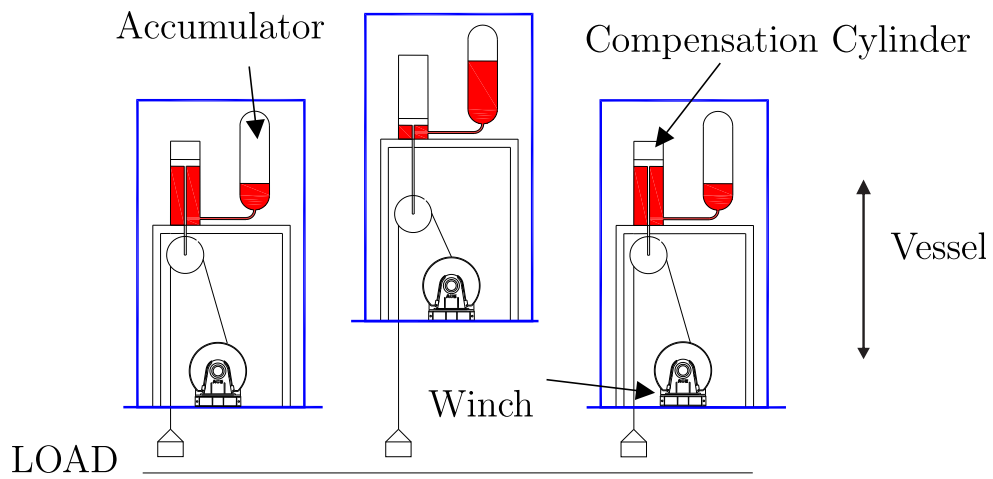


Figure 2.17: Passive heave compensation system [28]



Figure 2.18: Lower Cursor System [27]

2.4.7 Deployment Procedure

As discussed in on section 2.1.4, module deployment through the moonpool is a critical procedure limiting the operability of RLWI vessels. Understanding of the procedure for module deployment is, therefore, an important step to carry a thorough analysis. A detailed manual of procedures for installation, operation, and retrieval of RLWI stack is prepared by FMC and carried on board the vessel. An overview of these procedures is outlined below.

- Step 1:** Preparation of WCP in its sea fastened hanger position and lock its running tool (RT)
- Step 2:** Remove the sea fastening from the WCP and move into Moonpool and the WCP RT will be connected to main winch.
- Step 3:** Connect the Umbilical to the WCP
- Step 4:** Deploy Guide wires one by one through Guide funnels
- Step 5:** Deploy the WCP with constant tension on the umbilical at 50m/min. WCP is supported by a cursor system until an estimated 1 meter above the bottom moonpool end
- Step 6:** The WCP will be run in accordance with procedure until the distance between subsea tree and the Subsea tree Adapter (connected at bottom of WCP) is approximately 6m.
- Step 7:** Land WCP with active heave compensator to limit landing velocity to maximum 0.5 m/s.
- Step 8:** When landing is confirmed, disconnect WCP running tool and retrieve back to vessel.
- Step 9:** Prepare LS for deployment, connect LS running tool
- Step 10:** Deploy LS with guide wires
- Step 11:** Lock LS to WCP, immediate followed by disconnect of LS RT
- Step 12:** Perform tests and retrieve LS RT
- Step 13:** Prepare PCH in moonpool
- Step 14:** Prepare wireline
- Step 15:** Run PCH with wireline tool string
- Step 16:** PCH will now be landed onto top of LS and connector locked
- Step 17:** Retrieve PCH RT

Step 18: Sluice the wireline tool into the well

Step 19: Wireline operation is performed

Step 20: When the run is done, the tool string is parked in the tool catcher inside the PCH and is retrieved to surface using the PCH running tool

Step 21: The process is repeated, with the PCH going up to the surface using the RT, depending on how many runs the well require

Step 22: Reverse the installation process when retrieve the stack

Chapter 3

Analysis Basis

Within the scope of this thesis, a comprehensive analysis method is sought for the evaluation of module deployment operation in RLWI units. Every attempt has been made to achieve this goal. This chapter describes the details of why a specific analysis decision is made and how it is implemented into the analysis software.

3.1 Define Operation Class and Select Field

The entire analysis is dependent on a correct definition of the operation type. As stated in section 2.1.3 on page 8, the sub-operations in RLWI are relatively independent. That is to mean, except during intervention, the sub operations can be halted at a given time and brought back to safe condition in a limited time. In addition, the operations are shown to take less than 72 hours or can be halted within that time through emergency disconnect system. DNV [29], classifies such type of operations as *Weather Restricted*. Module deployment operation takes less than 40 hours to be completed, and hence is defined as a weather restricted operation. It is also classified as moonpool operation since it will involve moonpool deployment.

The location of the operation is selected to be in the Norwegian Sea. We take Åsgard field as a case study because it has a large number of subsea wells (57) and also the wells have been in operation over ten years and would probably need to have more frequent intervention works [30]. Moreover, the Åsgard field has depth ranging from 280 – 380 m. Such depth is considered *deep water condition*, $\frac{d}{L} > 0.5$, for wave periods smaller than 18.9s, which realistically, they are within this range. Deep water conditions would be very suitable for a simpler analysis to be carried out for this thesis scope. This project will assume a design water depth of 350 m in Åsgard field. More information on Åsgard field can be obtained on Appendix F.

By using this information, the DNV recommended approach for the analysis is found to be *time domain analysis in regular wave for the moonpool operations and time domain irregular wave analysis for operations outside the moonpool* [21].

3.2 Analysis Software

The choice of time domain analysis software has been an ambiguous task. Several commercial software are available, qualified to simulate module deployment operation in moonpool. Some researchers have utilized DNV developed software packages such as SIMO and MACSI for similar operations [31, 32]. The main advantage of DNV software packages seems to be robustness and operation specificness. However, they have less friendly user interfaces and also, for our case, lack the needed close software support to complete this project in due time.

Consequently, for this time domain analysis, it is opted to use Orcaflex 9.7 software package. Orcaflex 9.7a is beta tested and used by several clients for dynamic analysis of offshore marine systems. It is developed to simulate large number of technical offshore scenarios such as riser, mooring, installation, and many other systems. Developed by Orcina co. in United kingdom, the software package is readily available at the University of Stavanger in its latest version 9.7a. Further more, it has a highly user friendly interface, in addition to a quick and helpful on-line software support. The only disadvantage is it is not tailor made for splash zone analysis, but can handle the analysis to an acceptable level.

3.3 Marine Environment Modelling

For a complete analysis, several parameters of the environment need to be considered such as density, wind, current, waves, directionality, and combination effects of these parameters. Several simplifications and assumptions shall be made to make the analysis feasible within the time limit. The environmental parameters will be dependent on the type of time domain analysis and field location as described in section 3.1. Åsgard metocean design basis is used for statistical data.

3.3.1 Design Density

Density changes with temperature and salinity. According to Åsgard metocean design basis, average monthly temperatures ranges between 6 to 12 °C at sea surface and is held at 6.5 °C at seabed . This ranges only make slight difference and it is logical to ignore

temperature and salinity effects and hold it constant at 10 °C. Density of sea water at 10 °C is $\rho = 1026.9 \text{ kg/m}^3$. This value will be used for our analysis.

3.3.2 Design Current

Since, the type of operation is classified as weather restricted, a restricting maximum current velocity should be defined, and a joint criteria with wave parameters based on joint probability should be assigned. However, to set a single criteria of weather limitation (i.e wave parameters), it is opted to classify the operation as current unrestricted and design the current based on 10-year return period value, as per recommended for *weather unrestricted* operations in section D100 of DNV offshore standard for marine operations. This will allow us to find maximum restricting wave parameters when current velocity is already maximum. However, this option is considered too conservative. This is mainly because, designing a 10-year return period current value for an operation lasting less than 3 weeks is exaggerated. We refer to section C602 of the same standard which suggests alternative method for unrestricted design wave heights. As stated in table 3.1, for operation reference period T_R less than 30 days, a 1 year return period should be defined. This means, the probability of the design current magnitude will be encountered in a given year is a binomial distribution with a probability of about 0.63. This is acceptable as long as the encounter probability of the restricting wave parameters is higher. The significant wave height with such an encounter probability in Åsgard field is 6.5 m. This is quite high and the operation will most likely has a lower restricting limit, which makes our assumption to take 1 year current some what acceptable. The 1-year return period for Åsgard field is estimated after consulting the design basis (see table 3.2).

Table 3.1: Acceptable return periods for H_s

| Reference Period, T_R | Return Period, T_d |
|-----------------------------|----------------------|
| $T_R \leq 3days$ | $T_d \geq 1month$ |
| $3days < T_R \leq 7days$ | $T_d \geq 3months$ |
| $7days < T_R \leq 30days$ | $T_d \geq 1year$ |
| $30days < T_R \leq 180days$ | $T_d \geq 10years$ |
| $T_R \geq 180days$ | $T_d \geq 100years$ |

3.3.3 Design Wave Parameters

The duration of the module deployment operation dictates the type of wave environment to be modeled. Since the deployment operation lasts less than 30 minutes in the splash zone, a regular wave would have been sufficient. However, the operation involves moonpool

Table 3.2: 1 year current for Åsgard [35]

| Depth, m | Speed cm/s |
|----------|------------|
| 0 | 71 |
| 20 | 62 |
| 50 | 61 |
| 100 | 57 |
| 200 | 49 |
| 300 | 47 |
| 350 | 41 |

deployment. Hence, DNV recommends the use of regular wave analysis for a module within a moonpool (section 3.4.2 of the recommended practice for modelling and analysis of marine operations) and irregular wave analysis for a module beneath the moonpool keel as per section 3.5.6.2 of the same document.

Regular Wave Analysis

For regular wave analysis, we chose to use Airy Wave theory, with linear stretching. This is mainly driven by the need to model a *moonpool sea state* (see section 3.5.2) in Orcaflex. The software can only manage to perform such modelling using the Airy Wave theory only.

Irregular Wave Analysis

The location specific *met-ocean design basis* is necessary for determining the type of irregular wave environment to be modelled. This is obtained from Åsgard metocean criteria. Accordingly, the Torsethaugen Two-Peak wave spectrum is selected. Modelling Torsethaugen spectrum, however, not recommended in Orcaflex. This is mainly because it can not allow different directions of the *swell wave train* and *windsea wave train*. It is recommended, however, to model the irregular wave as two wave trains of JONSWAP spectrum, as recommended by Orcaflex manual. One for swell and the other for wind sea. This option does not take into consideration of the modification to JONSWAP spectrum in Torsethaugen spectrum. Therefore, we decided to model the irregular sea with both sea waves and swell in the same direction. This is usually not the case in reality and regarded as conservative. However, it is a necessary simplification to reduce number of simulations.



Figure 3.1: Complex subsea module, Well Control Package

Wave Height and Period

Once the type of wave analysis is selected, the restricting maximum wave height and associated wave period shall be analyzed. Regular waves will have a wave height equal to a maximum wave height $2 \times H_s$ according to DNV-RP-H103, section 3.4.2.8. For irregular waves, the waves shall be randomly discretized for their respective significant wave heights. Irregular wave analysis is performed over several seeds (5 in our case) and parametric values was taken as the average.

According to Åsgard metocean design basis [35], the range of wave periods with annual probability of exceedance of 10^{-2} is between 2 to 27 s. When data is not available, DNV recommends the use of T_z range obtained from equation (3.1). It also recommends to perform simulation by varying the peak period every one second. However, this could result in large number of simulations. We shall perform some regular wave simulations and narrow down this range to a practical 5 s interval.

$$8.9 \cdot \sqrt{\frac{H_s}{g}} \leq T_z \leq 13 \quad (3.1)$$

3.4 Subsea Equipment Modelling

The well control package, shown in figure 3.1 is a complex structure. The main goal is to capture the load incurred by the structure at any given time and location as accurately as possible. For this we need to know several things about the module.

- Geometry of object
- Structural mass and mass moment of inertia

- Volume
- Hydrodynamic coefficients

The first three items in the above list is found from past experience with the equipment and are tabulated in table 3.3. Estimation of accurate hydrodynamic coefficients, however, is a challenging task.

Table 3.3: General MKII module data [2]

| Parameter | Unit | Value |
|--------------------------|----------------|-------|
| Weight | t | 50 |
| Width | m | ≈ 4 |
| Length | m | ≈ 4 |
| Height | m | 6 |
| Fully submerged volume | m ³ | ≈ 38 |
| Perforation ¹ | % | 65 |

Estimating Global Hydrodynamic Coefficients

For complex structures such as the well control package, DNV recommends the use of model tests. However, this project doesn't have the privilege of performing such tests large and complex tests. Other alternative methods are sought.

There are two ways we can reasonably estimate the hydrodynamic coefficients: 1) DNV recommended simplified method, and 2) use model tests carried by O.Øritsland [22]. Both of these methods are empirically derived. To question or criticize their validity, however, is beyond the level of the thesis. Therefore, hydrodynamic coefficients shall be calculated by using either of these methods where it is believed to be applicable.

Method 1: DNV recommended simplified method ²

- Step 1) Divide the structure into sub-elements with known shapes as shown in figure 3.2.
- Step 2) Determine the global hydrodynamic coefficients based on DNV provided tables, and
- Step 3) Calibrate these values according to proximity moonpool walls, proximity to water surface, percentage of perforation, trapped water, shielding and interaction effects.

¹Approximated overall value. For individual values of module members, refer to appendix ***

² Used for added mass estimation. See appendix B for added mass coefficients on known shapes

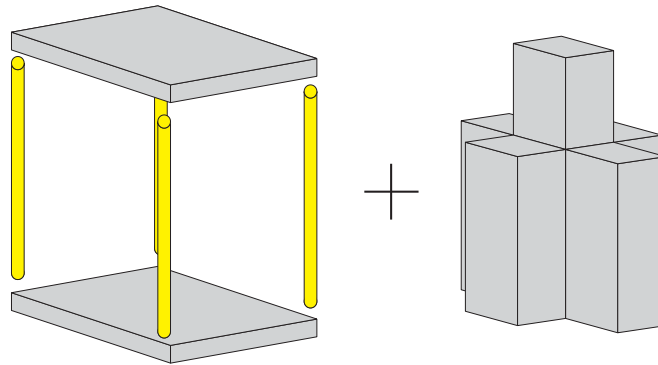


Figure 3.2: Simplified model of module for added mass calculation

Method 2: Adopt O.Øritsland Model Test Results ³

- Step 1) From a series of 3D modules where model tests have been performed, select one that has similar feature with module at hand.
- Step 2) Use the determined hydrodynamic coefficient values from previous model tests on the select module(s)
- Step 3) Calibrate these values for proximity to moonpool walls and to water surface.

Appendix B show that these methods only provides values for hydrodynamic coefficients in the three principal directions of the object (C_x , C_y and C_z). This implies the following simplification of the coefficient matrix is necessary.

$$\left| C_{ij} \right|_{6 \times 6} \Rightarrow \begin{vmatrix} C_{11} & & & & & \\ & C_{22} & & & & \\ & & C_{33} & & & \\ & & & C_{44} & & \\ & & & & C_{55} & \\ & & & & & C_{66} \end{vmatrix} \Rightarrow \begin{vmatrix} C_x & & 0 \\ & C_y & \\ 0 & & C_z \end{vmatrix}$$

Poisson effects are to be neglected. However, to compensate for the loss of values C_{44} , C_{55} and C_{66} it is important to divide each body into a many parts, similar to what is shown in the figure 3.3. This is done to better account the effect of coupling (moments) due to hydrodynamic forces.

³ Used for drag coefficient estimation. See appendix B for drag coefficients on some complex shapes

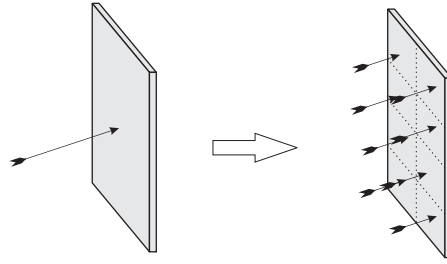


Figure 3.3: Modelling mesh on Orcaflex to account for hydrodynamic coupling coefficients

Calibrating Global Hydrodynamic Coefficients

The third step in both methods is to calibrate the global coefficients. DNV recommends using equations (3.2) and (3.3) for perforation and moonpool walls proximity. Added mass calibration for proximity to water surface is as shown in figure 3.4 [36].

- modification of added mass for perforation, DNV –RP-H103 ”Section 4.6.4”.

$$\mathbf{A}_p = \begin{cases} A_0 & p \leq 5 \\ A_0 \times \left(0.7 + 0.3 \times \cos \left[\pi \times \frac{p-5}{34}\right]\right) & 5 < p < 34 \\ A_0 \times \left(e^{\frac{10-p}{28}}\right) & 34 < p < 50 \end{cases} \quad (3.2)$$

- modification of coefficients for proximity to moonpool walls

$$\begin{aligned} \frac{C_A}{C_{A_0}} &= 1 + 1.9 \left(\frac{A_b}{A}\right)^{\frac{9}{4}} & \frac{A_b}{A} < 0.8 \\ \frac{C_D}{C_{D_0}} &= \frac{1 - 0.5 \frac{A_b}{A}}{\left(1 - \frac{A_b}{A}\right)^2} & \frac{A_b}{A} < 0.8 \end{aligned} \quad (3.3)$$

- modification for proximity to water surface, as shown in figure 3.4.

When using **method 1** above, shielding effects shall also be considered. To avoid double counting and shielding of module parts, buoys dedicated for a specific direction shall be modelled. Module parts completely shielded by another module part in a given direction will receive no hydrodynamic loading in that given direction. Interaction effects however, are extremely complicated and hence will be ignored. Again DNV recommends to use drag coefficients no less than 2.5 and no more than 8. This has been carefully looked at through out the process. The calculated results for different load cases using this method are shown in appendix C.

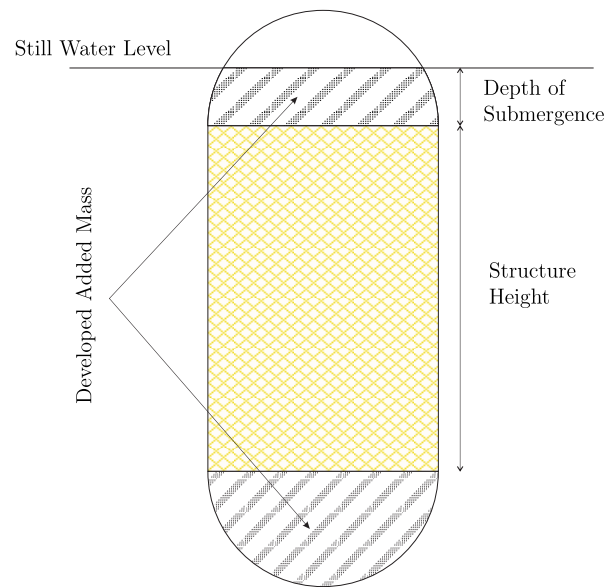


Figure 3.4: Modification for added mass proximity to water surface

3.5 Module Handling System Modelling

Any structure in the operation that has something to do with the motion of the subsea equipment is understood to be part of the handling system. Part of this system include, the vessel acting as a platform, Moonpool for shielding of translational motions, guide wires for limiting lateral movement of the module, heave compensated crane wire for vertical motion control, and the *tower and cursor system* for transferring load from module to the vessel safely at desired locations.

3.5.1 Vessel

Important parameters for modelling of the vessel have been obtained from confidential sources. These parameters include

- Vessel length
- Draught
- Structural mass
- Displacement RAO (motion transfer function)
- RAO reference point

The vessel is assumed to be unaffected by the module weight because of small weight proportions. Hence Load QTF RAO's are not used. Drift scenario is unknown.

3.5.2 Moonpool

Modelling the moonpool is challenging. Orcaflex suggest using the trapped water function, however, this does not capture moonpool sea state as per the desired accuracy. We refer to DNV-RP-H103 section 3.5, which describes a simplified sea state of the moonpool based on certain assumptions and other particular parameters. The main assumption are;

Assumption 1: The ratio of moonpool dimensions to the breadth of the ship is small.

Assumption 2: Only vertical motion of the water plug and equipment is considered

Assumption 3: Module dimensions are small enough to neglect the blocking effect of module to vertical motion of water.

Assumption 4: Cursor systems are installed to prevent lateral motion of the object

Based on these assumptions, it is shown that horizontal wave velocity in the moonpool is assumed to be zero. The vertical (heave) amplitude ratio between moonpool and wave sea state is given by equation (3.4).

$$\frac{\zeta}{\zeta_w} = \frac{\frac{G_w}{\rho g A} + 2ig\eta \frac{\omega}{\omega_0}}{1 - \frac{\omega^2}{\omega_0^2} + 2i\eta \frac{\omega}{\omega_0}} \quad (3.4)$$

where

$$G_w = \frac{F_w}{\zeta_w} = \rho A \left(ge^{-kD} - \omega^2 K \sqrt{A} \cdot RAO_s \right)$$

To implement this into Orcaflex 9.7, one can utilize the 'sea state RAO' for a given vessel at specified location. This function is only available for Airy Wave theory only. Also, this feature is not able to make horizontal velocities to be zero. To compensate this, we limit the hydrodynamic coefficients in the horizontal directions to be zero.

$$\begin{aligned} C_{A_x} &= 0 & C_{M_x} &= 0 & C_{D_x} &= 0 \\ C_{A_y} &= 0 & C_{M_y} &= 0 & C_{D_y} &= 0 \end{aligned}$$

3.5.3 Constant Tension Guide Wires

The guide wires shall all be modelled as constant tensioned. The constant tension winch in our case will be modelled as an absolute function, i.e as having near perfect performance. The guide wire properties taken from Certex.Co in figure E.1 are as shown in table 3.4.

3.5.4 Heave Compensated Crane Wire

A single crane wire attached to the vessel at 25m from deck shall be modelled. This is according to the current design of the lubricator system which is 22 m in length. The crane wire properties are shown in table 3.4. The wire properties are taken from a high performance wire manufacturer Certex Co. A snap shot of the manual for Big Hydra wire is shown in figure E.2.

Table 3.4: Wire Properties [37]

| Wire Properties | Unit | Guide wire | Crane Wire |
|-------------------------------|-----------------|------------|------------|
| External diameter | m | 0.019 | 0.0699 |
| Bending stiffness (EI) | Nm ² | 100 | 1000 |
| Axial Stiffness (EA) | N | 5.87E+07 | 2.70E+08 |
| Torsional Stiffness (GJ) | Nm ² | 2.26E+06 | 1.98E+08 |
| Unit weight in Air | kg/m | 2.226 | 20.8 |
| Tension Capacity | kN | 316 | 3599 |
| Drag Coefficient, C_D | - | 1 | 1 |
| Added Mass Coefficient, C_m | - | 1 | 1 |

3.5.5 Tower and Cursor System

The tower and lower cursor system are load bearing components which transfer the total load into the vessel. The tower is assumed to be fully capable of supporting the load, which is reasonable assumption. Modelling the cursor system, however is advantageous in understanding the impact load that it sustains. However, as far as this project was concerned, there was not enough information on the stiffness and capability of the equipment. Moreover, Orcaflex does not currently possess a feature that captures the banging type of loads a cursor system will need to bear. Hence, it is decided that, we evaluate the velocity and acceleration of the equipment within a moonpool and determine the expected impact energy transferred into the cursor system.

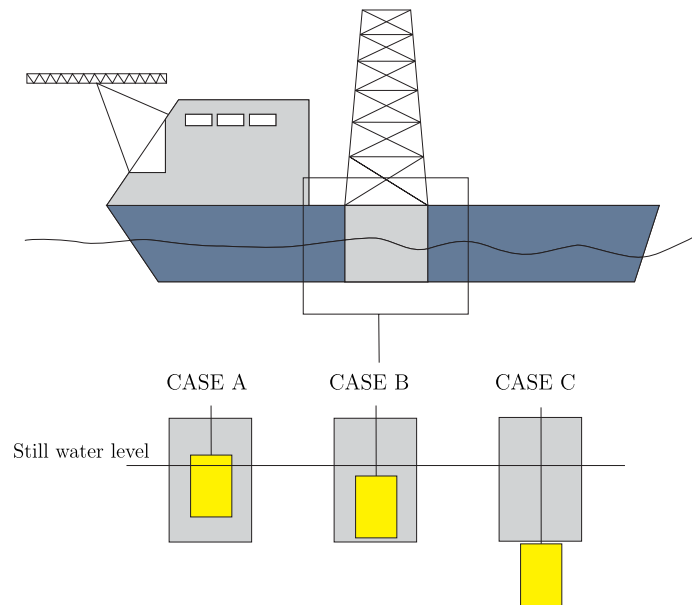


Figure 3.5: Load case definition based on module elevation

3.6 Load Case and Load Combination

Several Load cases and load combinations are to be studied. For each *load case* the module is hanged at a specified location and simulation are run for each *load combination*. The summary of the simulation is outlined.

3.6.1 Load Cases

- Case A: Module top 1m above still water surface (inside moonpool, regular wave analysis),
- Case B: Module top 1m below still water surface (inside moonpool, regular wave analysis) and
- Case C: Module top in-line with vessel keel (below moonpool, irregular wave analysis)

3.6.2 Load Combinations

- 2 wave headings (180 ° and 150 °)
- 5 wave periods (6s-10s)
- 5 seeds (for irregular wave analysis only)

- Selected significant wave heights (from 1 m-4 m \approx 3).

3.6.3 Sensitivity Studies (Based on selected constant wave height)

- 3 vessel length, Lpp (84m, 102m, and 137m)
- 4 moonpool sizes (7.6m, 7.8m, 8.0m, and 8.2m)
- 4 Guide Wire Tension (5kN, 20kN, 35kN and 50kN)
- 4 Percentage Heave compensation winch (0%, 60%, 75% and 90% heave compensation)

Each simulation of regular wave analysis shall have a minimum duration of 4 wave periods for dynamic simulation and a wave period for the starting phase. Each irregular wave analysis has seed duration of 8 times wave period. The seed time are carefully selected so that they contain the highest wave rise or fall. This decision is made upon consulting several analysts to reduce the amount of simulation time. With this conclusion, a regular analysis is 60 s long and irregular wave analysis is 150 s long.

3.7 Design Principle

The design codes for use are stated in DNV-OS-H102 section D. They are namely Load and Resistance Factor Design (LRFD), Working Stress Design (WSD) and Probabilistic method. The first two are commonly used in design, However, LRFD method gives better results although more complex to achieve. Details on these design codes may be referred to Norsok or DNV standards[33,34].

3.7.1 Load and Resistant Factor Design (LRFD)

In the LRFD (load- and resistance factor design) method the design load effect S_d is obtained by multiplying the characteristic loads with a certain load factors and combine them so that they would yield the worst possible load condition, i.e.,

$$S_d = S (F_{d1} + \dots + F_{dn}) \quad (3.5)$$

S_d = design load effect

Where: F_d = design load(s)

S = load effect function

Depending on the load factors and their combination, one can have Ultimate limit state design, fatigue limit state design, Accidental limit state and serviceability limit state. This method yields the best results, however, at a cost of a more complicated task.

Table 3.5: Basic Usage factors η_o for WSD method [33]

| Loading Conditions | | | | | |
|--------------------|-------------------|-------------------|-----|-----|-----|
| | (a) | (b) | (c) | (d) | (e) |
| η_o | 0.60 ⁴ | 0.80 ⁴ | 1.0 | 1.0 | 1.0 |

3.7.2 Working Stress Design (WSD)

By the Working Stress Design method the target safety is obtained by calibrating an inverted safety factor which is applied to the characteristic value of the structural resistance. The inverted safety factor is normally referred to as the permissible usage factor. Generally the factors should be defined such that the safety level will be equal or greater than obtained with the LRFD method.

In this analysis, we employ the Working Stress Design method. An inverted safety factor of 0.84 is to be used, when applicable, for this analysis based on DNV standard as shown in table 3.5. Loading condition b is for “maximum combination of environmental loads and associated functional loads” (DNV-RP-C201).

3.8 Acceptance Criteria

The analysis basis is completed by analyzing the possible failure modes and failure mechanisms for each load case set in section 3.6. We then set out a limiting design criteria based on appropriate design codes on the structures that are in place to prevent such failure. A limiting wave parameters is determined when the design load exceeds the design resistance as explained in section 3.7.

3.8.1 Failure Modes

The RLWI deployment operation can fail in many ways. A failure modes and effect analysis (FMEA) is conducted to analyze the possible failure modes, shown in appendix D. A summary of the critical failure modes shown in figure 3.6 considered are:

Load Case A and B:

1. Main crane wire failure due to excessive loading/snapping beyond capacity
2. Lower cursor system failure due to high impact loading from module

Load Case C:

⁴ For units unmanned during extreme environmental conditions, the usage factor η_o may be taken as 0.84 for loading condition (b)

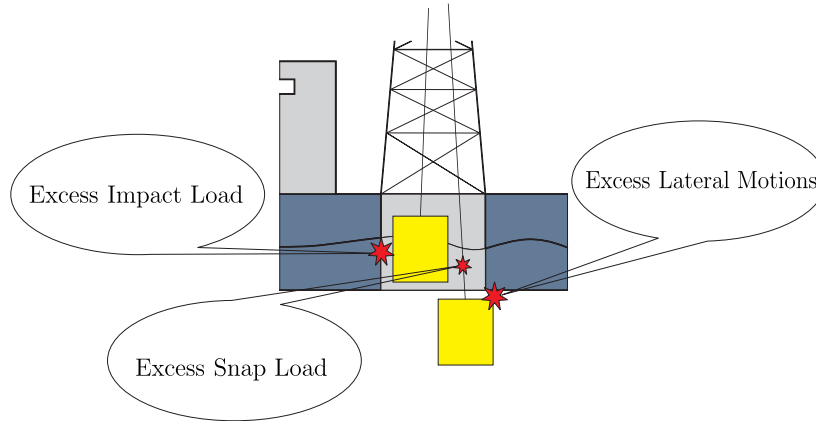


Figure 3.6: Critical structural failure modes considered for analysis

3. Main crane wire failure due to excessive loading/snapping beyond capacity
4. Module component failure because of clashing to moonpool bottom edges during deployment and/or retrieval

Other failure modes are listed in appendix D. Such failure modes are out of this thesis scope as its focus is mainly structural failures.

3.8.2 Safety Factors (Failure Limit)

Firstly, to address the first failure mode, the crane wire effective tension should not exceed minimum breaking strength divided by the safety factor. This is clearly stated on page 38 of DNV standard for certification of lifting appliances [38]. It shall be taken as no less than 3 or greater than 5.

$$\text{Safety factor, } S_f = \frac{10^4}{(0.885 \cdot SWF + 1910)} \quad (3.6)$$

For our case, the safe working load (SWL) is 50 t. Substituting this into equation (3.6), gives us a $S_f = 4.25$. This implies that for the system to comply with this standard acceptance criteria, the minimum breaking strength (MBS) of the crane wire must fulfil equation (3.7).

$$MBS \geq 4.25 \cdot S \quad (3.7)$$

where S= expected design load

Secondly, the lateral impact energy of module should not exceed the capacity of the lower cursor system. We can estimate the impact energy by calculating the kinetic energy (3.8).

$$K \cdot E = \frac{1}{2}mv^2 \quad (3.8)$$

Lastly, the lateral motion of module in case C, should not exceed the safe zone which determines the minimum moonpool clearance. This value is calculated by (3.9)

$$\text{Minimum moonpool clearance} = \text{Available moonpool clearance} \cdot S_f \quad (3.9)$$

Where $S_f = 0.84$ according to WSD method.

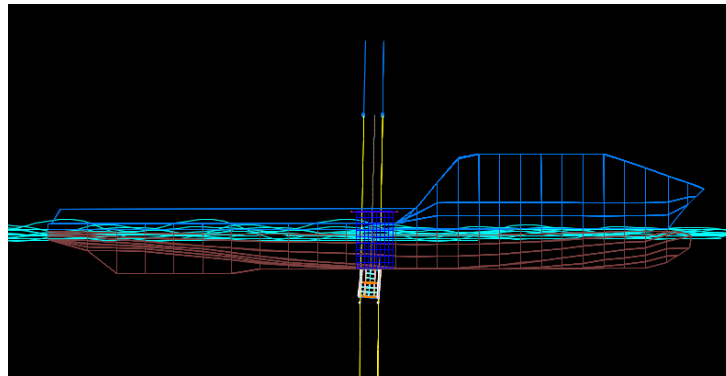
Chapter 4

Results

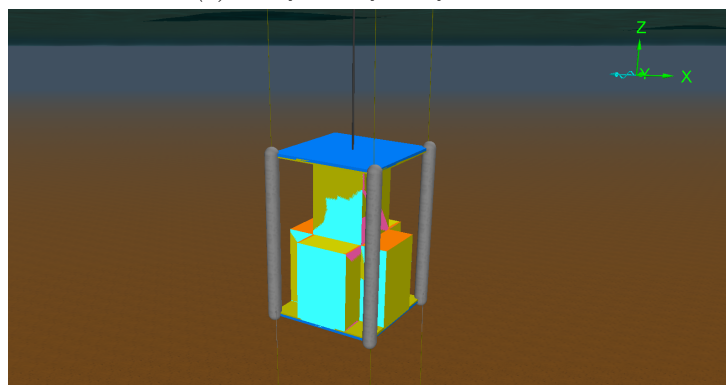
In the previous chapter, it is shown why a specific analysis method is chosen and implemented. Accordingly, the simulation is then run on Orcaflex 9.7a software according to the load cases described in section 3.6. This chapter is dedicated to presenting the results for the specific case of moonpool deployment of Mark II riser-less light well intervention subsea well control package. Selected results are presented after observation on their critically. The implication of the results on a general operation of moonpool deployment is discussed in chapter 5.

4.1 General

The Orcaflex computer model is shown in figure 4.1. Since the total perforation of the module is expected to be more than 50%, it is modelled as a combination of 'sub-members' with perforations of less than 50%. The sub-members are of made known shapes (i.e hollow cylinders, rectangular blocks and plates). The data input for the equipment is shown in table 3.3. The raw added mass coefficients for the fully submerged module far from the surface of water, before the effect of moonpool walls, perforation, shielding, interaction or trapped water are accounted is shown in Table 4.1. The hydrodynamic coefficient calculation results for each load case and each specific moonpool after accounting for shielding, perforation, moonpool wall proximity and water surface proximity are tabulated in Appendix C. Interaction effects between sub-members was difficult to compute, hence taken as a factor of 1. This is generally accepted as conservative.



(a) Wireframe of Orcaflex model



(b) 3D view of MKII stack model used

Figure 4.1: Orcaflex model results**Table 4.1:** Global added mass coefficients for module parts

| Object | Funnels | Roof | Floor | Block Type 1 | Block Type 2 | Block Type 3 | Block Type 4 |
|-------------------------|-----------------|-------------|-------------|--------------------------|--------------------------|--------------------------|--------------------------|
| Shape | Hollow Cylinder | Rect. Plate | Rect. Plate | Rect. Block ⁵ | Rect. Block ⁵ | Rect. Block ⁵ | Rect. Block ⁵ |
| Width/Dia. | 0.25 | 4.0 | 4.0 | 1.0 | 2.0 | 2.0 | 2.0 |
| Length/Thick.r | 0.01 | 4.0 | 4.0 | 2.0 | 2.0 | 2.0 | 3.0 |
| Height | 6.0 | 0.1 | 0.1 | 3.0 | 6.0 | 3.0 | 4.0 |
| Added Mass Coefficients | | | | | | | |
| C_x | 0.96 | 0.00 | 0.00 | 0.99 | 1.29 | 1.07 | 0.92 |
| C_y | 0.96 | 0.00 | 0.00 | 1.36 | 1.29 | 1.07 | 1.20 |
| C_z | 0.96 | 0.58 | 0.58 | 1.28 | 0.98 | 0.91 | 1.13 |
| Reference Volumes | | | | | | | |
| V_{R_x}, m^3 | 0.29 | 50.27 | 50.27 | 9.42 | 18.85 | 9.42 | 28.27 |
| V_{R_y}, m^3 | 0.29 | 50.27 | 50.27 | 2.36 | 18.85 | 9.42 | 12.57 |
| V_{R_z}, m^3 | 0.29 | 50.27 | 50.27 | 1.57 | 6.28 | 6.28 | 9.42 |

⁵ Added mass coefficient: x-value for largest projected area and z-values for the smallest projected area of the block

Table 4.2: Drag coefficients used for analysis

| Load Case | moonpool Size (m) | | | |
|-----------|-------------------|------|------|------|
| | 7.6 | 7.8 | 8 | 8.2 |
| CASE A | 6.12 | 5.96 | 5.82 | 5.69 |
| CASE B | 6.67 | 6.50 | 6.34 | 6.21 |
| CASE C | 3.93 | 3.93 | 3.93 | 3.93 |

The drag coefficients were calculated based on the suggestions of O.Øritsland's drag coefficient plot shown in Appendix B. We selected subsea module item no.12, which is ROT+ROT type module, to be the most suitable due to similarity in size and perforation level. Necessary adjustments were made for proximity to moonpool walls. The results are tabulated in table 4.2

4.2 Base Case

The base case particulars are outlined below. The selection of these particulars as *base case* is simply based on convenience to available data.

| | |
|------------------------|---|
| Vessel length (Lpp) | = 137 m |
| Vessel gross weight | = 21,460 t |
| Draught | = 7.74 m |
| Moonpool size | = $7.8 \times 7.8 \text{ m}^2$ |
| Moonpool damping ratio | = 30% |
| Guide wire tension | = 35 kN |
| Heave Compensation | = 0% |
| Tower height | = 25 m from deck level |
| Load case A and B | : Regular wave analysis (Airy wave theory, no current) |
| Load case C | : Irregular wave analysis (Torsethaugen wave spectra, 1-year current) |

Load cases A, B and C are simulated for these particulars. The hydrodynamic coefficients and moonpool sea state RAO are adjusted for their respective cases. As per our acceptance criteria in section 3.8, the results for crane-wire end forces, module heave motions, lateral velocity and accelerations as well as the moonpool contact clearance are presented in figures 4.2 through 4.4.

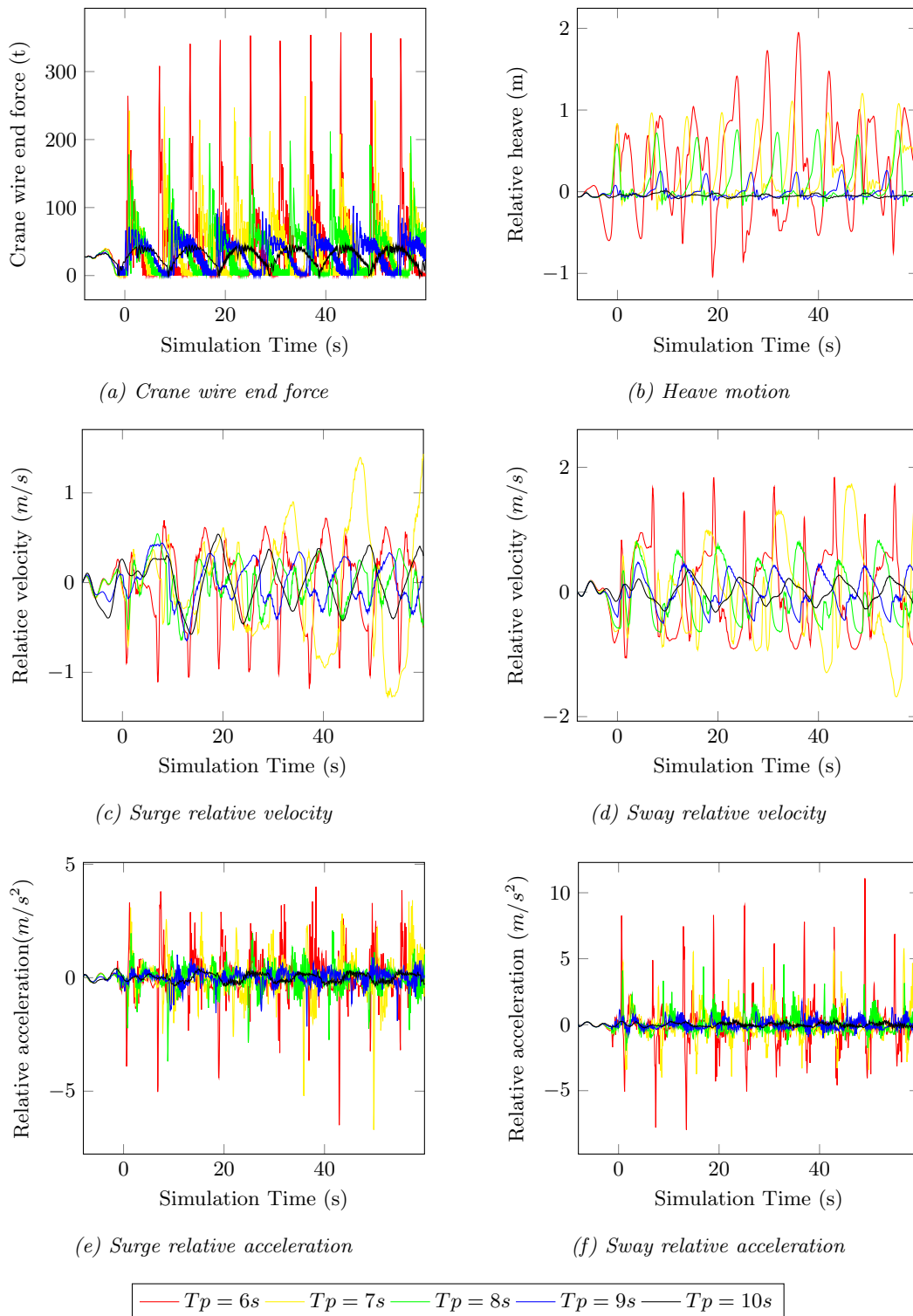


Figure 4.2: Base Case A: Results relative to moonpool at $H_S = 2.5m$ and 180° wave direction

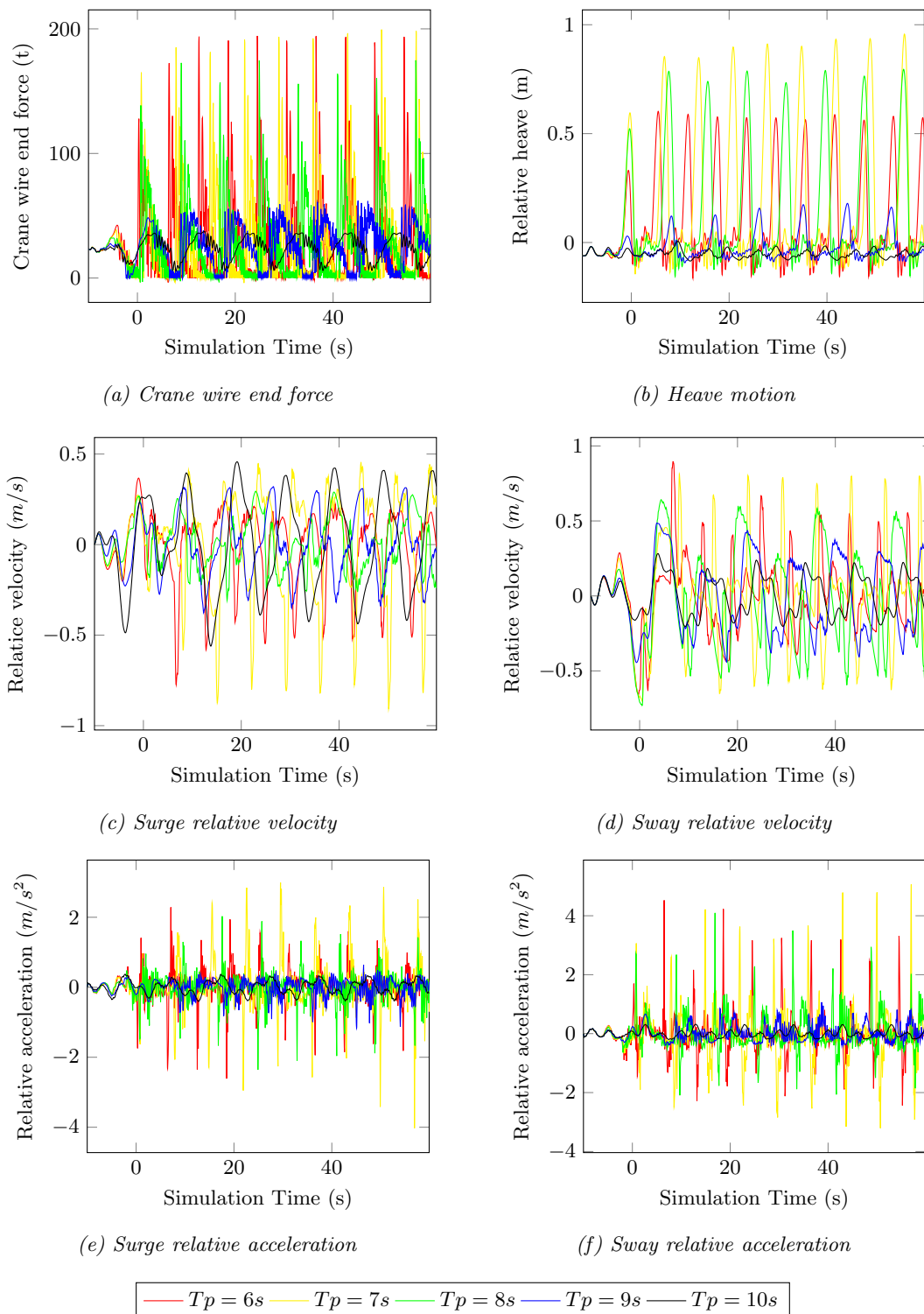
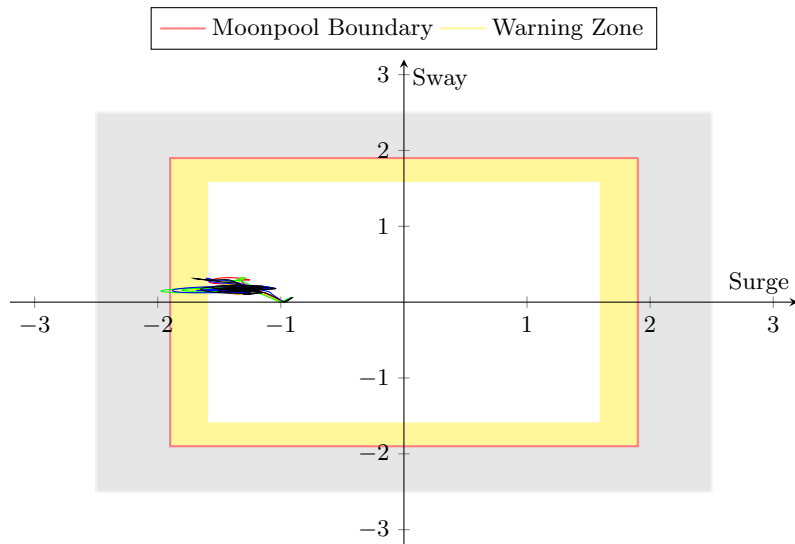
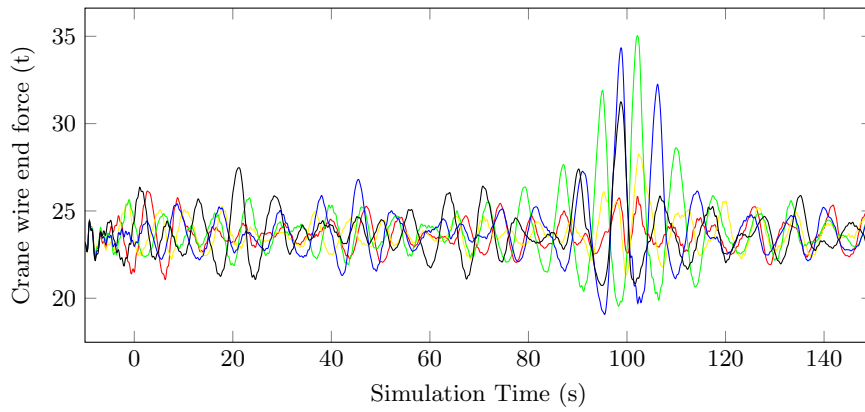


Figure 4.3: Base Case B: Results relative to moonpool at $H_S = 2.5m$ and 180° wave direction



(a) Module contact clearance from moonpool bottom edges (Maximum Values) (m)



(b) Crane wire end force

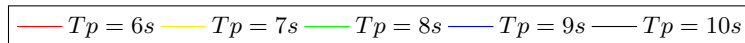


Figure 4.4: Base Case C: Results relative to moonpool at $H_S = 2.5\text{m}$ and 180° wave direction

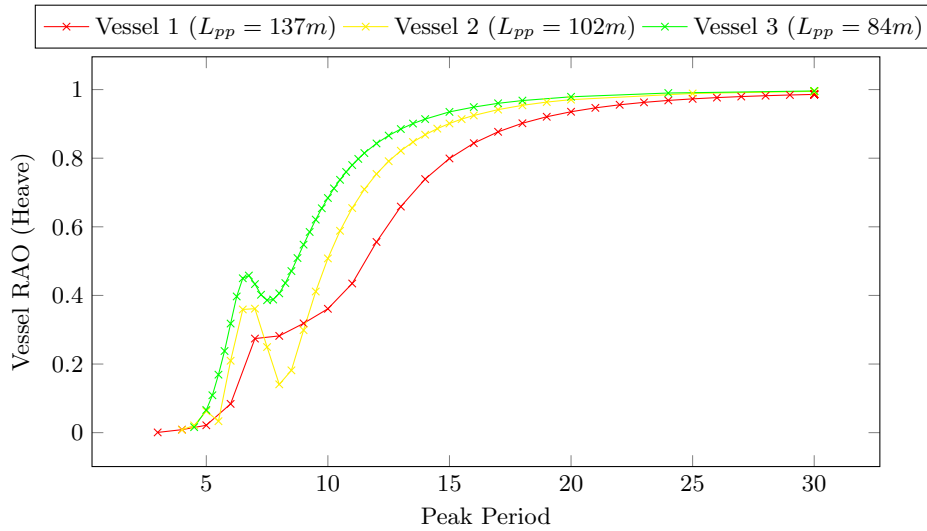


Figure 4.5: Vessel heave RAOs at 180° wave direction

4.3 Sensitivity Study

4.3.1 Vessel Particulars

To determine the effect of vessel particulars on moonpool deployment operation, two other vessels were tested and compared with the base case. Data on these vessels were obtained from a company which preferred to remain anonymous. For this reason, we will not be mentioning the names of the vessels. Relevant information on the vessels is outlined in Table 4.3. Motion transfer functions (RAO's) are plotted in Figure 4.5 Results from the simulations were generated and are presented in figures A.1 through A.3. In addition to the vessel motions (in terms of RAO's), the sensitive parameter was the moonpool sea state, which was computed by using equation (3.4).

Table 4.3: Vessel sensitivity particulars

| Vessel type | Vessel 1 | Vessel 2 | Vessel 3 |
|----------------------|----------|----------|----------|
| Length, L_{pp} (m) | 137 | 102 | 84 |
| Width (m) | 27 | 25 | 20 |
| Dead Weight (t) | 11300 | 8500 | 7000 |
| Draught (m) | 7.7 | 7.7 | 7.2 |
| DP Class (m) | III | III | II |

4.3.2 Active Heave Compensation

To determine the effect of active heave compensation the load cases described, we test three different heave compensations relative to the base case. The heave compensator is regarded to reduce the heave motions at the crane tip (25m from deck level) by a certain percentage. 60%, 75% and 90% heave compensation is simulated. The results are compared with the base case (0% compensated) and are presented in Figures A.4 through A.6.

4.3.3 Moonpool Width

The effect of moonpool size on deployment operation has been studied. We limit our study to square moonpool shapes with cofferdam walls. Cofferdam wall have damping ratio of 0.3. Changing the moonpool size affects several factors including the moonpool sea-state and hydrodynamic coefficients. The moonpool side lengths under consideration are 7.6m, 7.8m, 8.0m and 8.2 meter. The damping ratios are to be kept the same as the base case. The variance of heave transfer function for the different moonpool side width is shown in figure 5.6.

4.3.4 Guide Wire Tension

The guide wires act as a lateral restraint to the module during lowering and retrieval operations. They also assist the lower cursor module in limiting the lateral loads and motions. The tension in the guide wires has, to a large extent, a contribution to this purpose. To determine the sensitivity of the operation to guide wire tensions, four different values of guidewire tensions were tested. The results are presented in figures A.9 through A.11

4.4 Recommended Particulars

The final phase of the study was to determine a recommended configuration of the module handling system and analyze the total effect on the failure modes. It is noted from the results and the subsequent discussion in chapter 5, the following system parameters could lead to the best results in minimizing the risk of failure:

- 90% heave compensation
- 8.2 m wide moonpool opening
- 84 m long vessel number 3
- 50 kN guide wire tensions

This system configuration was tested for wave headings 180° , significant wave heights of 1.5 – 4.5 m, and for peak periods 6 – 10 s. The results for significant wave height of 2.5 m are selected for comparison and shown in figures 4.6 through 4.8.

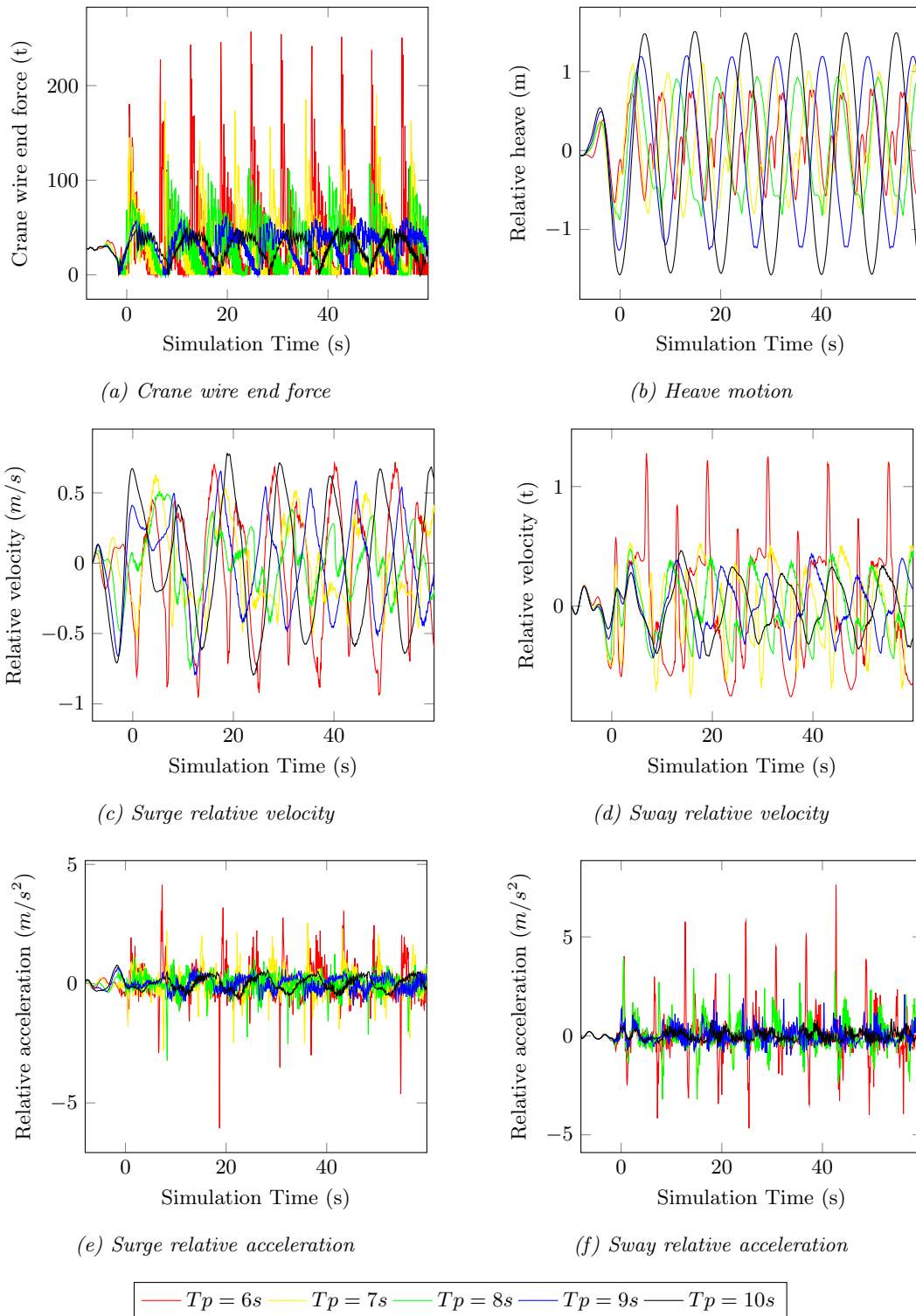


Figure 4.6: Recommended Case A: Results relative to moonpool at $H_S = 2.5m$ and 180° wave direction

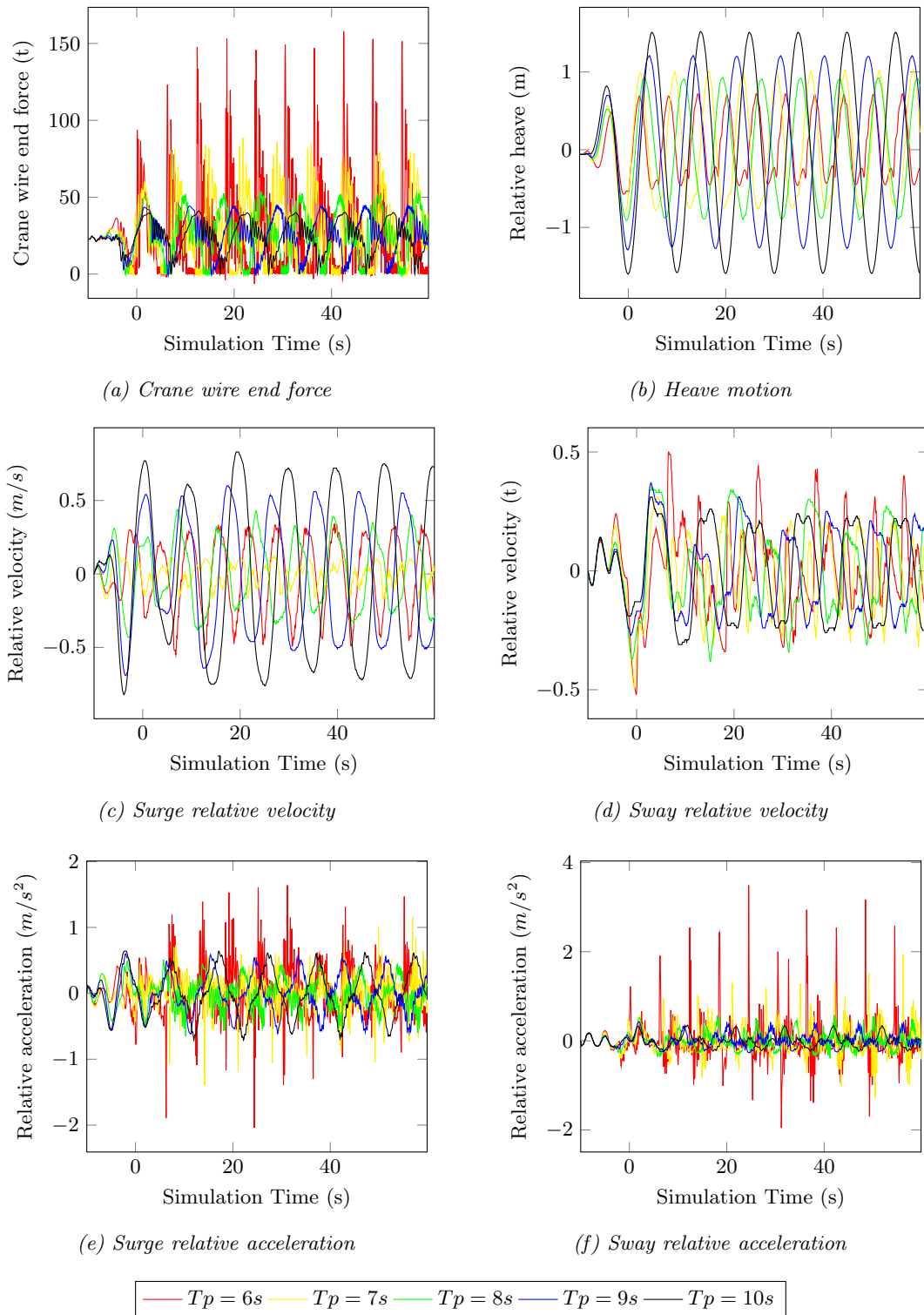
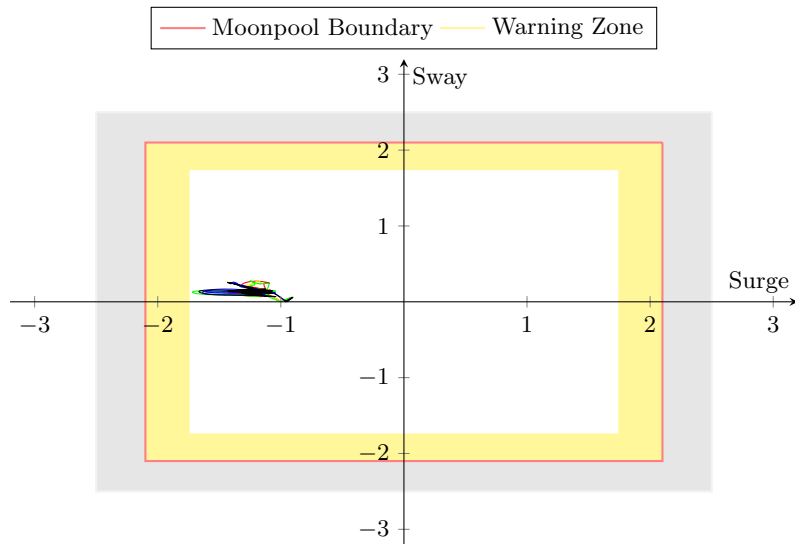
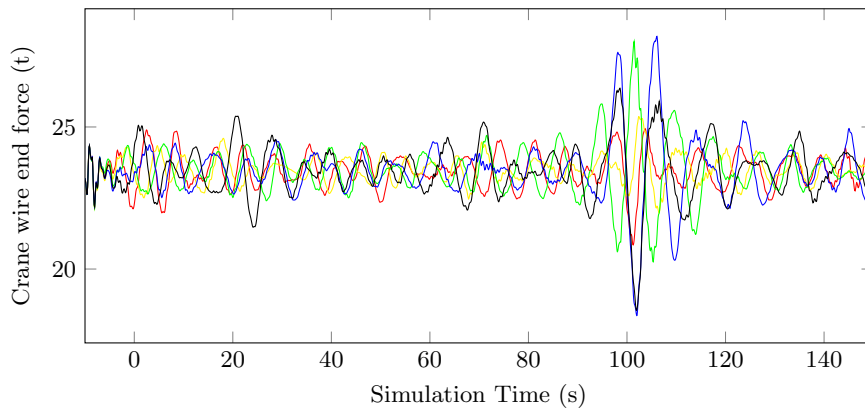


Figure 4.7: Recommended Case B: Results relative to moonpool at $H_S = 2.5m$ and 180° wave direction



(a) Module contact clearance from moonpool bottom edges (Maximum Values) (m)



(b) Crane wire end force

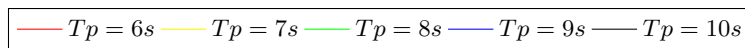


Figure 4.8: Recommended Case C: Results relative to moonpool at $H_S = 2.5\text{m}$ and 180° wave direction

Chapter 5

Discussion

According to our FMEA analysis, we focused on critical areas of failure. These are, crane wire loading, impact velocity when module is inside the moonpool, and lateral motions of the module at keel level. The results were presented in chapter 4. This chapter illustrates the significance of the results and discuss possible reasons why the results could have been as per observation.

5.1 Base Case Study

The base case is used as a bench mark get an idea of the operation and the expected loads involved. The three load cases (A, B and C) are tested for various wave heights, wave periods and wave headings. Results for significant wave height $H_s = 2.5m$ were selected for this discussion after observation on the other results. For the base case, the following observations were made:

1. Loads due to 180° wave headings were observed to have larger impact than 150° wave headings.
2. Crane wire loads are observed to be larger on load case A and get reduced as the module goes down the moonpool as witnessed in load cases B and C.
3. Maximum crane wire loads could reach up to 350 t, implying the minimum breaking limit of the wire to be $4.25 \times 350 = 1486t$ well above the crane wire specification limit of 367 t.
4. Minimum crane wire loads are near zero on load cases A and B, indication the presence of snap loading.
5. Relative to the moonpool/vessel, the module could have maximum heave motions up to 2 m at 6 s wave periods.

6. Impact surge velocity could reach up to 1.6 m/s, while sway impact velocity could reach up to 2 m/s.
7. Maximum acceleration of module in the moonpool could reach up to 5 m/s^2 while Sway acceleration could be double that amount.
8. At keel level, the module has maximum lateral motion of 2.2 m exceeding the moonpool boundaries limit of 1.9 m, indicating the possibility of clashing to the moonpool walls.

The first point indicates crane wire forces are larger on 180° wave headings. To understand this result, one needs to know the factors affecting crane wire loads. There are two main factors affecting crane wire end loads: crane tip motions and hydrodynamic loads on the structure. For the base case, using vessel 1, the crane tip motions mainly depend on heave motion transfer functions. These are shown to be lower for waves heading in the 180° direction compared to waves in the 150° direction, ref figure 5.1). The effect of having lower transfer function for a module within splash zone, is that, it increases the relative velocity of the sea water to the module. Hence increasing the upward hydrodynamic load that is applied in the module. In addition, when the wave is heading at 180° , the moonpool sea state RAO is slightly 'worse off', fig 5.2. This again, will result in higher hydrodynamic loading.

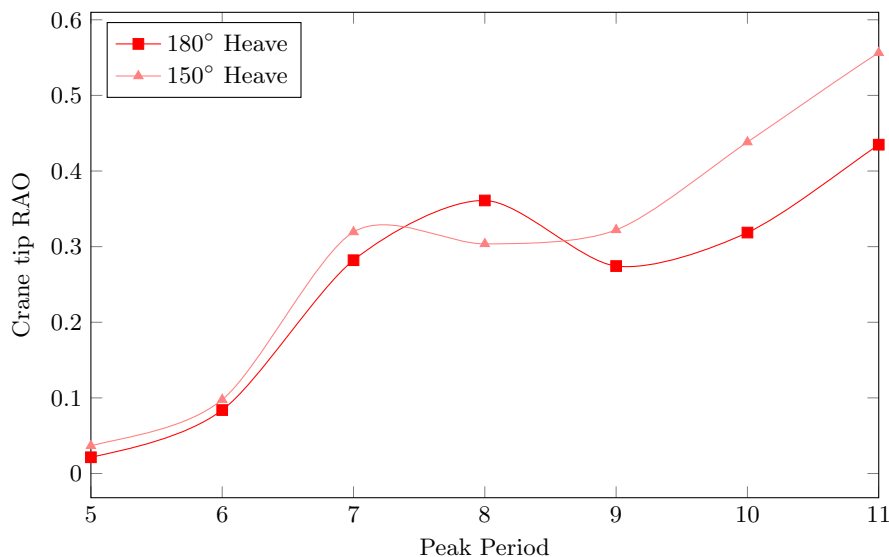


Figure 5.1: Crane tip heave motion transfer functions

Next point states that, load case A shows a higher loading condition than other load cases simulated. This is in line with basic hydrodynamic theories which state that wave loads decrease as we go down the depth.

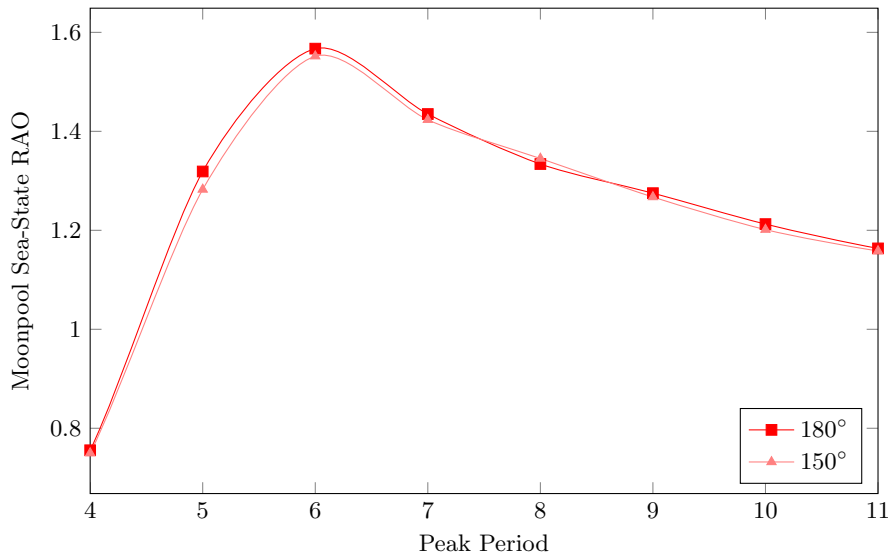


Figure 5.2: Vessel moonpool sea state RAO different wave heading

Points three and four show, the crane wire loads observed to be of high value and indication of snapping. Snapping occurs when the upward hydrodynamic loads on the module are greater than its static weight. This was evident in simulation results in load cases A and B. It should be noted that when using the regular wave analysis, the wave height used is the maximum wave height valued at 2 times the value of the significant wave height. In addition, the hydrodynamic drag coefficient of 6.5 used is the maximum drag coefficient for the module and is purposely conservative. Also, the buoyancy force contributes largely to the upward hydrodynamic load because of the geometry of the module. Therefore, snapping is expected for a wave height of as large as 5 m, however, the values could be highly cautious.

In point five, the motion of the module could reach up to 2 m high. With the assumption that the lower cursor module is only responsible for restraining lateral motions, it will be challenging for it to serve this purpose with a module vertical movement of such heights. Hence it could be a possible constraint to the weather criteria.

In point six, the impact velocity of the object reaching as high as 2 m/s. The kinetic energy produced with such magnitude of velocity is equivalent to 100 kJ. This is the value obtained if we take the static weight of the object. The buoyant weight with added mass would be slightly variant but expected to be less than the static weight. To determine the impact force would require strict understanding of the stiffness and exact configuration of the lower cursor system. This information was unavailable, but one can make a remark here that, the impact load is expected to be within limit.

A maximum 10 m/s² sway motion acceleration is mentioned in point seven. This large acceleration could result in an inertial loads of up to 50 t. The lower cursor module should

be designed to handle that as well.

Lastly, in point eight, the module has a high possibility of clashing. This is due to high amount of current force coupled with lateral wave forces when the module is outside the moonpool region . In addition to this, the hydrodynamic coefficients are taken to a Conservative value. However, one can observe that the module is now, away from the splash zone and vertical hydrodynamic loads are minimal. as a result the crane wire loads are immensely reduced well below the crane wire capacity.

5.2 Sensitivity Parameters

For the three load cases studied, the effect of four sensitivity parameters were analyzed: Vessel month, moonpool dimensions, active heave compensation and guide wire tensions. The detailed results are presented in appendix A in figures A.1 to A.11. For comparing the sensitivity particulars, a spider diagram relative to base case particulars is plotted in figure 5.3. Only maximum values of each 'failure' parameters were considered. The plot is relative to the base case. The base case particulars can be found in section 4.2. From the results, the following observations can be made:

1. Maximum load parameters occur in load case A, constrained in peak periods 6 s and 7 s.
2. Vessel month has no direct correlation with the expected crane wire loads, lateral velocity or acceleration for moonpool deployment.
3. Increasing moonpool dimensions have little benefit in reducing loads, but provide increased moonpool clearance.
4. Guide wire tensions have no effect in vertical crane wire loading or heave but directly affect lateral motions and lateral velocity to a great extent.
5. Active heave compensation has a positive effect in all the parameters studied except for module surge acceleration.
6. In order of significance, vessel month has the highest impact followed by active heave compensation, guide wire tensions and finally moonpool dimensions.

As discussed previously for base case study, the maximum values appears always in load case A. Since load case A is in the splash zone, this is to be expected. The fact that peak periods 6 s and 7 s give the maximum drag and inertia loads simply implies that the relative velocity and accelerations of sea water to module are maximum according to the Airy Wave Theory used.

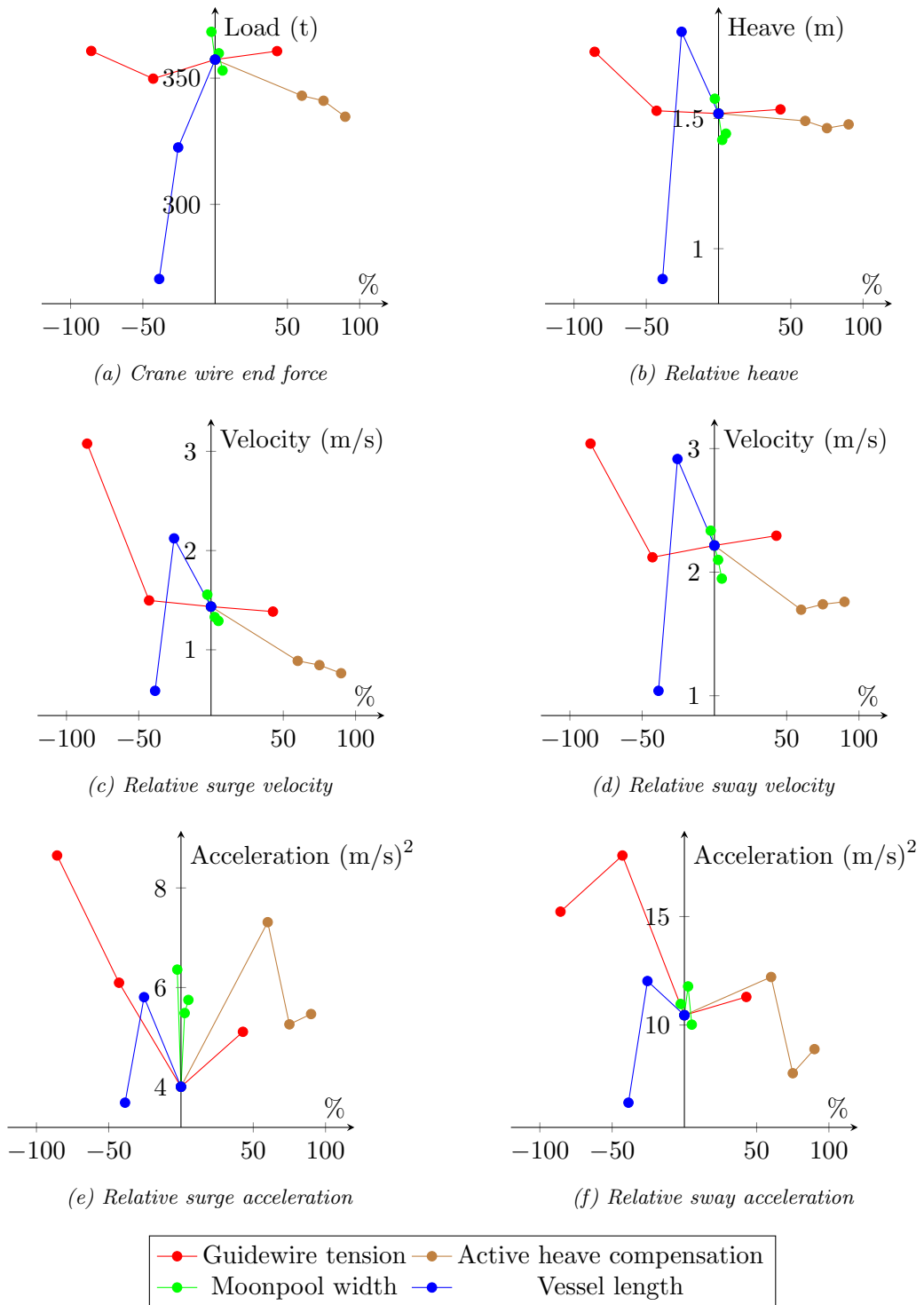


Figure 5.3: Spider diagram for sensitivity of failure parameters to system particulars (Maximum Values at $H_s = 2.5$ m for all load cases and peak periods 6 – 10 s)

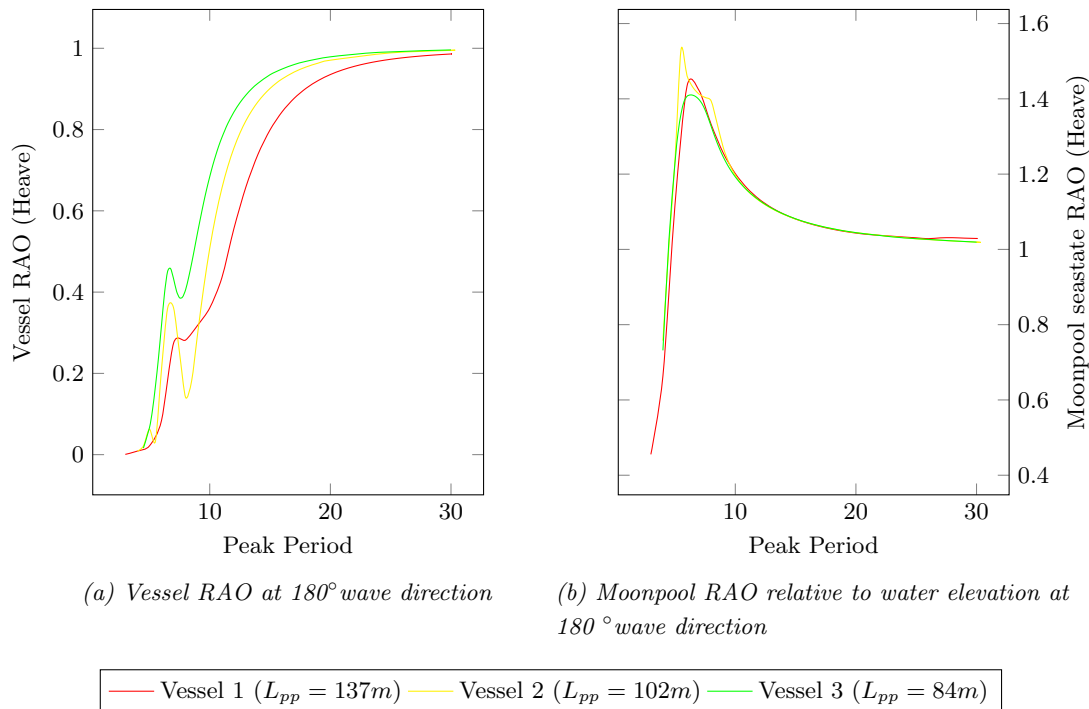


Figure 5.4: Vessel RAO Vs Moonpool Heave Seastate

Secondly, we can observe that there is no real correlation between vessel month and 'failure' parameters. One can expect that, as the vessel gets bigger, the operation loads would be reduced. But this expectation would go against the results of the simulation.

The main reason why the vessel month has not contributed directly to reducing operational loads is because of moonpool sea state transfer functions. Figure 5.4 shows a comparison between the vessels' heave RAO's relative to moonpool origin, and the respective moonpool sea-state RAO relative to the water elevation. In figure 5.4a it is clearly shown that vessel 3 ($L_{pp} = 84m$) has the least favorable motion transfer function. However, taking a look at figure 5.4b indicates a relatively better moonpool sea-state for the same vessel. This moonpool sea-state will determine the amount of hydrodynamic loading incurred by the equipment within the moonpool, which would then be expected to be highest on vessel 2 ($L_{pp} = 102m$). This is observed to the case in many of the 'failure' parameters.

The effect of the moonpool dimensions in the operation is three fold: 1) effect on the hydrodynamic coefficients; 2) effect on moonpool sea state; and 3) effect on moonpool clearance.

Its effect on drag and added mass coefficients is shown in appendix C. For added mass, the factor for proximity to moonpool walls changes from 1.11 to 1.075 for 7.6m and 8.2 m moonpool side width respectively. For drag, these effect is more visible with changes from 1.556 to 1.447 (cf equation (3.3). The effect of increasing moonpool dimensions on the

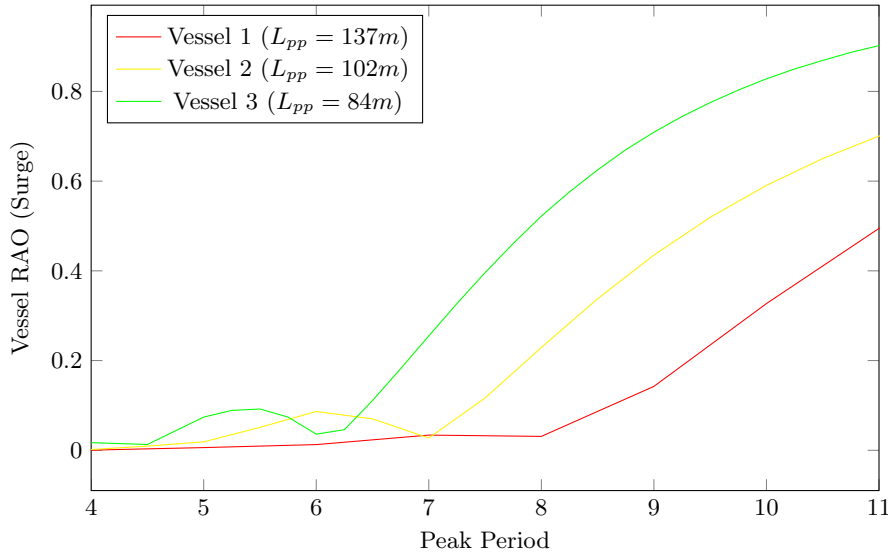


Figure 5.5: Vessel Surge RAO at 180° wave direction

moonpool sea state on vessel 1 (basecase) is also shown in figure 5.6. Only slight variation can be observed, however, small changes in sea state RAO's do happen to have notable effects on expected loads. Increasing dimensions from, say, 7.8 to 8.2m implies there is 0.2 m more room for the equipment at a given side. The moonpool clearance would rise from $0.84 \cdot 1.9 \approx 1.6$ m to $0.84 \cdot 2.1 \approx 1.75$ m.

From the studied moonpool sizes (7.6 m to 8.2 m), the sensitivity of the failure parameters to percentile dimension shown to be steep. In fact it has a steeper impact than any of the other system particulars. However it is important to note that, although failure parameters are seen to be highly sensitive to moonpool dimensions, one can only increase the moonpool size by a small percentage. Increasing moonpool further requires a vessel with broader breadth and subsequent design and cost implications. Hence, the total impact of increasing moonpool dimensions may not be felt as much. This can be shown in figure 5.3.

The issue of having a highly tensioned guide wires pays out markedly reducing the horizontal motions of the module at the keel level. This is shown in figure A.11 page 95 located in appendix A. Maximum horizontal surge motions relative to moonpool center are seen to be reduced from 2.57 m to 2.11 m when guide wires are tensioned up from 5 kN to 50 kN. This will reduce the risk of clashing, although it still exceeds the safe zone of maximum 1.6 m. Increased moonpool dimensions and/or other means of lowering module lateral motions are necessary.

When it comes to vertical loading, the guide wire tension has little to do with crane wire loads. Our result shown in figure 5.3 shows that, the case with 5 kN tension performed the worst, exhibiting the highest crane wire load, lateral velocity and acceleration. These parameters are greatly reduced for the case with 20 kN tension, however, the progress is

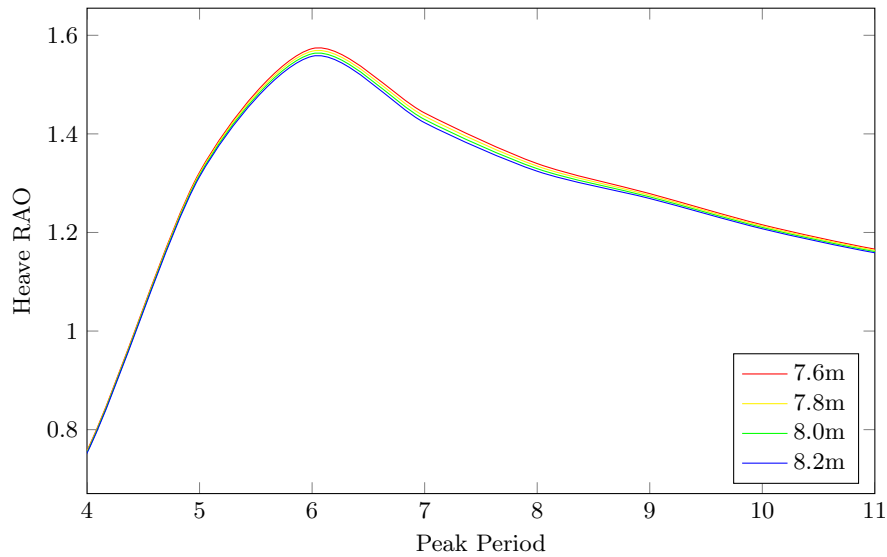


Figure 5.6: Variance of moonpool seastate RAO for different moonpool side width at 180° wave direction

subdued as we tensioned the guide wires further to 35 kN and 50 kN.

Lastly, it is clear to note that modifying the vessel would give the highest contribution in increasing the weather up time. This change however would be one of the most costly solutions. But one can take comfort knowing that, the vessel month is not necessarily the deciding factor in the vessel particulars. The resonance between the moonpool and the vessel RAO is much more essential. Guide wire tensions and active heave compensation both play considerable part in improving weather criteria, especially for lateral constraint of the module during lowering and retrieval. Moonpool size is responsible for creating more room for the equipment. Aside from that, however, increasing their dimension make little contribution in reducing failure risk due to inability to increase them significantly as desired.

5.3 Base Case Vs Recommended Case

Before starting to compare the base case to the recommended case, the reader should know that the recommended case is not the optimal solution to all type of RLWI module deployment operation. The recommended case is mainly drawn from only the parameters studied within this thesis. The extent of study for each parameters has been described in the previous section. We can therefore conclude that the recommended module handling system should be;

- A vessel with the most favorable moonpool sea state RAO.

- A vessel with surge RAO favoring the module lateral motions.
- An active heave compensator with high capacity
- A wider moonpool
- A highly tensioned guide wires.

Therefore, based on these conclusions of sensitivity study results, the best system configuration from the studied parameters is defined. Vessel 3 ($L_{pp} = 84$ m) is the better vessel, 8.2 m moonpool sidewidth, 50 kN tension, and 90 % active heave compensation are found to be the best scenarios for the deployment of RLWI stack MKII.

After conducting simulation using these values for the respective system particulars, the results are plotted in figures 4.6 to 4.8. Table 5.2 illustrates the total variation of the two systems, i.e. base case vs recommended case.

Table 5.1: Comparison between base case and recommended case on handling system particulars

| System Particular | Base case | Recommended case | Difference |
|------------------------------|-----------|------------------|------------|
| guide wire tension , kN | 35 | 50 | 43% |
| Moonpool width, m | 7.8 | 8.2 | 5% |
| Active heave compensation, % | 0 | 90 | 90% |
| Vessel month, L_{pp} | 137 | 84 | -39% |

Table 5.2: Comparison between base case and recommended case on maximum parametric values for $H_s = 2.5$ m and 180° wave direction, $T_p = 6 - 10$ s

| Failure Parameter (Max. Values) | Base Case | Recommended Case | Difference | Load Case |
|--------------------------------------|-----------|------------------|------------|-----------|
| Crane Wire Load, t | 357.37 | 257.13 | -28.0% | A |
| Surge Velocity, m/s | 1.43 | 0.78 | -45.6% | A |
| Surge Acceleration, m/s ² | 4.01 | 4.14 | 3.3% | A |
| Sway Velocity, m/s | 2.22 | 1.28 | -42.3% | A |
| Sway Acceleration, m/s ² | 10.45 | 7.63 | -27.0% | A |
| Heave Motion, m | 1.52 | 1.10 | -27.3% | A |
| Surge Motion, m | -2.58 | -1.72 | -33.4% | C |

5.4 Effect of Operational Weather Criteria on Up-time in Norwegian Continental Shelf

We looked at several literature to estimate the amount of waiting time is expected to perform a RLWI operation with a given weather limit. Employing the method proposed by Rich T.Walker [39], did not yield results anywhere near the expected values. This may be due to erroneous metocean design basis values, or error in methodology, or the methods

inability to cover wave heights above $2mH_s$. Nonetheless, we attempt to give a rough estimate of the expected waiting on weather based on the following accounts.

The probability of occurrence of a sea state having HS below a given value H is given by the Weibull distribution

$$F = P(H_s < H) = 1 - e^{-\frac{(H-B)^k}{A}}$$

where B = location parameter, A is scale parameter and k is shape coefficient.

The probability of a sea state will have $H_s < H$ for consecutive X hours is given as

$$P = P(H_s < H)^{x/3}$$

Hence, the expected amount of 3-hour sea states an operation has to wait before getting a consecutive $H_s < H$ is given by a geometric distribution

$$E(x) = \frac{1}{P(H_s < H)^{x/3}}$$

Converting into hours, the amount of waiting hours will be;

$$E(X) = 3 \times \frac{1}{P(H_s < H)^{x/3}}$$

Then we can conclude that for a given month (assume 30 days), the expected waiting time will be evaluated by

$$E(X) = \begin{cases} 3 \times \frac{1}{P(H_s < H)^{x/3}} & \text{for } E(X) < 720 \text{ hours/month} \\ 720 & \text{for } E(X) > 720 \text{ hours/month} \end{cases} \quad (5.1)$$

Performing this calculation for each month and finally estimating the total waiting on weather in percentage form

$$\%WOW = \frac{\sum_{i=1}^{12} E(X)_i}{24 \times 365} \quad (5.2)$$

Finally, we need to make a correct assumption of the value of x consecutive hours needed for the operation. It is stated that the total deployment operation takes an estimated 40 h. This includes the total time including testing of equipment. Since only two of the three components are large enough to be limited by weather conditions, we will take x as the time it takes until the completion of deploying the Lubricator section. With equal amount of testing time expected in all three components, the value of x can be approximated as one third of the total time. This gives us a value of $40/3 \approx 13 \text{ hours}$. We base our calculation with this number, the result are shown in figure 5.7. To compare the difference in the reference period of the operation an T_R value of 26 h is shown as a comparison

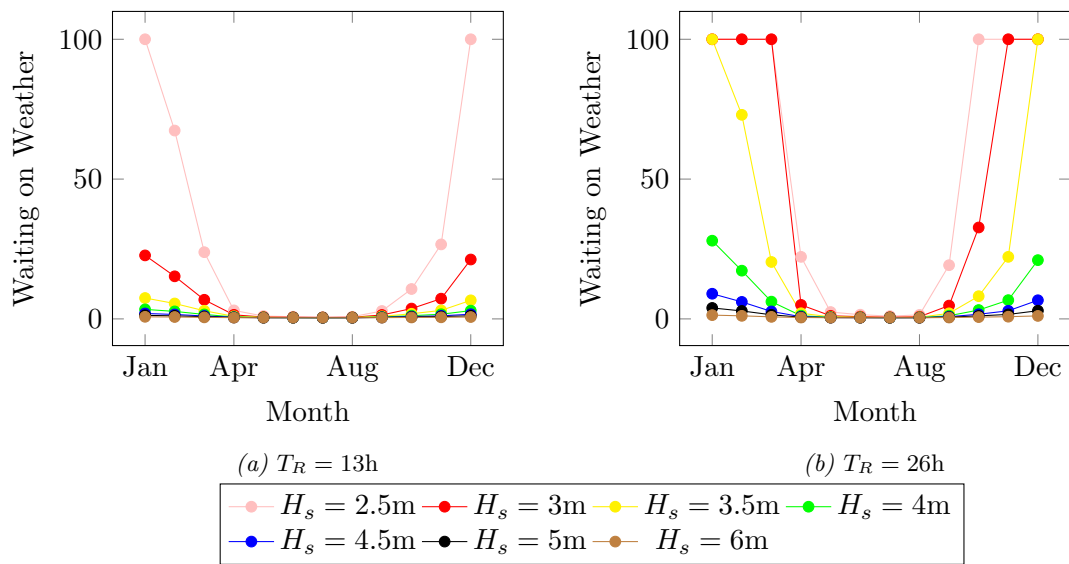


Figure 5.7: Percentage waiting on weather calculated based on expected reference period of module deployment operation

Chapter 6

Conclusion and Recommendations

In this thesis work, we have analyzed the module deployment operation of a riser-less light well intervention unit with the objective of improving its present weather limit. We have looked through the main structural components that play a part in handling environmental forces caused by harsh weather conditions. This chapter is a summary of the findings and recommendations on an improved module handling system.

The Vessel

The vessel is the main platform for the operation. It plays the most significant role when attempting to deploy in harsh weather conditions. The study conducted sensitivity on three vessels with different length between perpendiculars. Commonly, it is assumed the larger vessel would suppress environmental loads on the module. However, the findings of this study showed quite to the contrary. This was mainly because bigger vessels showed higher oscillation amplitudes to the same wave conditions and same moonpool designs. It is concluded that the vessel length doesn't necessarily improve weather limits on a module deployment operation of RLWI stack. In addition, longer vessels are, to no surprise, more costly. However, bigger vessels have the advantages of better motion transfer functions. This are favorable when considering drift scenarios, topside operations, personnel comfort etc... Hence there should be a necessary give and take on the vessel length.

The Moonpool

In the analysis of the moonpool design, we looked at the effect on moonpool dimensions on the operation. The results showed a steep correlation between the moonpool dimensions and the hydrodynamic loads on a structure inside a moonpool. The drag coefficients are reduced as well as the moonpool sea state is much improved. However, we were able to observe that, moonpool dimension changes are limited due to their dependency to the vessel's breadth. That is to mean one can only have a bigger moonpool, if the vessel's width is large enough. Due to this effect, moonpool dimensions make little contribution to improve the weather limit of the operation.

On the other hand, damping mechanism in place seems to have the bigger contribution. This variable has not been quantitatively studied in this thesis. However, we have been able to observe that the moonpool sea state is a determining factor. Several damping designs exist in literature (cf. section 2.4.2, and the design with the highest relative damping ratio should be selected.

The Module

The current riser less light well intervention module has a 16 m² footprint and weights 50 t. There is not much one can do to the already manufactured module. In the moonpool, hydrodynamic force comes in the shape of upward heave. The hydrodynamic drag coefficients inside a moonpool are magnified due to proximity to moonpool walls. A bigger moonpool may help, but significant reduction should not be expected. Therefore, it is beneficiary to reduce the module footprint for future module designs.

A smaller footprint module has many advantages. It will have less drag area and reduce the effect of moonpool walls on drag coefficient. It will also allow more clearance between module and moonpool walls. However, this may mean that the module could have a larger height and larger drag area in transverse directions. Transverse hydrodynamic loads are present only when the module is outside or near the bottom of the moonpool. Guide wire tensions and lower cursor system are responsible for supporting lateral loads and will have to be analyzed.

The Guide Wires

Guide wires are connected to the guide posts on the sea bed, pass through guide funnels on the equipment and are tensioned at the tower top through constant guideline tensioners. During module retrieval operation, it is expected that the lower cursor system will grasp the

equipment some way after the module top enters the moonpool. Guide wires are, therefore, the only support to the module lateral motions when entering the moonpool. Needless to say, it is highly important to assure guideline systems are fully reliable. Tensioners should be checked for capability and reliability. In this thesis, we have assumed the guide wire tensioners are fully reliable. Our conservative study analyzed four guide wire tension values and assessed their significance in supporting lateral motions. If tensioned at 5 t each, the system will provide the desired operability. However, guide wires do not provide any form of shield to vertical motions, as would be expected.

The Heave Compensator

Traditionally, the heave compensator main purpose is for landing operations of the moonpool. To see the effect of active heave compensation, we evaluated three different compensations with varying residuals. The active heave compensator showed positive improvement coming only second to vessel particulars in terms of significance. It should also be remarked that, the heave compensator resulted in reduced loads on support structures regardless of the presence of snapping conditions. Therefore, employing a heave compensator is an added advantage in deployment operations through moonpools.

The Crane Wire

The crane wire end load has been studied for different load cases. It is almost always the case that the crane wire is heavily loaded when the module is in the moonpool and close to the water surface. Logically, the crane wires with higher breaking loads are more suitable in these situations. The crane wire in one of the RLWI vessels has a safe working load of 100 t. This capacity fell short of the analyzed crane wire load at 2.5 m significant wave height and 6 s peak period. The analysis witnessed a snapping effect at this wave height. However, the analysis has also been conservative due to: 1) regular time domain analysis; and 2) conservative hydrodynamic coefficients. A comprehensive approach for moonpool analysis should be sought for a more accurate solution. In addition, model tests should be carried to determine better estimate of hydrodynamic coefficients.

The Lower Cursor System

In our study, the lower cursor system has not been modelled. Orcaflex on-line support was consulted and their proposed modelling approach resulted in unrealistic model behavior and increased simulation time immensely. Therefore, the approach was to determine the

expected impact energy on the lower cursor system. We have made an assumption that the lower cursor system will only serve as horizontal motion support. The results showed that, the cursor system could be loaded with impact energy of up to 100 kN. To understand the corresponding impact force, one needs to know the arrangement and stiffness of the the structure with a good level of accuracy. Nonetheless, the cursor system with the addition of guide wire support shall reach its structural limit before other system elements.

In addition, the heave motion of the module inside the moonpool was observed to be large, up to 1.5 m. This again is mainly due to conservative nature of the study, however, it should be remarked that the module could slip from the lower cursor's prongs in high wave conditions. Lowering the bottom drag area of the module would significantly improve such failure modes from occurring.

It may be concluded that, adjusting system components does affect the deployment operation significantly and therefore each parameter should be carefully selected. The results of this study should also be carefully referred for moonpool operations as we have made some strong assumptions due to lack of recommended tests and data. One should also analyse the effect of adjusting system particulars such as vessel length on other operations such as transiting and wire-line runs. This study is, therefore, a supplementary study to a larger evaluation of riser-less light well intervention vessels for improving their waether resistance.

References

- [1] Karlsen, O. E., Morrison, B. J., and Maciel, P. (2013), *Improved recovery rate in brownfield subsea wells using riser less light well intervention*. Offshore Technology Conference, doi:10.4043/24367-MS.
- [2] Statoil (2013), Personal Experience.
- [3] Statoil (2013), *Fact sheet CAT A*. On-line at: <http://www.statoil.com/en/NewsAndMedia/PressRoom/Pages/PressKitCatA.aspx>. Accessed on: 05-06-2014.
- [4] Schlumberger (2014), *Well intervention*. On-line at: http://www.slb.com/services/well_intervention.aspx. Accessed on: 14-03-2014.
- [5] Statoil (2014), *Fit for purpose rigs*. On-line at: <http://www.statoil.com/en/NewsAndMedia/PressRoom/Pages/28032012Rigger.aspx>. Accessed on: 05-06-2014.
- [6] NORSOK (2004), *Well integrity in drilling and well operations*. The Norwegian Oil Industry Association (OLF), Norwegian Standard.
- [7] Mathiassen, E. and Skeels, H. B. (2008), *Field experience with riser less light well intervention*. Offshore Technology Conference, doi: 10.4043/19552-MS.
- [8] FMC Technologies Brochure (2013), *Riser less light well intervention system*. On-line at: <http://www.fmctechnologies.com/SubseaSystems/Technologies/AdvancingTechnologies/Intervention/LWI.aspx>. Accessed on: 15-06-2014.
- [9] Drillingwellsolutions (2013), *RLWI – Riserless well intervention – The equipment*. On-line at: <http://drillingwellsolutions.wordpress.com/2013/02/19/rlwi-riserless-well-intervention-the-equipment/>. Accessed on: 15-06-2014.
- [10] Neumann, B (2012), *Global ambitions for our light well intervention business*. WellLinked : Your Global Energy Connection.
- [11] Friedberg, R., and Joessang, S., and Gramstad, B., and Dalane, S. (2010), *Subsea well intervention: Experiences from operating new generation riserless light well intervention units in the North Sea: Challenges and future opportunities*. Offshore Technology Conference, doi:10.4043/20418-MS.

- [12] Jossang, S.N., Friedberg, R., Buset, P. and Buset, B. (2008), *Present and future well intervention on subsea wells*. Society of Petroleum Engineers, **doi:10.2118/112661-MS**.
- [13] Zijderveld, G. H. T., Tiebout, H. J., Hendriks, S. M., and Poldervaart, L. (2012), *Subsea well intervention vessel and systems*. Offshore Technology Conference, **doi:10.4043/23161-MS**.
- [14] Jahnsen, B. (2011), *The future of well intervention services using RLWI*. FMC Technologies.
- [15] Pierson, W.J., Newman, G. Jr., and James, R.W. (1955), *Practical methods of observing and forecasting ocean waves by means of wave spectra and statistics*. U.S. Navy Hydrographic Office.
- [16] Michel, W. H. (1999), *Sea spectra revisited*. MAR TECHNOL, **36/4**. pp 211–227.
- [17] Liu, Z. and Frigaard, P. (1999), *Generation and analysis of random waves*. Aalborg Universitet, Denmark
- [18] Det Norske Veritas AS (2010), *Environmental loads and environmental conditions*. Recommended Practice: DNV-RP-C205.
- [19] Chakrabarti, S. K. (1987), *Hydrodynamics of offshore structures*. WIT press.
- [20] Le Méhauté, B. (1976), *An introduction to hydrodynamics and water waves*. Springer, **Isbn: 0387072322**.
- [21] Det Norske Veritas AS (2011), *Modelling and analysis of marine operations*. Recommended Practice: DNV-RP-H103.
- [22] Øritsland, O. (1989), *A summary of subsea module hydrodynamic data*. Marine Operations Part III.2, **70** 511110.05.
- [23] Strand, J. P., Sørensen, A. J., Ronæss, M., Fossen, T.I. (2002), *Positioning control systems for offshore vessels*. In: The Ocean Engineering Handbook.
- [24] Det Norske Veritas AS (2011), *Dynamic positioning systems*. Rules for Classification of Ships, Part 6 Chapter 7.
- [25] Kooiker, K. (2011), *Moonpool mysteries*. MARIN Report, **104**. pp 18–19
- [26] WireCo Worldgroup (2008), *Wire rope users' Handbook*. Form No. 1001F.
- [27] Juel, H., Ranum, H., Mjaaland, S., Varne, T., Solberg, D. B., and Bjorndal, R. (2009), *Wireline tractor milling operations from a riserless light-well intervention vessel at the high-temperature Åsgard Field*. Society of Petroleum Engineers. **doi:10.2118/121481-MS**

- [28] ACE Winches (2012), *Active heave compensation winch system presentation*. On-line at: http://www.ace-winches.com/images/uploads/Active_Heave_Compensation_v6.pdf. Accessed on: 15-06-2014.
- [29] Det Norske Veritas (2011), *Marine operations, General*. Offshore Standard: DNV-OS-H101.
- [30] Haaland, S., Fortmuller, C. G., Pollen, T., and Roosmalen, J. J. (1996). *Asgard: Simultaneous development of an oil and gas cluster in the Norwegian Sea*. Society of Petroleum Engineers, **doi:10.2118/36876-MS**
- [31] Valen, M. (2010), *Launch and recovery of ROV: Investigation of operational limit from DNV recommended practices and time domain simulations in SIMO*. in: Department of Marine Technology, Norwegian University of Science and Technology.
- [32] Roti, I. (2012), *Sea state limitations for the deployment of subsea compression station modules*. in: Department of Marine Technology, Norwegian University of Science and Technology.
- [33] Det Norske Veritas (2012), *Structural design of offshore units (WSD Method)*. Offshore Standard, DNV-OS-C201.
- [34] Det Norske Veritas (2012), *Marine operations, design and fabrication*. Offshore Standard, DNV-OS-H102.
- [35] Statoil (2012), *Asgard metocean design basis*.
- [36] Sarkar, A., and Gudmestad, O. T. (2010), *Splash zone lifting analysis of subsea structures*. In ASME 2010 29th International Conference on Ocean, Offshore and Arctic Engineering, pp. 303-312. American Society of Mechanical Engineers.
- [37] Certex Manual (2013), *Wire ropes*. In: Catalog, Certex.
- [38] Det Norske Veritas (2011), *Lifting appliances*. Standard for Certification, No. **22**.
- [39] Walker, R. T., v.Nieuwkoop-McCall, J., Johanning, L., and Parkinson, R. J. (2013), *Calculating weather windows: Application to transit, installation and the implications on deployment success*. Ocean Engineering, **68**, pp 88–101, ISSN 0029-8018.

Appendix A

Sensitivity Plots

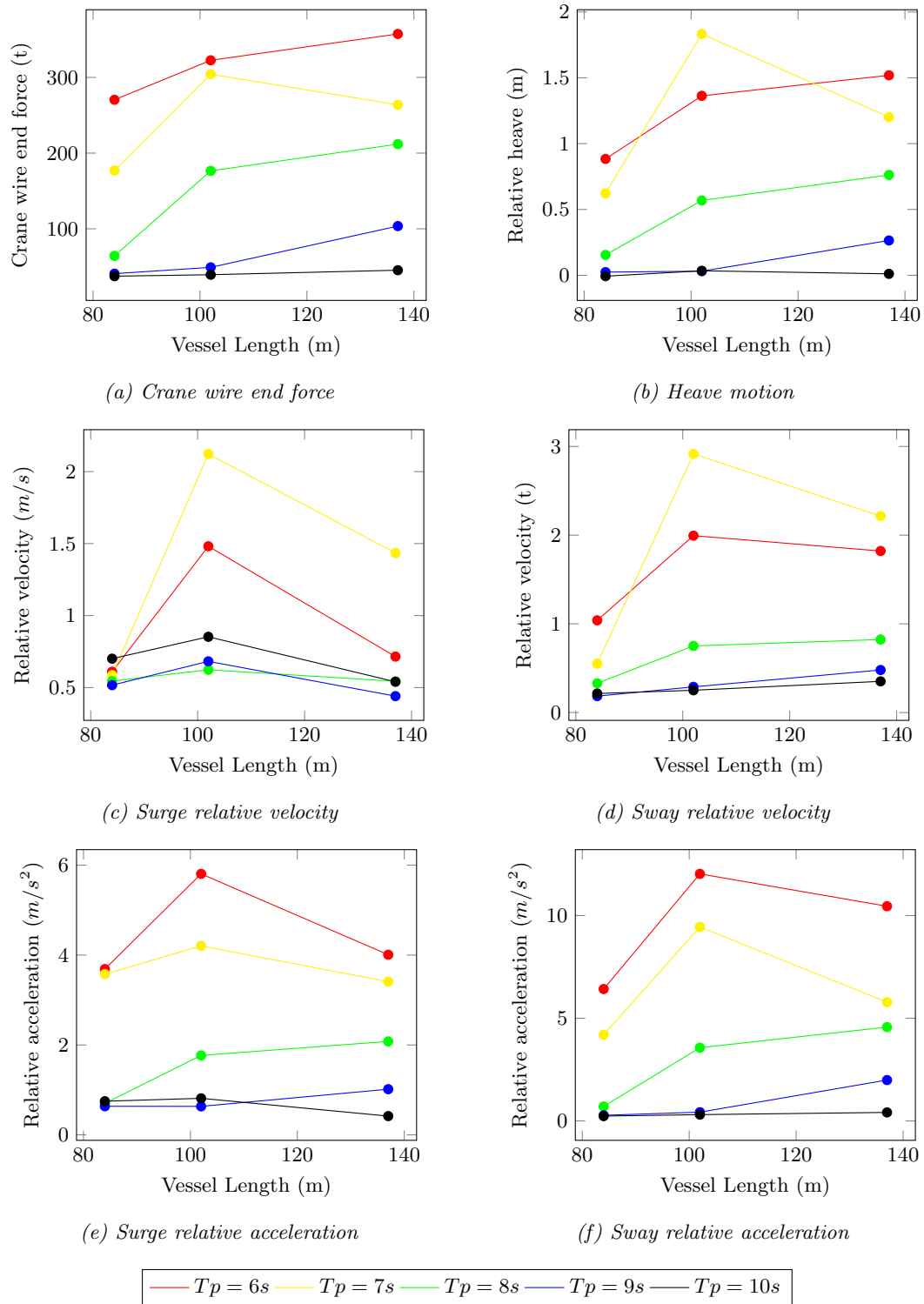
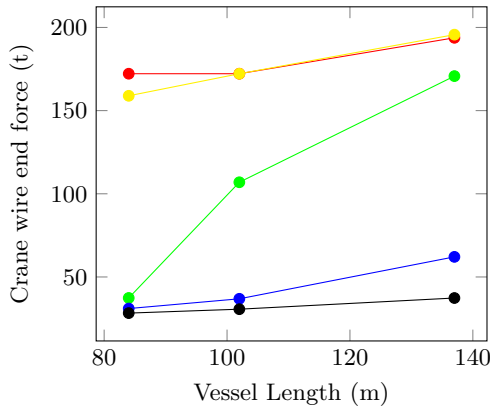
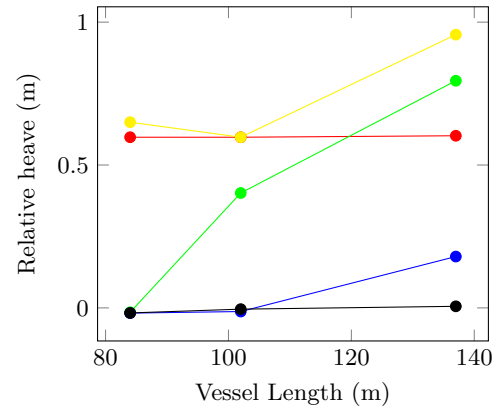


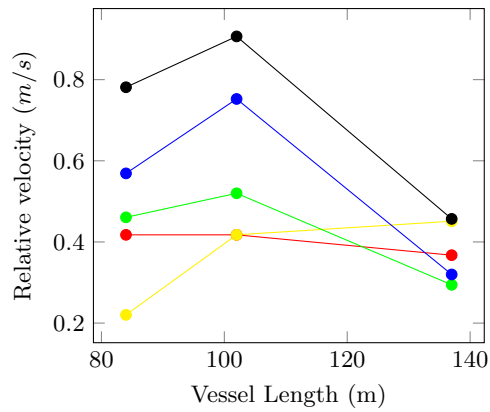
Figure A.1: Vessel Sensitivity Case A: Results relative to moonpool at $H_S = 2.5m$ and 180° wave direction



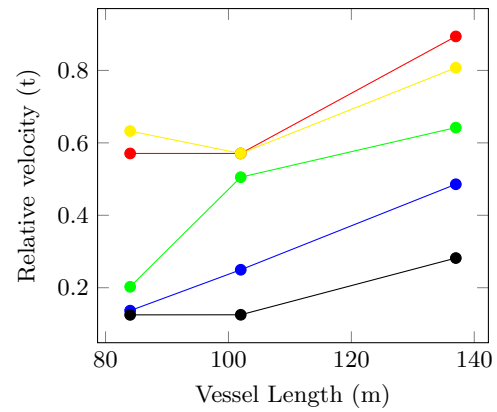
(a) Crane wire end force



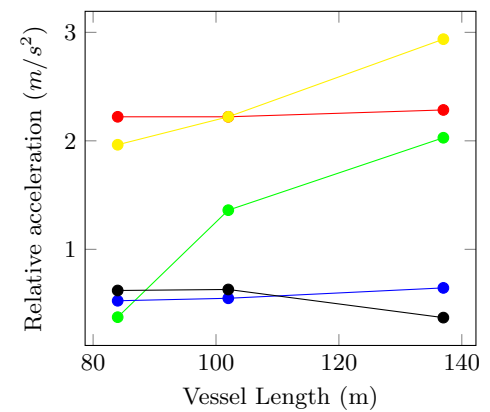
(b) Heave motion



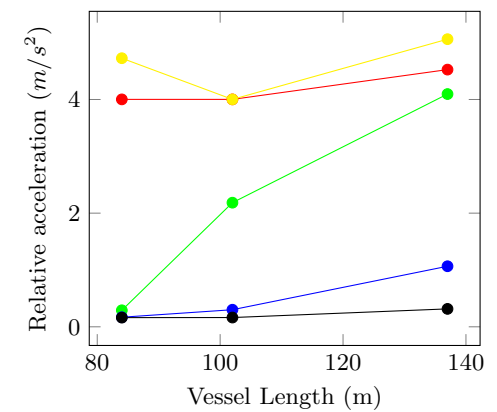
(c) Surge relative velocity



(d) Sway relative velocity



(e) Surge relative acceleration



(f) Sway relative acceleration

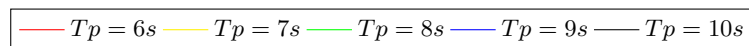
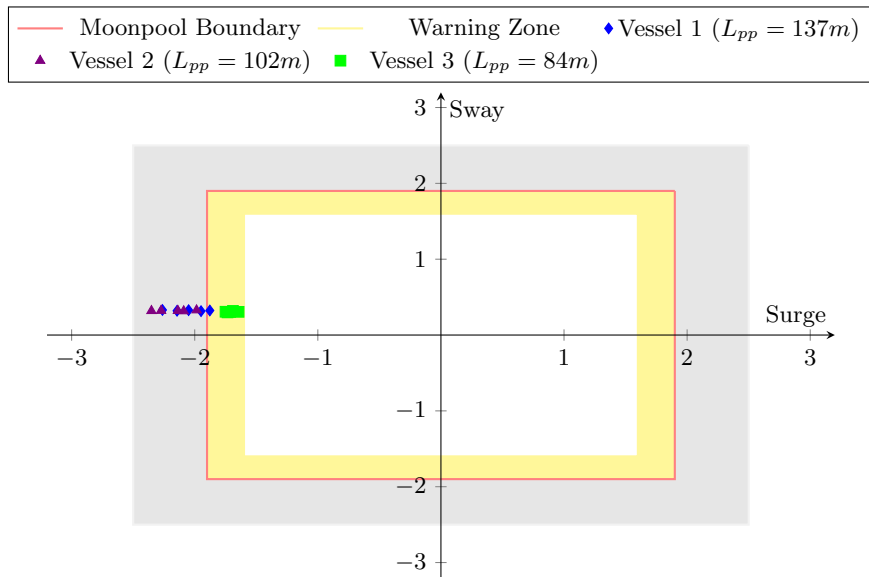
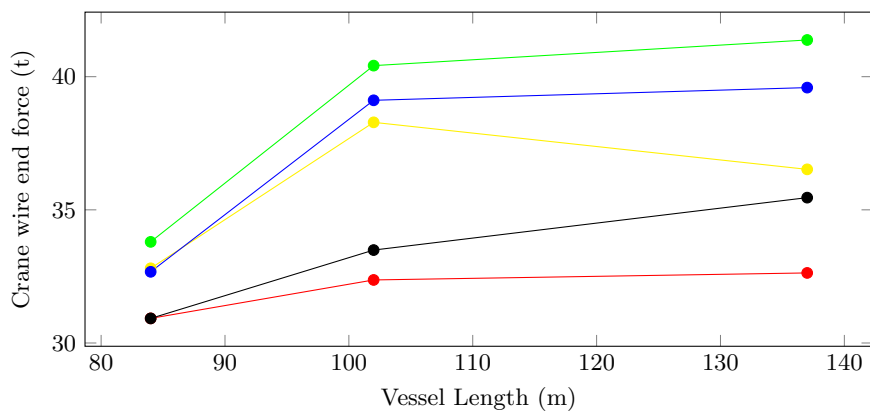


Figure A.2: Vessel Sensitivity Case B: Results relative to moonpool at $H_S = 2.5m$ and 180° wave direction



(a) Module contact clearance from moonpool bottom edges (Maximum Values) (m)



(b) Crane wire end force

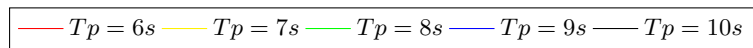


Figure A.3: Vessel Sensitivity Case C: Results relative to moonpool at $H_S = 2.5m$ and 180° wave direction

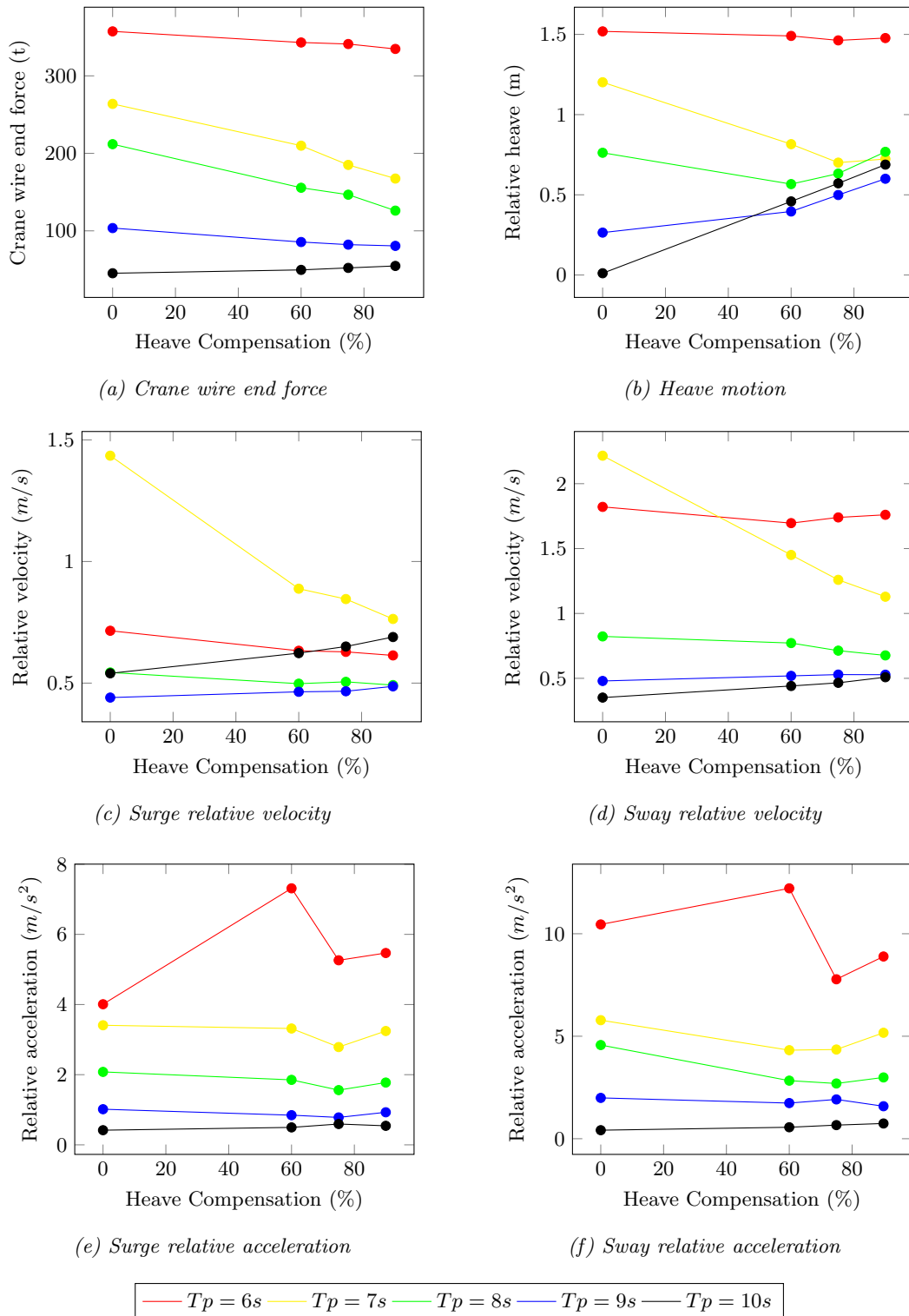


Figure A.4: Heave compensator Sensitivity Case A: Results relative to moonpool at $H_s = 2.5m$ and 180° wave direction

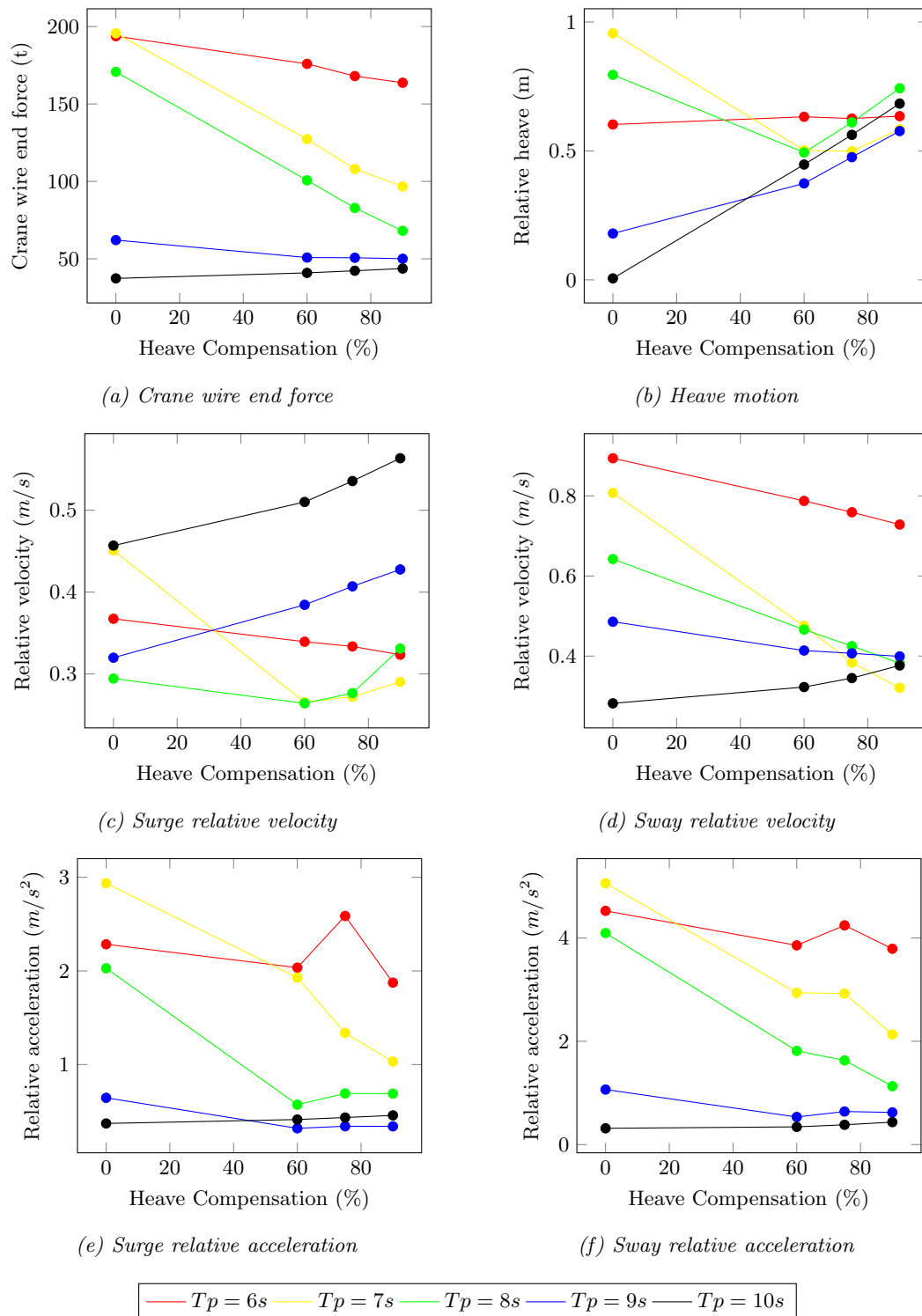
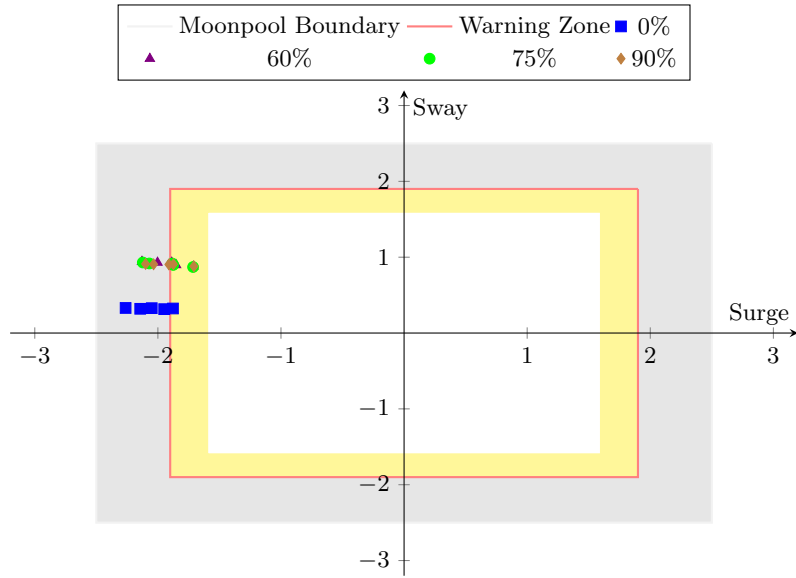
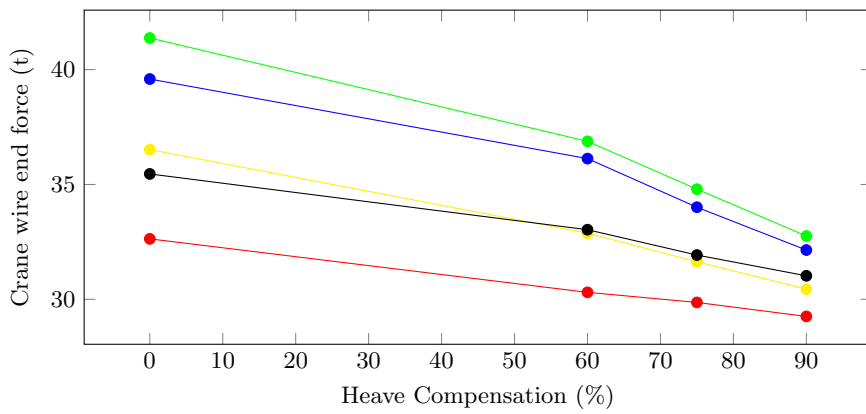


Figure A.5: Heave Compensator Sensitivity Case B: Results relative to moonpool at $H_S = 2.5m$ and 180° wave direction



(a) Module contact clearance from moonpool bottom edges (Maximum Values) (m)



(b) Crane wire end force

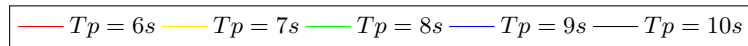


Figure A.6: Heave Compensator Sensitivity Case C: Results relative to moonpool at $H_S = 2.5m$ and 180° wave direction

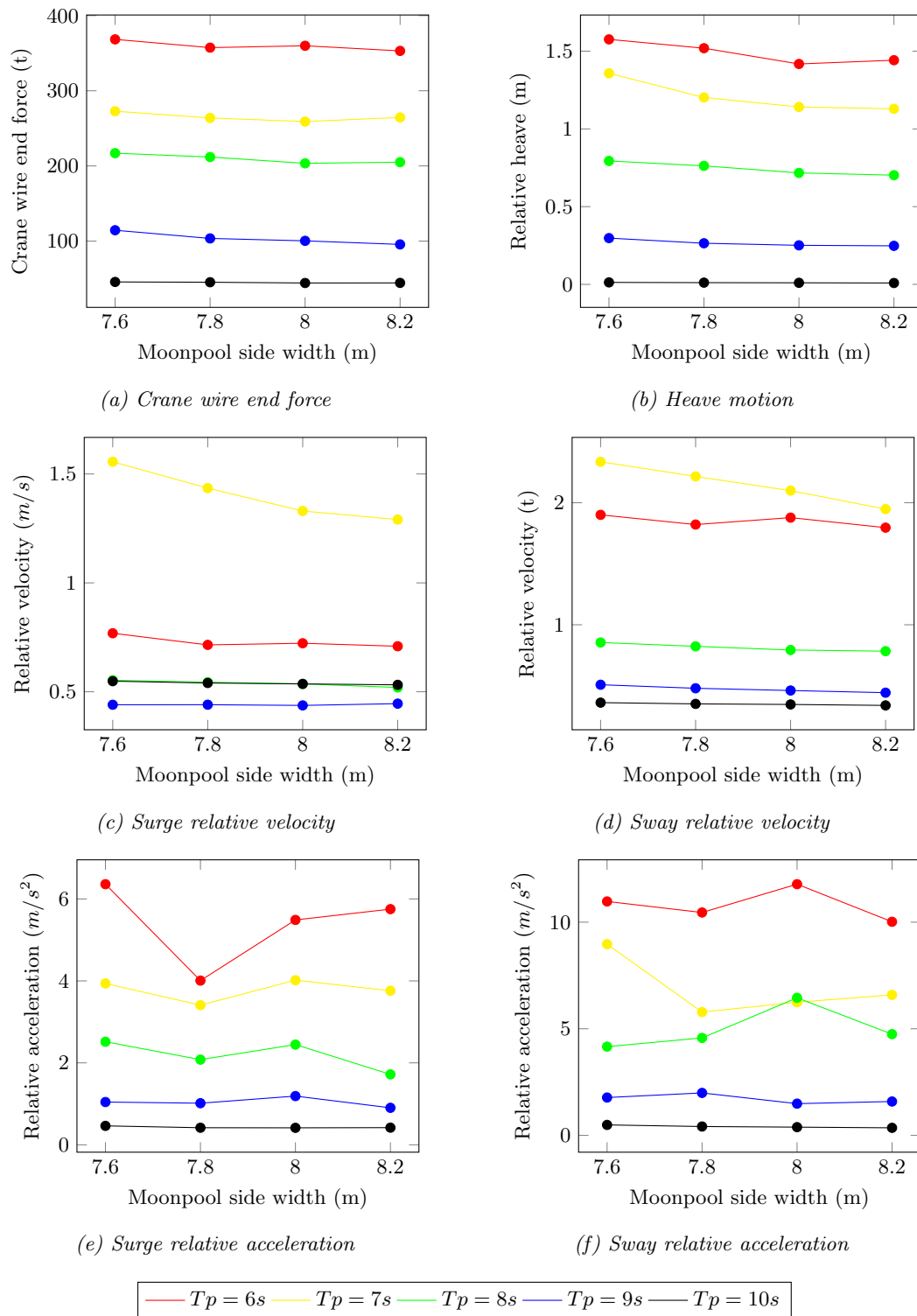


Figure A.7: Moonpool Particulars Case A: Results relative to moonpool at $H_S = 2.5m$ and 180° wave direction

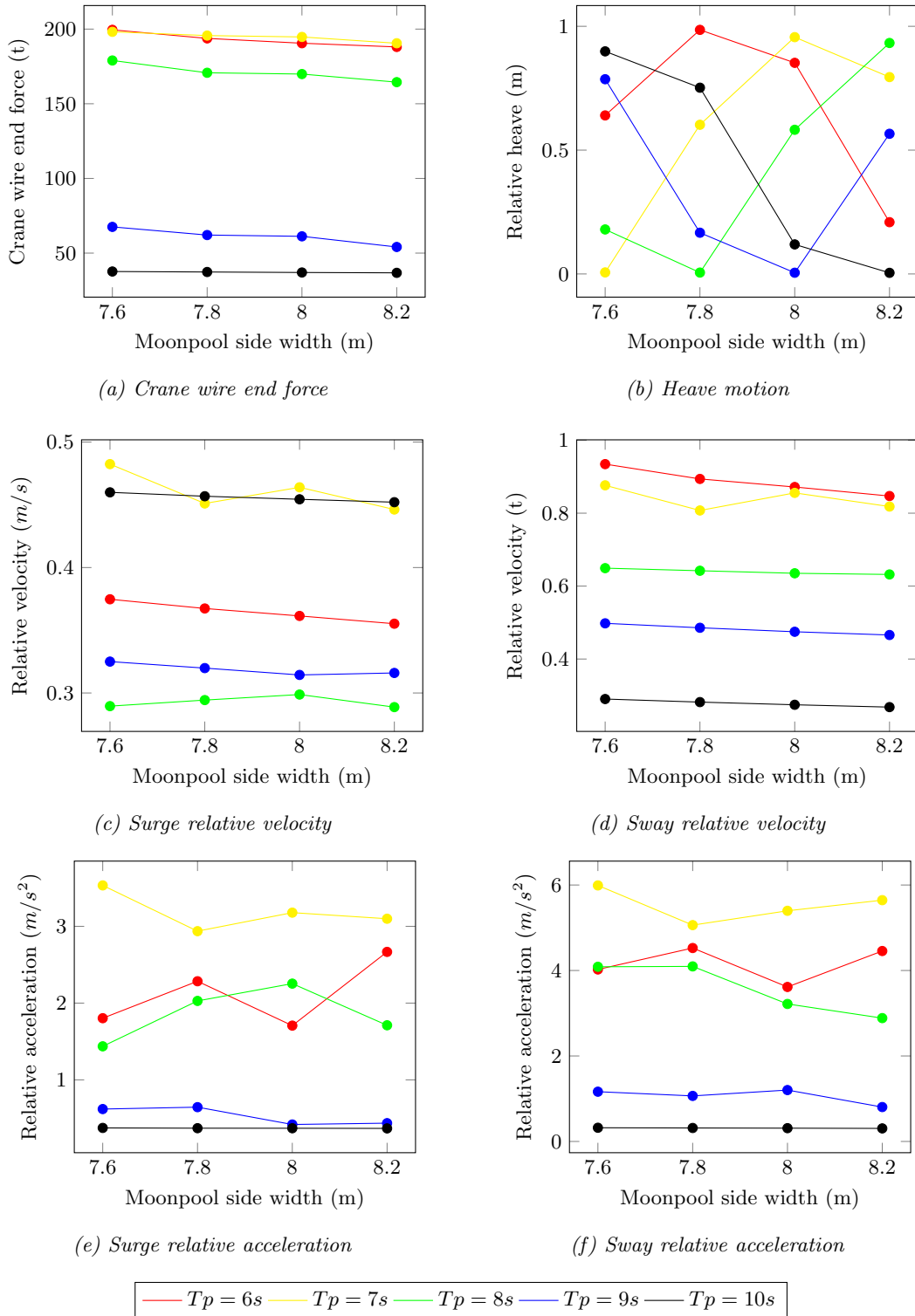


Figure A.8: Moonpool Particulars Case B: Results relative to moonpool at $H_S = 2.5m$ and 180° wave direction

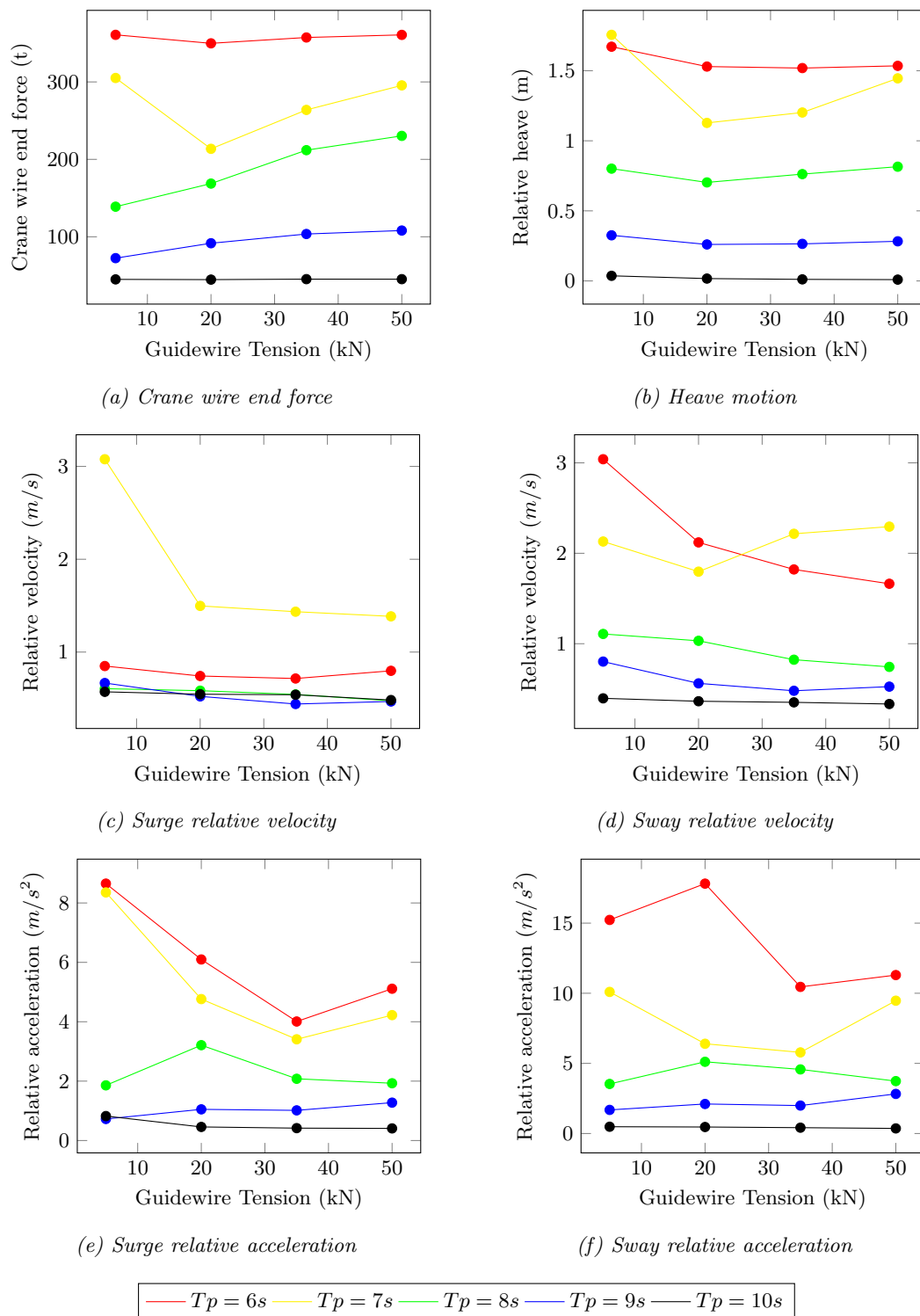


Figure A.9: Guidewire Tension Case A: Results relative to moonpool at $H_S = 2.5m$ and 180° wave direction

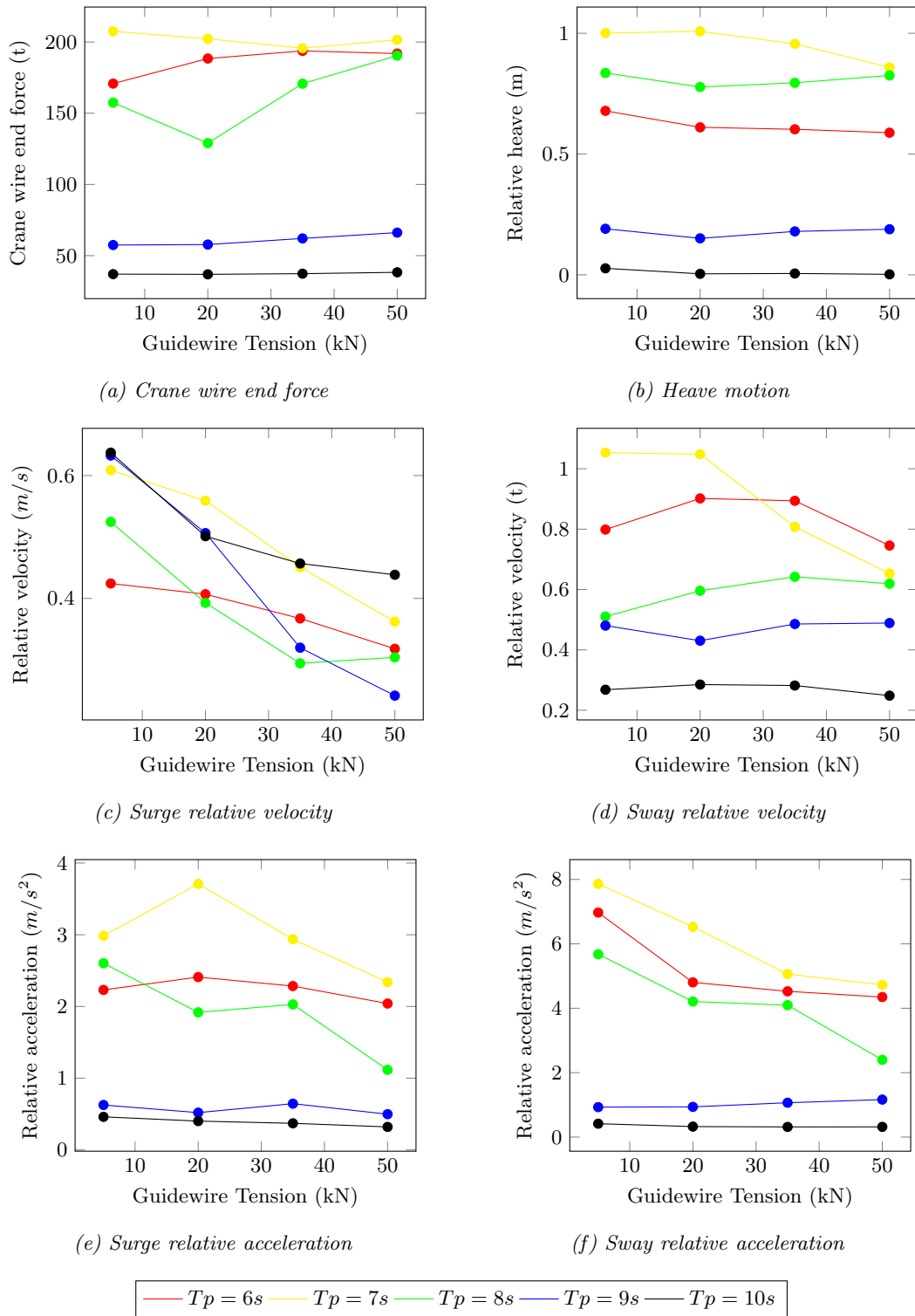
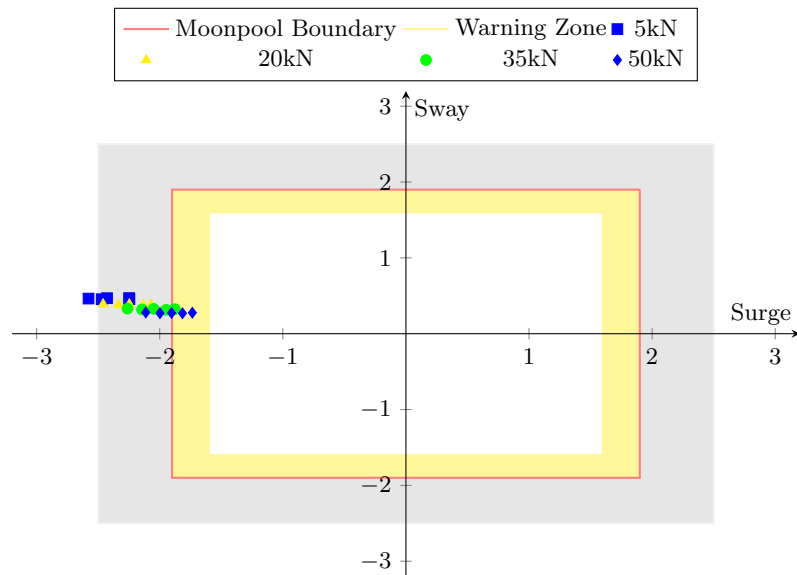
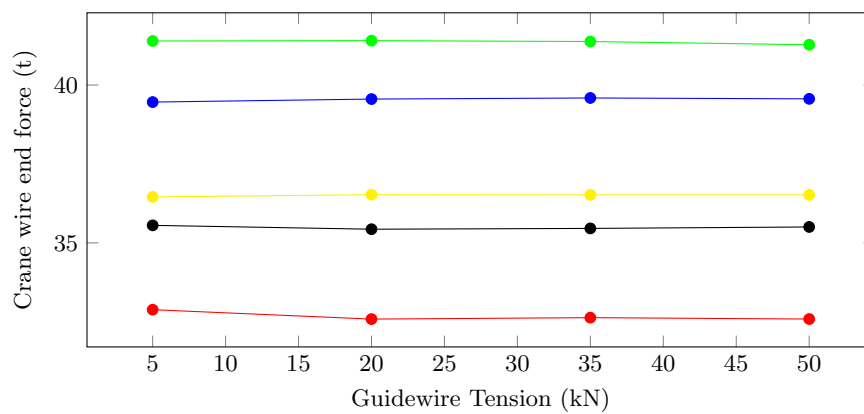


Figure A.10: Guidewire Tension Case B: Results relative to moonpool at $H_S = 2.5m$ and 180° wave direction



(a) Module contact clearance from moonpool bottom edges (Maximum Values) (m)



(b) Crane wire end force

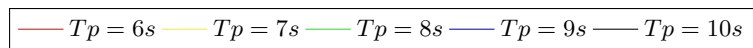
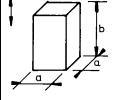
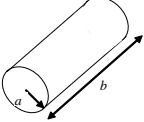
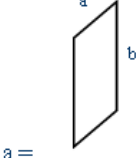


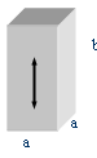
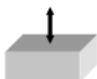
Figure A.11: Guidewire Tension Sensitivity Case C: Results relative to moonpool at $H_S = 2.5\text{m}$ and 180° wave direction

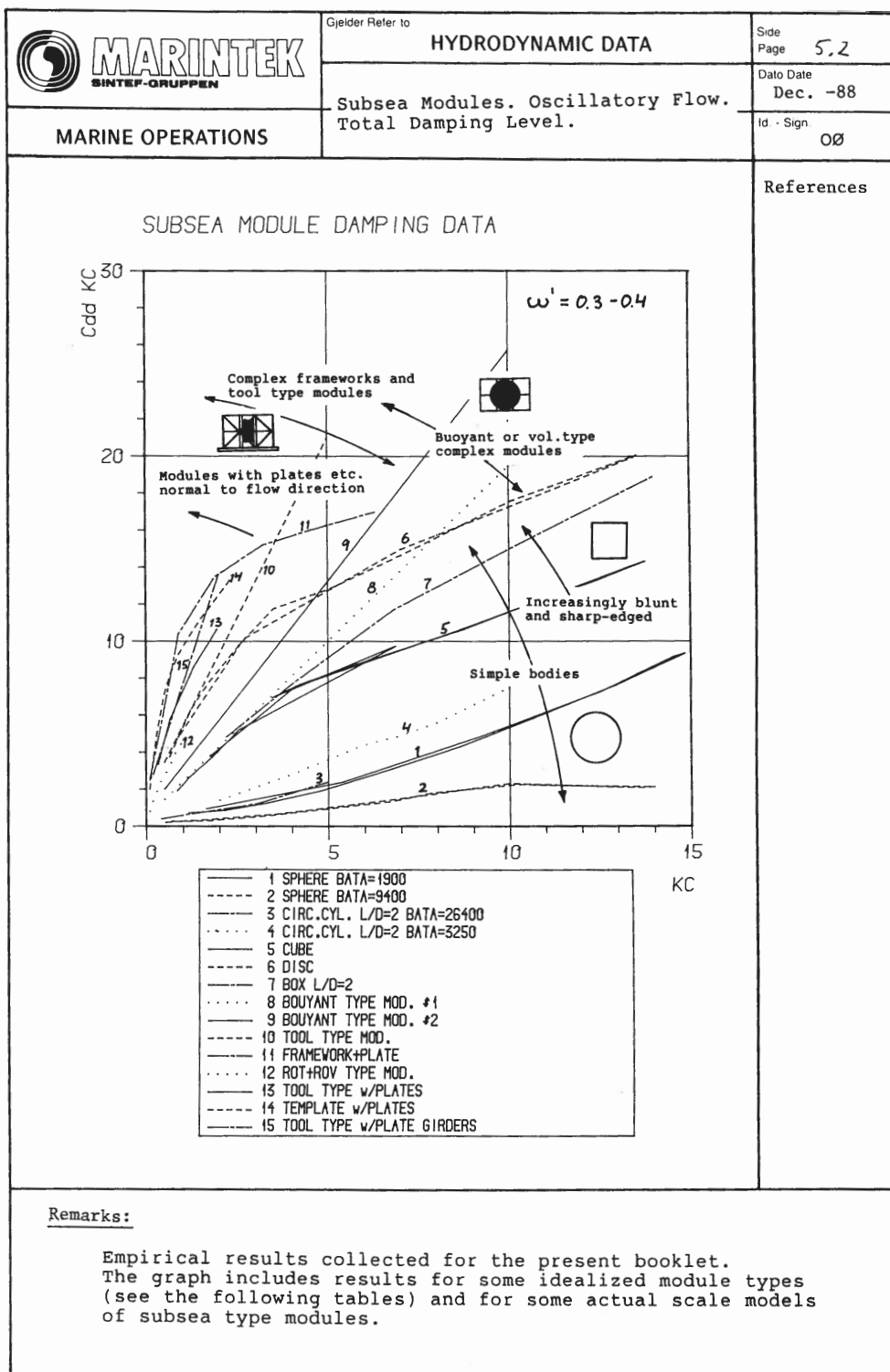
Appendix B

Global Hydrodynamic Coefficient Tables

| Table D-2 Analytical added mass coefficient for three-dimensional bodies in infinite fluid (far from boundaries). Added mass is $m_A = \rho C_A V_R$ [kg] where V_R [m ³] is reference volume. (Continued) | | | | |
|---|---------------------|----------|-------|-------------|
| Body shape | Direction of motion | C_A | | V_R |
| | | b/a | C_A | |
| Square prisms  | Vertical | | | $a^2 b$ |
| | | 1.0 | 0.68 | |
| | | 2.0 | 0.36 | |
| | | 3.0 | 0.24 | |
| | | 4.0 | 0.19 | |
| | | 5.0 | 0.15 | |
| | | 6.0 | 0.13 | |
| | | 7.0 | 0.11 | |
| 10.0 | 0.08 | | | |
| Right circular cylinder  | Vertical | $b/2a$ | C_A | $\pi a^2 b$ |
| | | 1.2 | 0.62 | |
| | | 2.5 | 0.78 | |
| | | 5.0 | 0.90 | |
| | | 9.0 | 0.96 | |
| | | ∞ | 1.00 | |

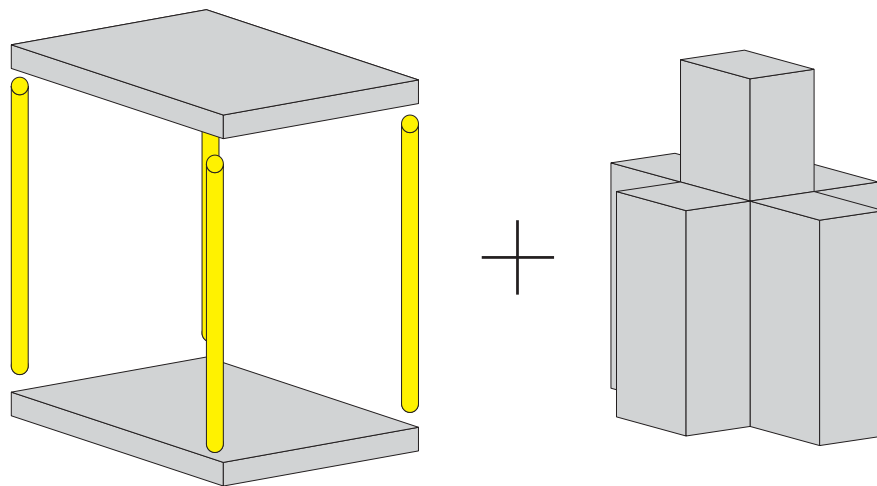
| Geometry | Formula | b/a | α |
|---|--|------|----------|
| Rectan- gular  a = shortest edge | $m_a = \alpha \rho V_c$ Cylinder volume: $V_c = \frac{\pi a^2}{4} b$ | 1.0 | 0.579 |
| | | 1.2 | 0.630 |
| | | 1.25 | 0.642 |
| | | 1.33 | 0.660 |
| | | 1.5 | 0.691 |
| | | 2.0 | 0.757 |
| | | 2.5 | 0.801 |
| | | 3.0 | 0.830 |
| | | 4.0 | 0.871 |
| | | 5.0 | 0.897 |
| | | 8.0 | 0.934 |
| 10.0 | 0.947 | | |

| Geometry | Formula | b/a | α | β |
|--|--|--|----------|---------|
| Rectangular block with quadratic base  a = base edge | $m_a = \alpha \rho V$ $= \beta \rho V_p$ $V = a^2 b$ $V_c = \frac{\pi a^2}{4} b$ | 0 | - | 1.00 |
| | | 0.1 | 5.139 | 1.13 |
| | | 0.3 | 2.016 | 1.33 |
| | | 0.50 | 1.310 | 1.44 |
| | | 0.75 | 0.916 | 1.51 |
| | | 1.00 | 0.705 | 1.55 |
| | | 1.25 | 0.575 | 1.58 |
| | | 1.60 | 0.458 | 1.61 |
| | | 2.00 | 0.373 | 1.64 |
| | | 2.40 | 0.316 | 1.67 |
| | | 2.80 | 0.274 | 1.69 |
| 3.60 | 0.217 | 1.72 | | |
| Rectangular block with rectangular base  | $m_a = \alpha \beta \rho V_c$ $V_p = 0.579 \cdot \frac{\pi a^3}{4}$ | α and V_c from rectangular plate, (1), Table 1 β from (1), this table | | |



Appendix C

Added Mass Calculations



Dividing the module to parts for added mass calculation

Table C.1: CASE A: 7.6 m moonpool size

| Name | | Legs | Roof | Floor | Block 1 | Block 2 | Block 3 | Block 4 |
|-----------------------|-----|----------|-------|-------|---------|---------|---------|---------|
| Shape Type | | Cylinder | Plate | Plate | R.Block | R.Block | R.Block | R.Block |
| Dimesions | a,r | 0.125 | 4 | 4 | 1 | 2 | 2 | 2 |
| | b,t | 0.015 | 4 | 4 | 2 | 2 | 2 | 3 |
| | h | 6 | 0.1 | 0.1 | 3 | 6 | 3 | 4 |
| Load Case | | A | A | A | A | A | A | A |
| Perforation | x | 0 | 0 | 0 | 30.00 | 20.00 | 20.00 | 25.00 |
| | y | 0 | 0 | 0 | 30.00 | 20.00 | 20.00 | 25.00 |
| | z | 90 | 25 | 15 | 30.00 | 20.00 | 20.00 | 25.00 |
| Location from surface | | 0.00 | 0.00 | 5.00 | 3.50 | 2.00 | 3.50 | 3.50 |
| Moonpoolsize | | 57.76 | 57.76 | 57.76 | 57.76 | 57.76 | 57.76 | 57.76 |
| Ca* | x | 0.96 | 0.00 | 0.00 | 0.99 | 1.29 | 1.07 | 0.92 |
| | y | 0.96 | 0.00 | 0.00 | 1.36 | 1.29 | 1.07 | 1.20 |
| | z | 0.96 | 0.58 | 0.58 | 1.28 | 0.98 | 0.91 | 1.13 |
| Reference Volume | x | 0.29 | 50.27 | 50.27 | 9.42 | 18.85 | 9.42 | 28.27 |
| | y | 0.29 | 50.27 | 50.27 | 2.36 | 18.85 | 9.42 | 12.57 |
| | z | 0.29 | 50.27 | 50.27 | 1.57 | 6.28 | 6.28 | 9.42 |
| Trapped Water | x | 0.23 | 0.00 | 0.00 | 0.00 | 0.00 | 0.00 | 0.00 |
| | y | 0.23 | 0.00 | 0.00 | 0.00 | 0.00 | 0.00 | 0.00 |
| | z | 0.00 | 0.00 | 0.00 | 0.00 | 0.00 | 0.00 | 0.00 |
| Perforation Factor | x | 1.00 | 1.00 | 1.00 | 0.56 | 0.76 | 0.76 | 0.64 |
| | y | 1.00 | 1.00 | 1.00 | 0.56 | 0.76 | 0.76 | 0.64 |
| | z | 0.00 | 0.64 | 0.88 | 0.56 | 0.76 | 0.76 | 0.64 |
| Surface Proximity | | 0.50 | 0.50 | 1.00 | 1.00 | 1.00 | 1.00 | 1.00 |
| Moonpool Factor | | 1.00 | 1.11 | 1.11 | 1.00 | 1.00 | 1.00 | 1.01 |
| Ca | x | 0.48 | 0.00 | 0.00 | 1.24 | 0.96 | 0.80 | 0.95 |
| | y | 0.48 | 0.00 | 0.00 | 1.70 | 0.96 | 0.80 | 1.22 |
| | z | 0.00 | 8.63 | 20.84 | 1.60 | 0.73 | 0.68 | 1.16 |
| Cm | x | 1.48 | 1.00 | 1.00 | 2.24 | 1.96 | 1.80 | 1.95 |
| | y | 1.48 | 1.00 | 1.00 | 2.70 | 1.96 | 1.80 | 2.22 |
| | z | 1.00 | 9.63 | 21.84 | 2.60 | 1.73 | 1.68 | 2.16 |
| Cs | x | 0.00 | 5.00 | 5.00 | 0.00 | 0.00 | 0.00 | 0.00 |
| | y | 0.00 | 5.00 | 5.00 | 0.00 | 0.00 | 0.00 | 0.00 |
| | z | 0.00 | 5.00 | 5.00 | 0.00 | 0.00 | 0.00 | 0.00 |
| Hydrodynamic Mass | x | 302 | 1643 | 1643 | 4313 | 19716 | 9858 | 18484 |
| | y | 302 | 1643 | 1643 | 4313 | 19716 | 9858 | 18484 |
| | z | 68 | 1232 | 1397 | 4313 | 19716 | 9858 | 18484 |

Table C.2: CASE A: 7.8 m moonpool size

| Name | | Legs | Roof | Floor | Block 1 | Block 2 | Block 3 | Block 4 |
|-----------------------|-----|----------|-------|-------|---------|----------|---------|---------|
| Shape Type | | Cylinder | Plate | Plate | R.Block | R.Block | R.Block | R.Block |
| Dimesions | a,r | 0.125 | 4 | 4 | 1 | 2 | 2 | 2 |
| | b,t | 0.015 | 4 | 4 | 2 | 2 | 2 | 3 |
| | h | 6 | 0.1 | 0.1 | 3 | 6 | 3 | 4 |
| Load Case | | A | A | A | A | A | A | A |
| Perforation | 1 | 0.00 | 0.00 | 0.00 | 30.00 | 20.00 | 20.00 | 25.00 |
| | 2 | 0.00 | 0.00 | 0.00 | 30.00 | 20.00 | 20.00 | 25.00 |
| | 3 | 90.00 | 25.00 | 15.00 | 30.00 | 20.00 | 20.00 | 25.00 |
| Location from surface | | 0.00 | 0.00 | 5.00 | 3.50 | 2.00 | 3.50 | 3.50 |
| Moonpoolsize | | 60.84 | 60.84 | 60.84 | 60.84 | 60.84 | 60.84 | 60.84 |
| Ca* | x | 0.96 | 0.00 | 0.00 | 0.99 | 1.29 | 1.07 | 0.92 |
| | y | 0.96 | 0.00 | 0.00 | 1.36 | 1.29 | 1.07 | 1.20 |
| | z | 0.96 | 0.58 | 0.58 | 1.28 | 0.98 | 0.91 | 1.13 |
| Reference Volume | x | 0.29 | 50.27 | 50.27 | 9.42 | 18.85 | 9.42 | 28.27 |
| | y | 0.29 | 50.27 | 50.27 | 2.36 | 18.85 | 9.42 | 12.57 |
| | z | 0.29 | 50.27 | 50.27 | 1.57 | 6.28 | 6.28 | 9.42 |
| Trapped Water | x | 0.23 | 0.00 | 0.00 | 0.00 | 0.00 | 0.00 | 0.00 |
| | y | 0.23 | 0.00 | 0.00 | 0.00 | 0.00 | 0.00 | 0.00 |
| | z | 0.00 | 0.00 | 0.00 | 0.00 | 0.00 | 0.00 | 0.00 |
| Perforation Factor | x | 1.00 | 1.00 | 1.00 | 0.56 | 0.76 | 0.76 | 0.64 |
| | y | 1.00 | 1.00 | 1.00 | 0.56 | 0.76 | 0.76 | 0.64 |
| | z | 0.00 | 0.64 | 0.88 | 0.56 | 0.76 | 0.76 | 0.64 |
| Surface Proximity | | 0.50 | 0.50 | 1.00 | 1.00 | 1.00 | 1.00 | 1.00 |
| Moonpool Factor | | 1.00 | 1.09 | 1.09 | 1.00 | 1.00 | 1.00 | 1.01 |
| Ca | x | 0.48 | 0.00 | 0.00 | 1.24 | 0.96 | 0.80 | 0.94 |
| | y | 0.48 | 0.00 | 0.00 | 1.70 | 0.96 | 0.80 | 1.22 |
| | z | 0.00 | 8.53 | 20.62 | 1.60 | 0.73 | 0.68 | 1.16 |
| Cm | x | 1.48 | 1.00 | 1.00 | 2.24 | 1.96 | 1.80 | 1.94 |
| | y | 1.48 | 1.00 | 1.00 | 2.70 | 1.96 | 1.80 | 2.22 |
| | z | 1.00 | 9.53 | 21.62 | 2.60 | 1.73 | 1.68 | 2.16 |
| Cs | x | 0.00 | 5.00 | 5 | 0.00 | 0.00 | 0.00 | 0.00 |
| | y | 0.00 | 5.00 | 5 | 0.00 | 0.00 | 0.00 | 0.00 |
| | z | 0.00 | 5.00 | 5 | 0.00 | 0.00 | 0.00 | 0.00 |
| Hydrodynamic Mass | x | 302 | 1643 | 1643 | 4312.98 | 19716.48 | 9858 | 18484 |
| | y | 302 | 1643 | 1643 | 4312.98 | 19716.48 | 9858 | 18484 |
| | z | 68 | 1232 | 1397 | 4312.98 | 19716.48 | 9858 | 18484 |

Table C.3: CASE A: 8.0 m moonpool size

| Name | | Legs | Roof | Floor | Block 1 | Block 2 | Block 3 | Block 4 |
|-----------------------|-----|----------|-------|-------|---------|---------|---------|---------|
| Shape Type | | Cylinder | Plate | Plate | R.Block | R.Block | R.Block | R.Block |
| Dimesions | a,r | 0.125 | 4 | 4 | 1 | 2 | 2 | 2 |
| | b,t | 0.015 | 4 | 4 | 2 | 2 | 2 | 3 |
| | h | 6 | 0.1 | 0.1 | 3 | 6 | 3 | 4 |
| Load Case | | A | A | A | A | A | A | A |
| Perforation | x | 0.00 | 0.00 | 0.00 | 30.00 | 20.00 | 20.00 | 25.00 |
| | y | 0.00 | 0.00 | 0.00 | 30.00 | 20.00 | 20.00 | 25.00 |
| | z | 90.00 | 25.00 | 15.00 | 30.00 | 20.00 | 20.00 | 25.00 |
| Location from surface | | 0.00 | 0.00 | 5.00 | 3.50 | 2.00 | 3.50 | 3.50 |
| Moonpoolsize | | 64.00 | 64.00 | 64.00 | 64.00 | 64.00 | 64.00 | 64.00 |
| Ca* | x | 0.96 | 0.00 | 0.00 | 0.99 | 1.29 | 1.07 | 0.92 |
| | y | 0.96 | 0.00 | 0.00 | 1.36 | 1.29 | 1.07 | 1.20 |
| | z | 0.96 | 0.58 | 0.58 | 1.28 | 0.98 | 0.91 | 1.13 |
| Reference Volume | x | 0.29 | 50.27 | 50.27 | 9.42 | 18.85 | 9.42 | 28.27 |
| | y | 0.29 | 50.27 | 50.27 | 2.36 | 18.85 | 9.42 | 12.57 |
| | z | 0.29 | 50.27 | 50.27 | 1.57 | 6.28 | 6.28 | 9.42 |
| Trapped Water | x | 0.23 | 0.00 | 0.00 | 0.00 | 0.00 | 0.00 | 0.00 |
| | y | 0.23 | 0.00 | 0.00 | 0.00 | 0.00 | 0.00 | 0.00 |
| | z | 0.00 | 0.00 | 0.00 | 0.00 | 0.00 | 0.00 | 0.00 |
| Perforation Factor | x | 1.00 | 1.00 | 1.00 | 0.56 | 0.76 | 0.76 | 0.64 |
| | y | 1.00 | 1.00 | 1.00 | 0.56 | 0.76 | 0.76 | 0.64 |
| | z | 0.00 | 0.64 | 0.88 | 0.56 | 0.76 | 0.76 | 0.64 |
| Surface Proximity | | 0.50 | 0.50 | 1.00 | 1.00 | 1.00 | 1.00 | 1.00 |
| Moonpool Factor | | 1.00 | 1.08 | 1.08 | 1.00 | 1.00 | 1.00 | 1.01 |
| Ca | x | 0.48 | 0.00 | 0.00 | 1.24 | 0.96 | 0.80 | 0.94 |
| | y | 0.48 | 0.00 | 0.00 | 1.70 | 0.96 | 0.80 | 1.22 |
| | z | 0.00 | 8.46 | 20.43 | 1.60 | 0.73 | 0.68 | 1.15 |
| Cm | x | 1.48 | 1.00 | 1.00 | 2.24 | 1.96 | 1.80 | 1.94 |
| | y | 1.48 | 1.00 | 1.00 | 2.70 | 1.96 | 1.80 | 2.22 |
| | z | 1.00 | 9.46 | 21.43 | 2.60 | 1.73 | 1.68 | 2.15 |
| Cs | x | 0.00 | 5.00 | 5.00 | 0.00 | 0.00 | 0.00 | 0.00 |
| | y | 0.00 | 5.00 | 5.00 | 0.00 | 0.00 | 0.00 | 0.00 |
| | z | 0.00 | 5.00 | 5.00 | 0.00 | 0.00 | 0.00 | 0.00 |
| Hydrodynamic Mass | x | 302 | 1643 | 1643 | 4313 | 19716 | 9858 | 18484 |
| | y | 302 | 1643 | 1643 | 4313 | 19716 | 9858 | 18484 |
| | z | 68 | 1232 | 1397 | 4313 | 19716 | 9858 | 18484 |

Table C.4: CASE A: 8.2 m moonpool size

| Name | | Legs | Roof | Floor | Block 1 | Block 2 | Block 3 | Block 4 |
|-----------------------|-----|----------|-------|-------|---------|---------|---------|---------|
| Shape Type | | Cylinder | Plate | Plate | R.Block | R.Block | R.Block | R.Block |
| Dimesions | a,r | 0.125 | 4 | 4 | 1 | 2 | 2 | 2 |
| | b,t | 0.015 | 4 | 4 | 2 | 2 | 2 | 3 |
| | h | 6 | 0.1 | 0.1 | 3 | 6 | 3 | 4 |
| Load Case | | A | A | A | A | A | A | A |
| Perforation | x | 0.00 | 0.00 | 0.00 | 30.00 | 20.00 | 20.00 | 25.00 |
| | y | 0.00 | 0.00 | 0.00 | 30.00 | 20.00 | 20.00 | 25.00 |
| | z | 90.00 | 25.00 | 15.00 | 30.00 | 20.00 | 20.00 | 25.00 |
| Location from surface | | 0.00 | 0.00 | 5.00 | 3.50 | 2.00 | 3.50 | 3.50 |
| Moonpoolsize | | 67.24 | 67.24 | 67.24 | 67.24 | 67.24 | 67.24 | 67.24 |
| Ca* | x | 0.96 | 0.00 | 0.00 | 0.99 | 1.29 | 1.07 | 0.92 |
| | y | 0.96 | 0.00 | 0.00 | 1.36 | 1.29 | 1.07 | 1.20 |
| | z | 0.96 | 0.58 | 0.58 | 1.28 | 0.98 | 0.91 | 1.13 |
| Reference Volume | x | 0.29 | 50.27 | 50.27 | 9.42 | 18.85 | 9.42 | 28.27 |
| | y | 0.29 | 50.27 | 50.27 | 2.36 | 18.85 | 9.42 | 12.57 |
| | z | 0.29 | 50.27 | 50.27 | 1.57 | 6.28 | 6.28 | 9.42 |
| Trapped Water | x | 0.23 | 0.00 | 0.00 | 0.00 | 0.00 | 0.00 | 0.00 |
| | y | 0.23 | 0.00 | 0.00 | 0.00 | 0.00 | 0.00 | 0.00 |
| | z | 0.00 | 0.00 | 0.00 | 0.00 | 0.00 | 0.00 | 0.00 |
| Perforation Factor | x | 1.00 | 1.00 | 1.00 | 0.56 | 0.76 | 0.76 | 0.64 |
| | y | 1.00 | 1.00 | 1.00 | 0.56 | 0.76 | 0.76 | 0.64 |
| | z | 0.00 | 0.64 | 0.88 | 0.56 | 0.76 | 0.76 | 0.64 |
| Surface Proximity | | 0.50 | 0.50 | 1.00 | 1.00 | 1.00 | 1.00 | 1.00 |
| Moonpool Factor | | 1.00 | 1.08 | 1.08 | 1.00 | 1.00 | 1.00 | 1.01 |
| Ca | x | 0.48 | 0.00 | 0.00 | 1.24 | 0.96 | 0.80 | 0.94 |
| | y | 0.48 | 0.00 | 0.00 | 1.70 | 0.96 | 0.80 | 1.22 |
| | z | 0.00 | 8.39 | 20.26 | 1.60 | 0.73 | 0.68 | 1.15 |
| Cm | x | 1.48 | 1.00 | 1.00 | 2.24 | 1.96 | 1.80 | 1.94 |
| | y | 1.48 | 1.00 | 1.00 | 2.70 | 1.96 | 1.80 | 2.22 |
| | z | 1.00 | 9.39 | 21.26 | 2.60 | 1.73 | 1.68 | 2.15 |
| Cs | x | 0.00 | 5.00 | 5.00 | 0.00 | 0.00 | 0.00 | 0.00 |
| | y | 0.00 | 5.00 | 5.00 | 0.00 | 0.00 | 0.00 | 0.00 |
| | z | 0.00 | 5.00 | 5.00 | 0.00 | 0.00 | 0.00 | 0.00 |
| Hydrodynamic Mass | x | 302 | 1643 | 1643 | 4313 | 19716 | 9858 | 18484 |
| | y | 302 | 1643 | 1643 | 4313 | 19716 | 9858 | 18484 |
| | z | 68 | 1232 | 1397 | 4313 | 19716 | 9858 | 18484 |

Table C.5: CASE B: 7.6 m moonpool size

| Name | | Legs | Roof | Floor | Block 1 | Block 2 | Block 3 | Block 4 |
|-----------------------|-----|----------|-------|-------|---------|---------|---------|---------|
| Shape Type | | Cylinder | Plate | Plate | R.Block | R.Block | R.Block | R.Block |
| Dimesions | a,r | 0.125 | 4 | 4 | 1 | 2 | 2 | 2 |
| | b,t | 0.015 | 4 | 4 | 2 | 2 | 2 | 3 |
| | h | 6 | 0.1 | 0.1 | 3 | 6 | 3 | 4 |
| Load Case | | B | B | B | B | B | B | B |
| Perforation | x | 0.00 | 0.00 | 0.00 | 30.00 | 20.00 | 20.00 | 25.00 |
| | y | 0.00 | 0.00 | 0.00 | 30.00 | 20.00 | 20.00 | 25.00 |
| | z | 90.00 | 25.00 | 15.00 | 30.00 | 20.00 | 20.00 | 25.00 |
| Location from surface | | 1.00 | 1.00 | 7.00 | 5.50 | 4.00 | 5.50 | 5.50 |
| Moonpoolsize | | 57.76 | 57.76 | 57.76 | 57.76 | 57.76 | 57.76 | 57.76 |
| Ca* | x | 0.96 | 0.00 | 0.00 | 0.99 | 1.29 | 1.07 | 0.92 |
| | y | 0.96 | 0.00 | 0.00 | 1.36 | 1.29 | 1.07 | 1.20 |
| | z | 0.96 | 0.58 | 0.58 | 1.28 | 0.98 | 0.91 | 1.13 |
| Reference Volume | x | 0.29 | 50.27 | 50.27 | 9.42 | 18.85 | 9.42 | 28.27 |
| | y | 0.29 | 50.27 | 50.27 | 2.36 | 18.85 | 9.42 | 12.57 |
| | z | 0.29 | 50.27 | 50.27 | 1.57 | 6.28 | 6.28 | 9.42 |
| Trapped Water | x | 0.23 | 0.00 | 0.00 | 0.00 | 0.00 | 0.00 | 0.00 |
| | y | 0.23 | 0.00 | 0.00 | 0.00 | 0.00 | 0.00 | 0.00 |
| | z | 0.00 | 0.00 | 0.00 | 0.00 | 0.00 | 0.00 | 0.00 |
| Perforation Factor | x | 1.00 | 1.00 | 1.00 | 0.56 | 0.76 | 0.76 | 0.64 |
| | y | 1.00 | 1.00 | 1.00 | 0.56 | 0.76 | 0.76 | 0.64 |
| | z | 0.00 | 0.64 | 0.88 | 0.56 | 0.76 | 0.76 | 0.64 |
| Surface Proximity | | 1.00 | 0.66 | 1.00 | 1.00 | 1.00 | 1.00 | 1.00 |
| Moonpool Factor | | 1.00 | 1.11 | 1.11 | 1.00 | 1.00 | 1.00 | 1.01 |
| Ca | x | 0.96 | 0.00 | 0.00 | 1.24 | 0.96 | 0.80 | 0.95 |
| | y | 0.96 | 0.00 | 0.00 | 1.70 | 0.96 | 0.80 | 1.22 |
| | z | 0.00 | 11.34 | 20.84 | 1.60 | 0.73 | 0.68 | 1.16 |
| Cm | x | 1.96 | 1.00 | 1.00 | 2.24 | 1.96 | 1.80 | 1.95 |
| | y | 1.96 | 1.00 | 1.00 | 2.70 | 1.96 | 1.80 | 2.22 |
| | z | 1.00 | 12.34 | 21.84 | 2.60 | 1.73 | 1.68 | 2.16 |
| Cs | x | 0.00 | 5.00 | 5.00 | 0.00 | 0.00 | 0.00 | 0.00 |
| | y | 0.00 | 5.00 | 5.00 | 0.00 | 0.00 | 0.00 | 0.00 |
| | z | 0.00 | 5.00 | 5.00 | 0.00 | 0.00 | 0.00 | 0.00 |
| Hydrodynamic Mass | x | 302 | 1643 | 1643 | 4313 | 19716 | 9858 | 18484 |
| | y | 302 | 1643 | 1643 | 4313 | 19716 | 9858 | 18484 |
| | z | 68 | 1232 | 1397 | 4313 | 19716 | 9858 | 18484 |

Table C.6: CASE B: 7.8 m moonpool size

| Name | | Legs | Roof | Floor | Block 1 | Block 2 | Block 3 | Block 4 |
|-----------------------|-----|----------|-------|-------|---------|---------|---------|---------|
| Shape Type | | Cylinder | Plate | Plate | R.Block | R.Block | R.Block | R.Block |
| Dimesions | a,r | 0.125 | 4 | 4 | 1 | 2 | 2 | 2 |
| | b,t | 0.015 | 4 | 4 | 2 | 2 | 2 | 3 |
| | h | 6 | 0.1 | 0.1 | 3 | 6 | 3 | 4 |
| Load Case | | B | B | B | B | B | B | B |
| Perforation | x | 0.00 | 0.00 | 0.00 | 30.00 | 20.00 | 20.00 | 25.00 |
| | y | 0.00 | 0.00 | 0.00 | 30.00 | 20.00 | 20.00 | 25.00 |
| | z | 90.00 | 25.00 | 15.00 | 30.00 | 20.00 | 20.00 | 25.00 |
| Location from surface | | 1.00 | 1.00 | 7.00 | 5.50 | 4.00 | 5.50 | 5.50 |
| Moonpoolsize | | 60.84 | 60.84 | 60.84 | 60.84 | 60.84 | 60.84 | 60.84 |
| Ca* | x | 0.96 | 0.00 | 0.00 | 0.99 | 1.29 | 1.07 | 0.92 |
| | y | 0.96 | 0.00 | 0.00 | 1.36 | 1.29 | 1.07 | 1.20 |
| | z | 0.96 | 0.58 | 0.58 | 1.28 | 0.98 | 0.91 | 1.13 |
| Reference Volume | x | 0.29 | 50.27 | 50.27 | 9.42 | 18.85 | 9.42 | 28.27 |
| | y | 0.29 | 50.27 | 50.27 | 2.36 | 18.85 | 9.42 | 12.57 |
| | z | 0.29 | 50.27 | 50.27 | 1.57 | 6.28 | 6.28 | 9.42 |
| Trapped Water | x | 0.23 | 0.00 | 0.00 | 0.00 | 0.00 | 0.00 | 0.00 |
| | y | 0.23 | 0.00 | 0.00 | 0.00 | 0.00 | 0.00 | 0.00 |
| | z | 0.00 | 0.00 | 0.00 | 0.00 | 0.00 | 0.00 | 0.00 |
| Perforation Factor | x | 1.00 | 1.00 | 1.00 | 0.56 | 0.76 | 0.76 | 0.64 |
| | y | 1.00 | 1.00 | 1.00 | 0.56 | 0.76 | 0.76 | 0.64 |
| | z | 0.00 | 0.64 | 0.88 | 0.56 | 0.76 | 0.76 | 0.64 |
| Surface Proximity | | 1.00 | 0.66 | 1.00 | 1.00 | 1.00 | 1.00 | 1.00 |
| Moonpool Factor | | 1.00 | 1.09 | 1.09 | 1.00 | 1.00 | 1.00 | 1.01 |
| Ca | x | 0.96 | 0.00 | 0.00 | 1.24 | 0.96 | 0.80 | 0.94 |
| | y | 0.96 | 0.00 | 0.00 | 1.70 | 0.96 | 0.80 | 1.22 |
| | z | 0.00 | 11.22 | 20.62 | 1.60 | 0.73 | 0.68 | 1.16 |
| Cm | x | 1.96 | 1.00 | 1.00 | 2.24 | 1.96 | 1.80 | 1.94 |
| | y | 1.96 | 1.00 | 1.00 | 2.70 | 1.96 | 1.80 | 2.22 |
| | z | 1.00 | 12.22 | 21.62 | 2.60 | 1.73 | 1.68 | 2.16 |
| Cs | x | 0 | 5 | 5 | 0 | 0 | 0 | 0 |
| | y | 0 | 5 | 5 | 0 | 0 | 0 | 0 |
| | z | 0 | 5 | 5 | 0 | 0 | 0 | 0 |
| Hydrodynamic Mass | x | 302 | 1643 | 1643 | 4313 | 19716 | 9858 | 18484 |
| | y | 302 | 1643 | 1643 | 4313 | 19716 | 9858 | 18484 |
| | z | 68 | 1232 | 1397 | 4313 | 19716 | 9858 | 18484 |

Table C.7: CASE B: 8.0 m moonpool size

| Name | | Legs | Roof | Floor | Block 1 | Block 2 | Block 3 | Block 4 |
|-----------------------|-----|----------|-------|-------|---------|---------|---------|---------|
| Shape Type | | Cylinder | Plate | Plate | R.Block | R.Block | R.Block | R.Block |
| Dimesions | a,r | 0.125 | 4 | 4 | 1 | 2 | 2 | 2 |
| | b,t | 0.015 | 4 | 4 | 2 | 2 | 2 | 3 |
| | h | 6 | 0.1 | 0.1 | 3 | 6 | 3 | 4 |
| Load Case | | B | B | B | B | B | B | B |
| Perforation | x | 0.00 | 0.00 | 0.00 | 30.00 | 20.00 | 20.00 | 25.00 |
| | y | 0.00 | 0.00 | 0.00 | 30.00 | 20.00 | 20.00 | 25.00 |
| | z | 90.00 | 25.00 | 15.00 | 30.00 | 20.00 | 20.00 | 25.00 |
| Location from surface | | 1.00 | 1.00 | 7.00 | 5.50 | 4.00 | 5.50 | 5.50 |
| Moonpoolsize | | 64.00 | 64.00 | 64.00 | 64.00 | 64.00 | 64.00 | 64.00 |
| Ca* | x | 0.96 | 0.00 | 0.00 | 0.99 | 1.29 | 1.07 | 0.92 |
| | y | 0.96 | 0.00 | 0.00 | 1.36 | 1.29 | 1.07 | 1.20 |
| | z | 0.96 | 0.58 | 0.58 | 1.28 | 0.98 | 0.91 | 1.13 |
| Reference Volume | x | 0.29 | 50.27 | 50.27 | 9.42 | 18.85 | 9.42 | 28.27 |
| | y | 0.29 | 50.27 | 50.27 | 2.36 | 18.85 | 9.42 | 12.57 |
| | z | 0.29 | 50.27 | 50.27 | 1.57 | 6.28 | 6.28 | 9.42 |
| Trapped Water | x | 0.23 | 0.00 | 0.00 | 0.00 | 0.00 | 0.00 | 0.00 |
| | y | 0.23 | 0.00 | 0.00 | 0.00 | 0.00 | 0.00 | 0.00 |
| | z | 0.00 | 0.00 | 0.00 | 0.00 | 0.00 | 0.00 | 0.00 |
| Perforation Factor | x | 1.00 | 1.00 | 1.00 | 0.56 | 0.76 | 0.76 | 0.64 |
| | y | 1.00 | 1.00 | 1.00 | 0.56 | 0.76 | 0.76 | 0.64 |
| | z | 0.00 | 0.64 | 0.88 | 0.56 | 0.76 | 0.76 | 0.64 |
| Surface Proximity | | 1.00 | 0.66 | 1.00 | 1.00 | 1.00 | 1.00 | 1.00 |
| Moonpool Factor | | 1.00 | 1.08 | 1.08 | 1.00 | 1.00 | 1.00 | 1.01 |
| Ca | x | 0.96 | 0.00 | 0.00 | 1.24 | 0.96 | 0.80 | 0.94 |
| | y | 0.96 | 0.00 | 0.00 | 1.70 | 0.96 | 0.80 | 1.22 |
| | z | 0.00 | 11.12 | 20.43 | 1.60 | 0.73 | 0.68 | 1.15 |
| Cm | x | 1.96 | 1.00 | 1.00 | 2.24 | 1.96 | 1.80 | 1.94 |
| | y | 1.96 | 1.00 | 1.00 | 2.70 | 1.96 | 1.80 | 2.22 |
| | z | 1.00 | 12.12 | 21.43 | 2.60 | 1.73 | 1.68 | 2.15 |
| Cs | x | 0.00 | 5.00 | 5.00 | 0.00 | 0.00 | 0.00 | 0.00 |
| | y | 0.00 | 5.00 | 5.00 | 0.00 | 0.00 | 0.00 | 0.00 |
| | z | 0.00 | 5.00 | 5.00 | 0.00 | 0.00 | 0.00 | 0.00 |
| Hydrodynamic Mass | x | 302 | 1643 | 1643 | 4313 | 19716 | 9858 | 18484 |
| | y | 302 | 1643 | 1643 | 4313 | 19716 | 9858 | 18484 |
| | z | 68 | 1232 | 1397 | 4313 | 19716 | 9858 | 18484 |

Table C.8: CASE B: 8.2 m moonpool size

| Name | | Legs | Roof | Floor | Block 1 | Block 2 | Block 3 | Block 4 |
|-----------------------|-----|----------|-------|-------|---------|---------|---------|---------|
| Shape Type | | Cylinder | Plate | Plate | R.Block | R.Block | R.Block | R.Block |
| Dimesions | a,r | 0.125 | 4 | 4 | 1 | 2 | 2 | 2 |
| | b,t | 0.015 | 4 | 4 | 2 | 2 | 2 | 3 |
| | h | 6 | 0.1 | 0.1 | 3 | 6 | 3 | 4 |
| Load Case | | B | B | B | B | B | B | B |
| Perforation | x | 0.00 | 0.00 | 0.00 | 30.00 | 20.00 | 20.00 | 25.00 |
| | y | 0.00 | 0.00 | 0.00 | 30.00 | 20.00 | 20.00 | 25.00 |
| | z | 90.00 | 25.00 | 15.00 | 30.00 | 20.00 | 20.00 | 25.00 |
| Location from surface | | 1.00 | 1.00 | 7.00 | 5.50 | 4.00 | 5.50 | 5.50 |
| Moonpoolsize | | 67.24 | 67.24 | 67.24 | 67.24 | 67.24 | 67.24 | 67.24 |
| Ca* | x | 0.96 | 0.00 | 0.00 | 0.99 | 1.29 | 1.07 | 0.92 |
| | y | 0.96 | 0.00 | 0.00 | 1.36 | 1.29 | 1.07 | 1.20 |
| | z | 0.96 | 0.58 | 0.58 | 1.28 | 0.98 | 0.91 | 1.13 |
| Reference Volume | x | 0.29 | 50.27 | 50.27 | 9.42 | 18.85 | 9.42 | 28.27 |
| | y | 0.29 | 50.27 | 50.27 | 2.36 | 18.85 | 9.42 | 12.57 |
| | z | 0.29 | 50.27 | 50.27 | 1.57 | 6.28 | 6.28 | 9.42 |
| Trapped Water | x | 0.23 | 0.00 | 0.00 | 0.00 | 0.00 | 0.00 | 0.00 |
| | y | 0.23 | 0.00 | 0.00 | 0.00 | 0.00 | 0.00 | 0.00 |
| | z | 0.00 | 0.00 | 0.00 | 0.00 | 0.00 | 0.00 | 0.00 |
| Perforation Factor | x | 1.00 | 1.00 | 1.00 | 0.56 | 0.76 | 0.76 | 0.64 |
| | y | 1.00 | 1.00 | 1.00 | 0.56 | 0.76 | 0.76 | 0.64 |
| | z | 0.00 | 0.64 | 0.88 | 0.56 | 0.76 | 0.76 | 0.64 |
| Surface Proximity | | 1.00 | 0.66 | 1.00 | 1.00 | 1.00 | 1.00 | 1.00 |
| Moonpool Factor | | 1.00 | 1.08 | 1.08 | 1.00 | 1.00 | 1.00 | 1.01 |
| Ca | x | 0.96 | 0.00 | 0.00 | 1.24 | 0.96 | 0.80 | 0.94 |
| | y | 0.96 | 0.00 | 0.00 | 1.70 | 0.96 | 0.80 | 1.22 |
| | z | 0.00 | 11.03 | 20.26 | 1.60 | 0.73 | 0.68 | 1.15 |
| Cm | x | 1.96 | 1.00 | 1.00 | 2.24 | 1.96 | 1.80 | 1.94 |
| | y | 1.96 | 1.00 | 1.00 | 2.70 | 1.96 | 1.80 | 2.22 |
| | z | 1.00 | 12.03 | 21.26 | 2.60 | 1.73 | 1.68 | 2.15 |
| Cs | x | 0.00 | 5.00 | 5.00 | 0.00 | 0.00 | 0.00 | 0.00 |
| | y | 0.00 | 5.00 | 5.00 | 0.00 | 0.00 | 0.00 | 0.00 |
| | z | 0.00 | 5.00 | 5.00 | 0.00 | 0.00 | 0.00 | 0.00 |
| Hydrodynamic Mass | x | 302 | 1643 | 1643 | 4313 | 19716 | 9858 | 18484 |
| | y | 302 | 1643 | 1643 | 4313 | 19716 | 9858 | 18484 |
| | z | 68 | 1232 | 1397 | 4313 | 19716 | 9858 | 18484 |

Table C.9: CASE C

| Name | | Legs | Roof | Floor | Block 1 | Block 2 | Block 3 | Block 4 |
|-----------------------|-----|----------|-------|-------|---------|---------|---------|---------|
| Shape Type | | Cylinder | Plate | Plate | R.Block | R.Block | R.Block | R.Block |
| Dimesions | a,r | 0.125 | 4 | 4 | 1 | 2 | 2 | 2 |
| | b,t | 0.015 | 4 | 4 | 2 | 2 | 2 | 3 |
| | h | 6 | 0.1 | 0.1 | 3 | 6 | 3 | 4 |
| Load Case | | C | C | C | C | C | C | C |
| Perforation | x | 0.00 | 0.00 | 0.00 | 30.00 | 20.00 | 20.00 | 25.00 |
| | y | 0.00 | 0.00 | 0.00 | 30.00 | 20.00 | 20.00 | 25.00 |
| | z | 90.00 | 25.00 | 15.00 | 30.00 | 20.00 | 20.00 | 25.00 |
| Location from surface | | 10.70 | 10.70 | 10.70 | 10.70 | 10.70 | 10.70 | 10.70 |
| Moonpoolsize | | 60.84 | 60.84 | 60.84 | 60.84 | 60.84 | 60.84 | 60.84 |
| Ca* | x | 0.96 | 0.00 | 0.00 | 0.99 | 1.29 | 1.07 | 0.92 |
| | y | 0.96 | 0.00 | 0.00 | 1.36 | 1.29 | 1.07 | 1.20 |
| | z | 0.96 | 0.58 | 0.58 | 1.28 | 0.98 | 0.91 | 1.13 |
| Reference Volume | x | 0.29 | 50.27 | 50.27 | 9.42 | 18.85 | 9.42 | 28.27 |
| | y | 0.29 | 50.27 | 50.27 | 2.36 | 18.85 | 9.42 | 12.57 |
| | z | 0.29 | 50.27 | 50.27 | 1.57 | 6.28 | 6.28 | 9.42 |
| Trapped Water | x | 0.23 | 0.00 | 0.00 | 0.00 | 0.00 | 0.00 | 0.00 |
| | y | 0.23 | 0.00 | 0.00 | 0.00 | 0.00 | 0.00 | 0.00 |
| | z | 0.00 | 0.00 | 0.00 | 0.00 | 0.00 | 0.00 | 0.00 |
| Perforation Factor | x | 1.00 | 1.00 | 1.00 | 0.56 | 0.76 | 0.76 | 0.64 |
| | y | 1.00 | 1.00 | 1.00 | 0.56 | 0.76 | 0.76 | 0.64 |
| | z | 0.00 | 0.64 | 0.88 | 0.56 | 0.76 | 0.76 | 0.64 |
| Surface Proximity | | 1.00 | 1.00 | 1.00 | 1.00 | 1.00 | 1.00 | 1.00 |
| Moonpool Factor | | 1.00 | 1.00 | 1.00 | 1.00 | 1.00 | 1.00 | 1.00 |
| Ca | x | 0.96 | 0.00 | 0.00 | 1.24 | 0.95 | 0.79 | 0.93 |
| | y | 0.96 | 0.00 | 0.00 | 1.70 | 0.95 | 0.79 | 1.21 |
| | z | 0.00 | 15.60 | 18.85 | 1.59 | 0.73 | 0.68 | 1.14 |
| Cm | x | 1.96 | 1.00 | 1.00 | 2.24 | 1.95 | 1.79 | 1.93 |
| | y | 1.96 | 1.00 | 1.00 | 2.70 | 1.95 | 1.79 | 2.21 |
| | z | 1.00 | 16.60 | 19.85 | 2.59 | 1.73 | 1.68 | 2.14 |
| Cs | x | 0.00 | 5.00 | 5.00 | 0.00 | 0.00 | 0.00 | 0.00 |
| | y | 0.00 | 5.00 | 5.00 | 0.00 | 0.00 | 0.00 | 0.00 |
| | z | 0.00 | 5.00 | 5.00 | 0.00 | 0.00 | 0.00 | 0.00 |
| Hydrodynamic Mass | x | 302 | 1643 | 1643 | 4313 | 19716 | 9858 | 18484 |
| | y | 302 | 1643 | 1643 | 4313 | 19716 | 9858 | 18484 |
| | z | 68 | 1232 | 1397 | 4313 | 19716 | 9858 | 18484 |

Appendix D

Failure Mode Effects Analysis

Table D.1: FMEA of RLWI deployment operation

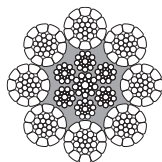
| No. | Equipment/ procedure name | Function | Failure mode | Failure Effect- local | Failure effect – end effect | Failure detection | Alternative provisions/ redundancy/ Barriers |
|-----|------------------------------|---|-----------------------------------|--------------------------------|---|---|---|
| 1. | Locking of WCP to RT | Lifting Support | Fracture Fatigue | Running tool disconnected | Lift off failure | Testing of valves and connection | Several locking mechanism |
| 2 | Moving WCP to moonpool | Positioning for next procedure | Getting trapped or stuck | Delay | Loss of rig time | Human detection | Lubrication/ maintenance |
| 3 | Umbilical Connection | Communication during Wireline runs | Electrical/ hydraulic/ mechanical | Loss of communication | Operation shut down | Work over control system (WOCS) | Proper design and analysis of the Umbilical Termination Head |
| 4 | Guide Wires | Guide the stack from lateral motions | Plastic deformation/ rupture | Loss of hydrodynamic stability | Clashing or drift off | Analysis of maximum expected hydrodynamic load | High tension capacity wires or Reduce weight of equipment |
| 5 | Landing of WCP | To lock the WCP | High landing speed | Impact force on WCP and XT | Damage the Equipment | Analysis of Maximum possible heave speed | Use active heave compensator to reduce the heave velocity |
| 6 | WROV | Disconnect Running tools | Mechanical/ electrical failure | unable to remove running tool | Operation halted until ROV fixed | ROV panel control system | Use additional WROV and continuous maintenance to reduce risk |
| 7 | WCP to LS connection | Seal the connection | Incorrect landing angle, fatigue | Drifting/ or buckling | Stack badly damaged, Risk of blowout | Testing on deck and WROV inspection | Follow procedures, and post machining of welds |
| 8 | Wireline Tool string | Wire to connect wireline tool to topside facilities | Plastic deformation/ rupture | Loss of wireline tool | Operation halt, complication on well management | Temperature and H2S detection from fiber optics | Appropriate quality wireline |
| 9 | Wire rope | Vertical hoisting support | Snatching due to snap load | Equipment sinking | Damage to XT, Stack and chance of loss of stability | Analysis of snap/ hydrodynamic loads | High quality crane wire |

Appendix E

Certex Wire Properties

HIGH PERFORMANCE WIRE ROPE

1



Endurance Dyform® 8/8PI

- **High breaking force** confirmed by Bridon's 'Powercheck' testing of a sample from each production length.
- **Superior bending fatigue life** when compared with other conventional eight strand ropes - confirmed by laboratory testing and extensive field experience.
- **Excellent resistance to crushing and abrasion** resulting from the overall compactness and robustness of the rope and the Dyform strands - recommended when multi-layer spooling is involved.
- **Reduced elongation** results from increased steel content and the Dyform process.
- **Optional plastic coating of IWRC** to further extend fatigue life, improve structural stability and resistance to corrosion.

Available as standard:

| Lay Type | | Lay Direction | | Finish | | Grade |
|----------|-------|---------------|-----------|--------|------|--------|
| Ordinary | Langs | Right Hand | Left Hand | Bright | Galv | Dyform |
| • | | • | | • | | • |

| Diameter | | Approx mass WSC | | Minimum breaking force | |
|----------|-----|--------------------|-------|------------------------|--------|
| | | | | Rope Grade | |
| in | mm | lb.ft | kg/ft | Dyform | |
| | | | | tons | kN |
| 3/8 | | 0.32 | 0.14 | 9.7 | 86.3 |
| | 10 | 0.30 | 0.14 | 9.8 | 87.3 |
| | 11 | 0.38 | 0.17 | 11.8 | 105.0 |
| 7/16 | | 0.40 | 0.18 | 12.4 | 110.4 |
| | 12 | 0.44 | 0.20 | 14.2 | 126.0 |
| 1/2 | | 0.51 | 0.23 | 16.2 | 143.7 |
| | 13 | 0.52 | 0.23 | 16.5 | 147.0 |
| | 14 | 0.60 | 0.27 | 19.2 | 171.0 |
| 9/16 | | 0.65 | 0.29 | 20.3 | 180.7 |
| | 5/8 | 0.80 | 0.35 | 25.0 | 222.5 |
| 5/8 | 16 | 0.78 | 0.35 | 25.2 | 224.0 |
| | 18 | 1.01 | 0.46 | 31.8 | 283.0 |
| | 19 | 1.12 | 0.51 | 35.5 | 316.0 |
| 3/4 | | 1.16 | 0.51 | 36.0 | 320.4 |
| | 20 | 1.24 | 0.56 | 39.3 | 350.0 |
| | 22 | 1.49 | 0.68 | 47.7 | 424.0 |
| 7/8 | | 1.58 | 0.70 | 48.3 | 429.4 |
| | 24 | 1.78 | 0.81 | 56.8 | 505.0 |
| 1 | | 2.05 | 0.91 | 62.8 | 558.5 |
| | 26 | 2.12 | 0.96 | 66.5 | 592.0 |
| | 28 | 2.47 | 1.12 | 77.2 | 687.0 |
| 1 1/8 | | 2.60 | 1.15 | 79.0 | 703.1 |
| 1 1/4 | | 3.22 | 1.42 | 98.0 | 872.2 |
| | 32 | 3.26 | 1.48 | 100.8 | 897.0 |
| 1 3/8 | | 3.90 | 1.72 | 117.0 | 1041.3 |
| | 36 | 4.07 | 1.85 | 127.9 | 1138.0 |
| 1 1/2 | | 4.62 | 2.04 | 138.0 | 1228.2 |

WARNING: Any warranties, expressed or implied, concerning the use of this product apply only to the nominal strength of new, unused wire rope. All equipment using this product must be properly used and maintained. Wire rope must be properly stored, handled, used and maintained. Most importantly, wire rope must be regularly inspected during use. Damage, abuse or improper maintenance can cause rope failure. Consult the AISI Wire Rope Users Manual, ASME or ANSI Standards, before usage. Wire rope removal criteria are based on the use of steel sheaves. If synthetic sheaves are used, consult the sheave equipment manufacturer. **WARNING!**

CERTEX

1-28

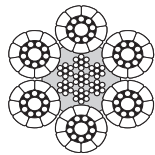
Figure E.1: Guide wire properties (Diameter-19 mm)

HIGH PERFORMANCE WIRE ROPE

Riser Tensioner Lines

Riser Tensioner Lines present a tough application for wire rope, repetitive highload bending over sheaves requiring a flexible solution with exceptional bend fatigue properties and resistance to wear & abrasion.

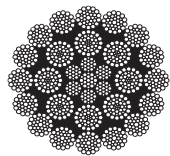
1



DYFORM® BRISTAR® 6

Dyform Bristar 6 ropes for riser tensioner applications are designed to give characteristics which enhance fatigue performance. The 'compacting' process facilitates excellent resistance to wear on the sheaves and drums.

| Rope diameter | | Approximate mass | | | | Minimum breaking force (F _{min}) | | | Axial stiffness @20% load | | Torque generated @20% load | | Metallic cross section | |
|---------------|-------|------------------|-------|-----------|-------|--|--------|---------|---------------------------|------|----------------------------|--------|------------------------|-----------------|
| | | In air | | Submerged | | IPS/1770 grade | | | Lang's lay | | Lang's lay | | Metallic cross section | |
| mm | in | kg/m | lb/ft | kg/m | lb/ft | kN | Tonnes | 2000lbs | MN | Mlbs | kN.m | lbs.ft | mm ² | in ² |
| 44 | | 8.59 | 5.77 | | | 1569 | 160 | 176 | 107 | 24 | 1.5 | 1110 | 1038 | 1.61 |
| 44.5 | 1 7/8 | 8.60 | 5.78 | | | 1569 | 160 | 176 | 109 | 25 | 1.5 | 1121 | 1059 | 1.64 |
| 47.6 | 1 7/8 | 10.1 | 6.81 | | | 1782 | 182 | 200 | 125 | 28 | 1.8 | 1364 | 1214 | 1.88 |
| 48 | | 10.4 | 6.99 | | | 1782 | 182 | 200 | 127 | 29 | 1.9 | 1375 | 1235 | 1.91 |
| 50.8 | 2 | 11.7 | 7.86 | | | 2010 | 205 | 226 | 142 | 32 | 2.2 | 1641 | 1383 | 2.14 |
| 52 | | 11.9 | 8.00 | | | 2067 | 211 | 232 | 149 | 34 | 2.3 | 1728 | 1449 | 2.25 |
| 54 | 2 1/8 | 12.4 | 8.33 | | | 2187 | 223 | 246 | 161 | 36 | 2.6 | 1898 | 1563 | 2.42 |
| 56 | | 13.3 | 8.94 | | | 2315 | 236 | 260 | 173 | 39 | 2.8 | 2084 | 1681 | 2.61 |
| 57.2 | 2 1/4 | 13.9 | 9.34 | | | 2373 | 242 | 267 | 180 | 41 | 3.0 | 2180 | 1751 | 2.71 |
| 60.3 | 2 1/4 | 15.0 | 10.1 | | | 2550 | 260 | 286 | 201 | 45 | 3.4 | 2472 | 1949 | 3.02 |
| 63.5 | 2 1/2 | 17.3 | 11.6 | | | 2922 | 298 | 328 | 223 | 50 | 4.0 | 2983 | 2161 | 3.35 |
| 64 | | 17.5 | 11.8 | | | 2970 | 303 | 334 | 226 | 51 | 4.1 | 3055 | 2195 | 3.40 |
| 66.7 | 2 1/2 | 19.0 | 12.8 | | | 3227 | 329 | 363 | 246 | 55 | 4.7 | 3460 | 2385 | 3.70 |
| 69.9 | 2 1/2 | 20.8 | 14.0 | | | 3599 | 367 | 404 | 270 | 61 | 5.5 | 4044 | 2619 | 4.06 |
| 73.0 | 2 3/4 | 22.6 | 15.2 | | | 3756 | 383 | 422 | 294 | 66 | 6.0 | 4407 | 2856 | 4.43 |
| 76.2 | 3 | 24.7 | 16.6 | | | 3923 | 400 | 441 | 321 | 72 | 6.5 | 4805 | 3112 | 4.82 |



Big Hydra

Big Hydra multi-strand ropes provide an opportunity to utilise large diameter 'Rotational Resistant' ropes ensuring an excellent fatigue performance and high strength. Big Hydra is available in conventional or Dyform® construction to suit your individual requirements.

| Rope diameter | | Approximate mass | | | | Minimum breaking force (F _{min}) | | | Axial stiffness @20% load | | Torque generated @20% load | | Metallic cross section | |
|---------------|-------|------------------|-------|-----------|-------|--|--------|---------|---------------------------|------|----------------------------|--------|------------------------|-----------------|
| | | In air | | Submerged | | IPS/1770 grade | | | Lang's lay | | Lang's lay | | Metallic cross section | |
| mm | in | kg/m | lb/ft | kg/m | lb/ft | kN | Tonnes | 2000lbs | MN | Mlbs | kN.m | lbs.ft | mm ² | in ² |
| 76 | | 26.1 | 17.6 | 22.7 | 15.3 | 4747 | 484 | 533 | 295 | 66 | 3.68 | 2717 | 2813 | 4.36 |
| 76.2 | 3 | 26.3 | 17.7 | 22.9 | 15.4 | 4777 | 487 | 537 | 297 | 67 | 3.72 | 2742 | 2828 | 4.38 |
| 80 | | 29.0 | 19.5 | 25.2 | 16.9 | 5249 | 535 | 590 | 327 | 74 | 4.18 | 3083 | 3117 | 4.83 |
| 82.6 | 3 1/4 | 30.9 | 20.8 | 26.9 | 18.1 | 5581 | 569 | 627 | 349 | 78 | 4.54 | 3351 | 3323 | 5.15 |
| 84 | | 31.9 | 21.4 | 27.8 | 18.6 | 5778 | 589 | 649 | 361 | 81 | 4.84 | 3569 | 3436 | 5.33 |
| 88 | | 35.0 | 23.5 | 30.5 | 20.5 | 6071 | 619 | 682 | 396 | 89 | 5.43 | 4004 | 3771 | 5.85 |
| 88.9 | 3 1/2 | 35.7 | 24.0 | 31.1 | 20.9 | 6194 | 631 | 696 | 404 | 91 | 5.57 | 4106 | 3849 | 5.97 |
| 92 | | 38.3 | 25.7 | 33.3 | 22.4 | 6634 | 676 | 745 | 433 | 97 | 6.36 | 4688 | 4122 | 6.39 |
| 95.3 | 3 3/4 | 41.0 | 27.6 | 35.7 | 24.0 | 7086 | 722 | 796 | 464 | 104 | 6.79 | 5009 | 4423 | 6.86 |
| 96 | | 41.6 | 28.0 | 36.2 | 24.3 | 7198 | 734 | 809 | 471 | 106 | 6.99 | 5155 | 4488 | 6.96 |
| 100 | | 45.2 | 30.4 | 39.3 | 26.4 | 7797 | 795 | 876 | 511 | 115 | 8.17 | 6021 | 4870 | 7.55 |
| 101.6 | 4 | 46.7 | 31.4 | 40.6 | 27.3 | 8103 | 826 | 910 | 528 | 119 | 8.31 | 6127 | 5027 | 7.79 |
| 108 | 4 1/4 | 52.9 | 35.5 | 46.0 | 30.9 | 9076 | 925 | 1020 | 596 | 134 | 9.84 | 7253 | 5680 | 8.80 |
| 114.3 | 4 1/2 | 59.1 | 39.7 | 51.4 | 34.6 | 10121 | 1032 | 1137 | 668 | 150 | 11.68 | 8616 | 6362 | 9.86 |
| 120.7 | 4 3/4 | 66.1 | 44.4 | 57.5 | 38.6 | 11240 | 1146 | 1263 | 745 | 167 | 13.69 | 10091 | 7095 | 11.00 |
| 127 | 5 | 73.1 | 49.1 | 63.6 | 42.7 | 12355 | 1259 | 1388 | 825 | 185 | 15.81 | 11661 | 7855 | 12.18 |
| 133.4 | 5 1/4 | 80.9 | 54.4 | 70.4 | 47.3 | 13616 | 1388 | 1530 | 910 | 205 | 18.10 | 13346 | 8666 | 13.43 |
| 139.7 | 5 1/2 | 88.5 | 59.5 | 77.0 | 51.7 | 14726 | 1501 | 1654 | 998 | 224 | 20.77 | 15316 | 9504 | 14.73 |

Values for ordinary lay are available on request.

Figure E.2: Crane wire properties (Diameter-69.9mm)

Appendix F

Information on Åsgard Field

Subsea Technology Features of Åsgard Field Development

Mohammed Ali Mohammed, Stavanger, Norway

Overview

New technology development has always been at the forefront of what drives the oil and gas industry. This is an industry which faces a number of new challenges as we look forward to develop fields discovered in the Arctic and ultra-deep waters. However, history tells us that with the right research and investment, economically feasible solutions are imminent. Some of the most remarkable and pioneering technology developed to tackle challenges in the Norwegian Sea for the past 25 years are testimony to that fact. One of the fields in the Norwegian Sea is the Åsgard field located in Haltenbanken area, about 260 km (162 miles) from N/W Trondheim and 50 km (30 miles) south of Heidrun field. In this paper, we overlook at some of the iconic subsea solutions developed in Åsgard field.

Åsgard field covers six blocks encompassing Midgard, Smørbukkk and Smørbukkk South sub-fields, discovered on 1981, 1984 and 1985 respectively. Collectively, the discoveries amounted to an estimated 100.4 million Sm³ of oil, 207.7 billion Sm³ of gas, 39.4 million tons of NGL and 17.1 million Sm³ of condensate (Alveberg and Melberg, 2013). The Haltenbanken area, which has depths ranging from 240 to 380 meters, has a harsh environment with high wave heights and high velocity in current and wind. Furthermore, due to the size of the individual deposits, separate development by standalone projects was deemed to be economically non-profitable (Totland et al., 2007). In 1994, these conditions led to the commissioning of the largest subsea development project of its time in an attempt to tie all three fields together. Upon successful development, Åsgard field gave its first oil in May 1999 followed by gas production in October 2000. Much of the reserve has since been produced, however significant amount still remains. In addition, the field has had new gas/oil discoveries years after it first started production.

Åsgard Field Development Concept

Norway's largest subsea development to date, the Åsgard field is completed with subsea wells through subsea templates that are tied by flow lines into a Floating Production Storage and Offloading vessel (Åsgard A) for oil, and a semi-submersible facility for processing of gas and condensate (Åsgard B). Åsgard B is also linked to a condensate storage vessel (Åsgard C). Gas is exported through the export pipeline Åsgard Transport to Kårstø north of Stavanger, while oil and condensate is exported using tankers. Among other things, the choice of using this subsea concept for was mainly influenced by size, type and distance between Smørbukkk, Smørbukkk south and Midgard and adjacent areas.

Smørbukkk field produces from Tilje formation that contains gas and light oil. Tilje formation has poor permeability having been split into several separate segments by barriers. The moderate quality Garn and the underlying Ile and Tilje formations are the main reservoirs for Smørbukkk south field. The formations contain oil and gas condensate respectively. Smørbukkk and Smørbukkk south fields are produced using a combined 32 production wells from 9 templates and 16 gas injection wells from 5 templates (Haaland et al., 1996). In 2011, Smørbukkk northeast field was developed through a satellite well hooked up to an existing template connected to Åsgard B.

Midgard field generally consists of four reservoir zones; Garn Not, Ile, and Tilje, and are found to contain lean gas with high level of permeability. Hence, Midgard field is produced by natural depletion using 9 gas producing wells developed with 3 templates. However, with current facilities, the field had reduced production than estimated on its initial PDO. To avert this scenario, a subsea compression system is planned for installment in 2015.

The design of templates used in Åsgard was influenced by the intention to perform all marine operations without using divers. Thereby, a new 'HOST template' designed by FMC has been implemented for all wells. The HOST template allows assembly of modules of the template on deck or at subsea by using a special UTIS tie-in tool from a moonpool of a floating rig.

Figure 1.0 shows a schematic diagram of the Åsgard field. Templates from Midgard are connected with Åsgard B in a 20" pipeline of an approximately 97 km long circular loop ("Midgard - loop"), where the templates are connected to pipelines by use of jumpers. One template from Midgard is also connected to gas templates from Mikkel field located 37 km south through to an 18" pipeline. In the north a different template from Midgard is connected to Yttergryta field template through an approximately 5.5 km long pipeline (18"). Templates from Smørbukkk and Smørbukkk south fields are connected to topside facilities by two 10" pipeline arranged separately and in bundles. Total infield flowlines utilized have an estimated length of 300 km with hydraulic/electric control umbilicals measuring about 145 km.

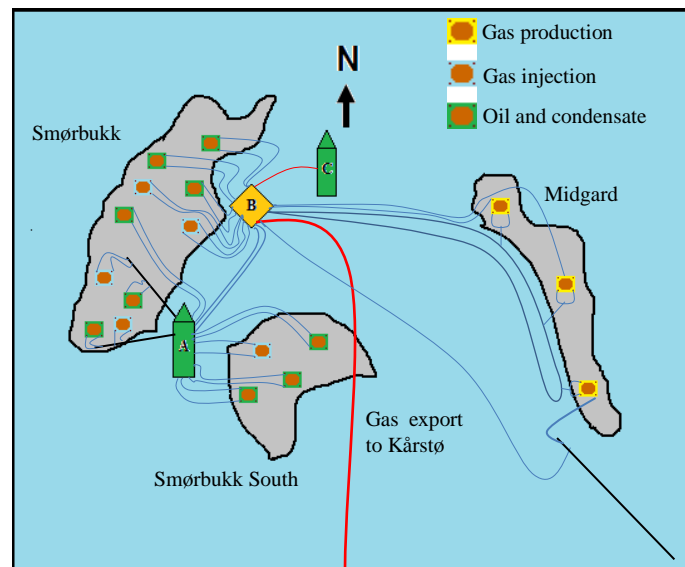


Figure 1.0 Åsgard unit field development layout

Notworthy Subsea Features of Åsgard

1. Horizontal Subsea Trees

A subsea tree can be simply described as an assembly of valves that serve as a main access to wells and are a physical barrier between well fluids and the sea during production. Depending on the type of assembly, there are two main types of subsea trees: Horizontal and Vertical. According to FMC, Åsgard field was developed entirely from horizontal subsea trees. Horizontal trees are designed to omit using a tubing head spool typically found on vertical trees. This enables the landing of tubing hanger to be performed after installation of the subsea tree. This important step provides a means for a direct access into the well without needing to disrupt the connection of wellhead/flowline/x-mass tree. In Åsgard, the horizontal trees had a 7"x2", 10000 Psi configurations. This implies there exists a 7" production bore accessible vertically with wire-line while protected by an isolation plug installed in the tubing hanger. A second isolation barrier also placed within the internal tree cap serving as a fail-safe. A 2" annulus bypass loop also allows the pressure between the tubing hanger and the annulus circulation to be equalized. The 10000 psi specification also refers to design capability of the valves at full pressure actuation. Once installed, a subsea electro-hydraulic system is used to remotely operate subsea trees.

2. Riser-less light well intervention (RLWI)

The recovery rate of subsea wells is significantly lower than dry wells because subsea well intervention is more costly than non-subsea wells. Hence, frequent well intervention has been a major concern for Åsgard. A new technology called Riser-less Light Well Intervention has been used over the past decade to address this issue. The technology, which utilizes subsea equipment deployed from a DP moored vessel, is faster and cheaper than previous riser based intervention rigs. It's use has given a significant boost to achieve improved recovery (IOR) of

subsea wells (Viken et al., 2007). The RLWI system currently in use has three sections: 1) Well control package (WCP), 2) Lubricator section (LS) and 3) Pressure control head. Each section deployed from a monohull vessel separately through a moonpool is connected at sea bed using remotely operated vehicles (ROV). Figure 2.0 below shows arrangement of the sections. The WCP acts as the main well barrier equipment consisting of subsea control module, hydraulic power unit, accumulator and electric umbilical station. The PCH is used as a grease seal for a moving wire line. A work over control system (WOCS) is used for temporary control of the well during light well intervention.

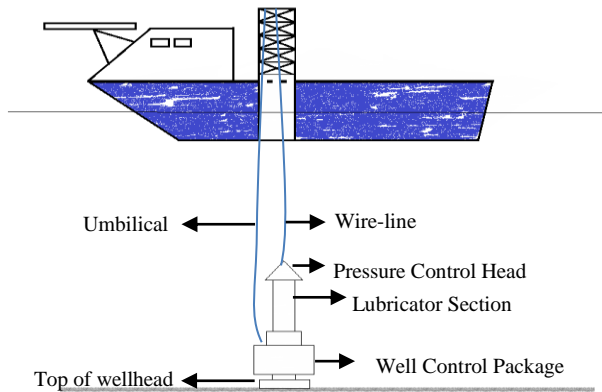


Figure 2: Riser-less light well intervention schematics

3. Direct Electric Heating of Flowlines

Prevention of wax and hydrate formation inside flowlines is prominent for regularity of production. The technology of Direct Electric Heating has been qualified for this purpose and implemented for the first time on Asgard production pipelines (Dretvik and Bornes, 2001). A total pipeline (10") length of 45 km from Smørbukk templates to Asgard B is equipped with direct electric heating. The technology involves heating of flowlines to keep them above the hydrate formation temperature by passing electric current generated from topside facilities. For Smørbukk field effluent, this temperature is 25 °C. The operator controls the current flowing through these pipes and is able to manage the temperature of the flow line. To keep the generated heat from escaping out, a pipe insulation system is used. However, it is economically non-profitable to ideally insulate the flowlines due to demand for cathodic protection to a large extent for corrosion prevention. Sacrificial anodes are used in 50 m gaps to connect the heating system to adjacent seawater. Finally, direct electric has added advantage of being environmental friendly, with little to no pollution hazards. Conventional remediation techniques, requiring pressure blowdown, hot oiling and chemical injection are costly and require long time, or environmentally unfriendly.

Subsea gas compression for Asgard field

Unforeseen pressure drop and water breakthrough in the Midgard field and its adjacent Mikkel field has resulted in reduced gas flow rate than expected and increased risk of slug accumulation in flowlines in the future. To maintain gas recovery on par with the initial PDO estimate, two alternative solutions were proposed: 1) A subsea gas compression or 2) A floating compression platform. Other options such as drilling additional wells, modifying existing facilities to accommodate compression stations, onshore compression... etc were considered non-optimal solutions due to weight limits and technical/economic barriers.

1. Platform compression alternative

A floating platform will be installed in strategic location between the Midgard and Mikkel fields. The platform shall be equipped with a two train compressor station. Due to limitation on the size of the compressor station, the platform topside layout should have an estimated length of 100m and 70m width. A semi-submersible or TLP platform type is deemed to be suitable for this configuration. The total weight would be in the order of 30,000 tons (Bjerkreim, 2004). Once the platform is installed, the wellstream is to be connected to a distribution manifold which is used to re-route the wellflow into the newly installed risers. Each riser will be connected to the compression trains through supply headers. When the wellflow reaches the compression station, the gas and liquid phases will be separated. The gas will be compressed and heated and the liquid will be

boosted by pumps. An export pipeline connects the mixed multiphase flow back to the existing flowlines connected to Asgard B. Power shall be supplied locally at the platform. The platform will be manned and communication to other facilities would be wireless.

2. Subsea compression alternative

The subsea compression concept will have basically the same function. Major differences are that (Statoil, 2011);

- Compression station will be installed on the seabed (~240m depth) instead of platform.
- Power will be supplied through existing facilities on Asgard A
- Minor modification occur in Asgard B

There are a few challenges when choosing subsea compression concept. Firstly, subsea compression is a rather a new technology compared to a matured platform concept. Next, it has been only attempted once in the Ormen Lange project 2007 and the components of the subsea compression station will require to be "marinated" further. Moreover, underwater power supply is still a developing technology. Finally, interventions and maintenance works would also be challenging and more costly than on deck maintenance.

However, there are several advantages that make implementing a subsea gas compression the favored solution. A compression platform with comparable compression effect will have higher energy consumption due to well needed power supply to platform decks. Increased energy demand would also lead to greater emissions of the scroll, CO₂ and NO_x. In addition, due to the close proximity of the subsea compression station to the wellhead, subsea compression is considered to be a more energy efficient. Manufacturing a 30,000 ton platform compared to 3600 ton subsea compressor will also be more expensive and inefficient way of using material (steel). Platforms will normally have installations for flaring of gas. The seabed based compressor station has no such dedicated discharge points. All or part of the gas stream would be recycled in a closed system, but never released to the surroundings. Finally, there will be minor staff changes to operate the subsea compressor compared to a whole crew needed to operate a platform with a compression unit, thereby further reducing the operational costs.

Risk Assessment

The risk encountered on Asgard field development can be attributed to environmental impact, economic loss, and personal exposure.

1. Environmental impact

During subsea development in Asgard we risk disturbing fishing activities and coral reefs. Emissions of greenhouse gases are kept to minimum by using less energy. Discharges of fluids to the environment are also monitored. Risk of accidental blowout is apparent and necessary design specifications are made for fail safe barriers.

2. Economic loss

The subsea solution has less CAPEX but has higher OPEX. Risk of expenditure (RISKEX) due to unintended operations is higher. This can be seen from the need for subsea compression system discussed earlier. Changes in oil price, accidental blow out, un-mature technology, unforeseen weather conditions all contribute to risk of economic loss.

3. Personal exposure.

Implementing subsea development for Asgard has minimized the personnel exposed to operation. Hence, risk of fatality is considerably reduced. Risk is increased due to in-experience of subsea installation and operation of newly developed technology.

- BJERKREIM, B. 2004. Subsea gas compression - A future option. *Offshore Technology Conference*. Houston, Texas.
- DRETVIK, S. & BORNES, A. H. 2001. Direct Heated Flowlines In the Asgard Field. The International Society of Offshore and Polar Engineers.
- STATOIL 2011. Åsgard havbunnskompresjon - Edret plan for utbygging og drift : Del 2 Konsekvensutredning. *RE-MFP 00072*. Stavanger: Statoil.
- TOTLAND, T., PETERSEN, O. A., GRINI, P. G. & UTENGEN, S. F. 2007. The Norwegian Sea: The Development of a New Offshore Region. *Offshore Technology Conference*. Houston, Texas.
- VIKEN, V., HOVDE, E., SLETFJERDING, E., STOROE, P. A., MJAALAND, S., SAND, G. A., VASSENDEN, F. & LERDAHL, T. R. 2007. Light Well Intervention in the Asgard Field (Norway) as a Tool for Improved Reservoir Management. *Offshore Europe*. Aberdeen, Scotland, U.K.: Society of Petroleum Engineers.